Title: Tidal Streams and Debris Flows: Dark Matter Velocity Substructure and Direct Detection

Date: Sep 23, 2011 02:00 PM

URL: http://pirsa.org/11090085

Abstract: High resolution simulations of Galactic Cold Dark Matter halos reveal staggering amounts of substructure, both in configuration and velocity space. In this talk I will focus on the latter. In addition to spatially localized subhalos and streams, I will also discuss so-called debris flows -- incompletely phase-mixed material originating in numerous accretion and merging events that are the hallmark of the hierarchical build-up of the host halo. Finally, I will briefly discuss the presence and direct detection consequences of a dark disk in the Eris simulation, a cosmological simulation including baryonic physics of the formation of a realistic looking disk galaxy.

Tidal Streams and Debris Flows: Dark Matter Velocity Substructure and Direct Detection

Michael Kuhlen, UC Berkeley

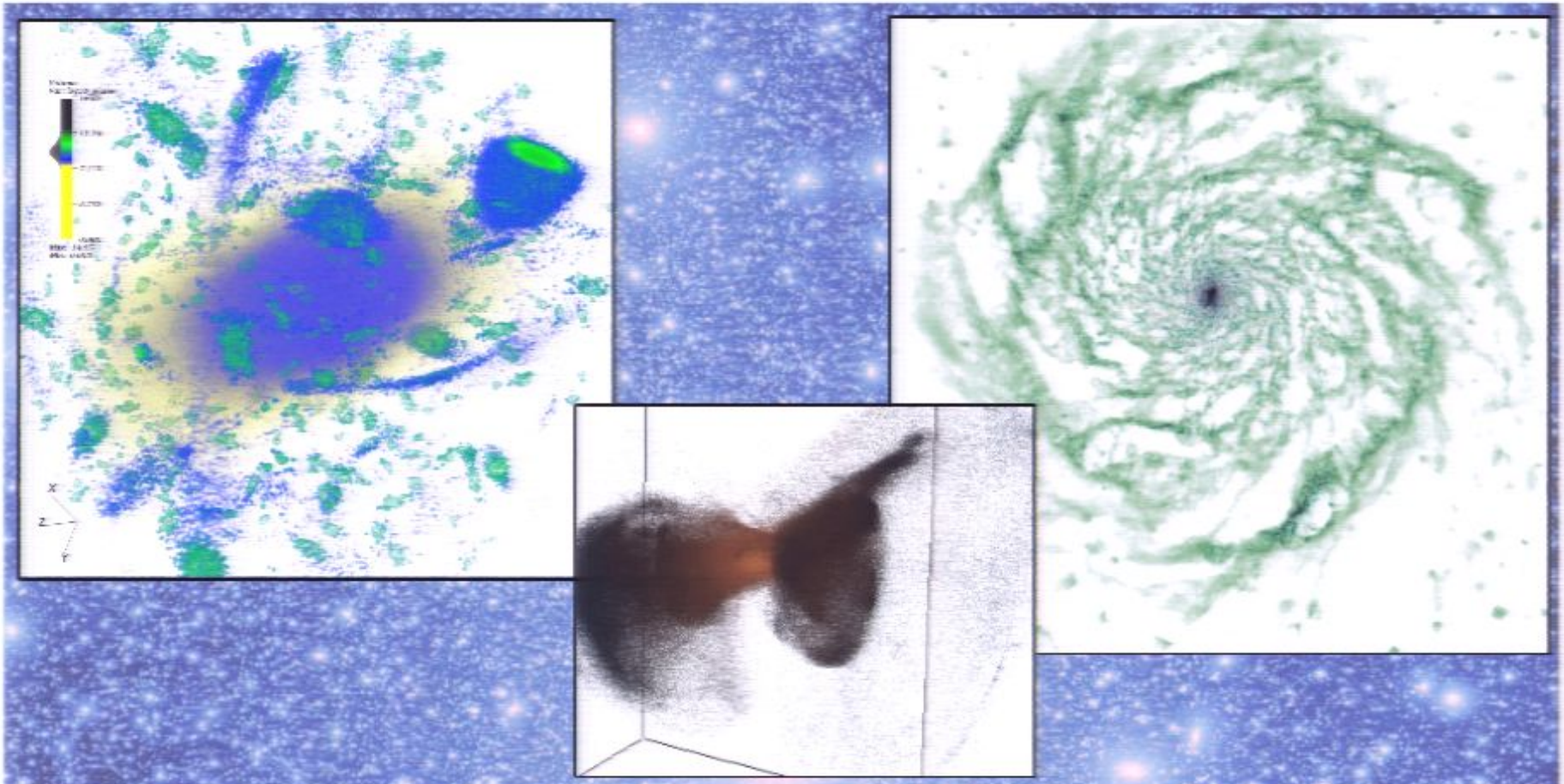

Collaborators: P. Madau (UCSC), J. Diemand (Zurich), M. Zemp (Michigan), B. Moore (Zurich), J. Stadel (Zurich), D. Potter (Zurich), N. Weiner (NYU), **Mariangela Lisanti (Princeton)**, **Javiera Guedes(Zurich)**

Velocity Space Substructure and Direct Detection

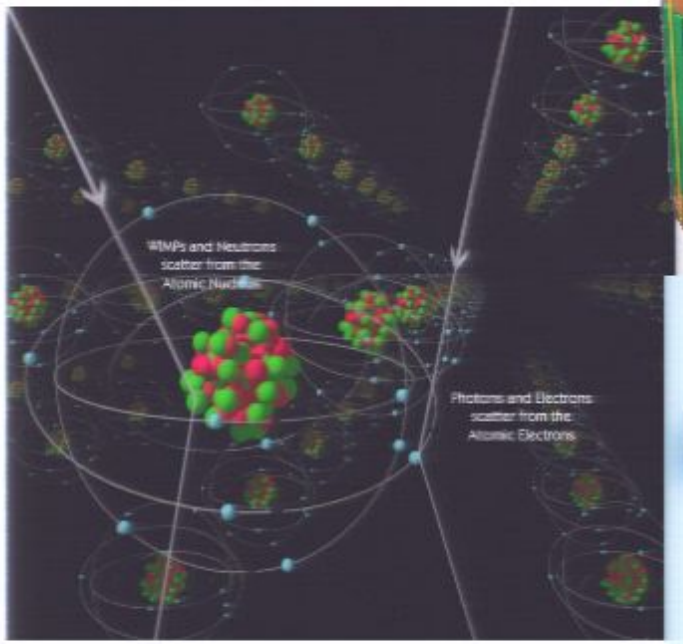

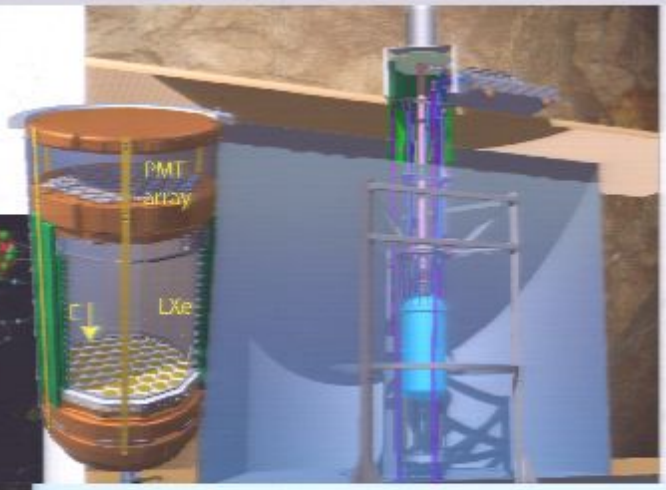

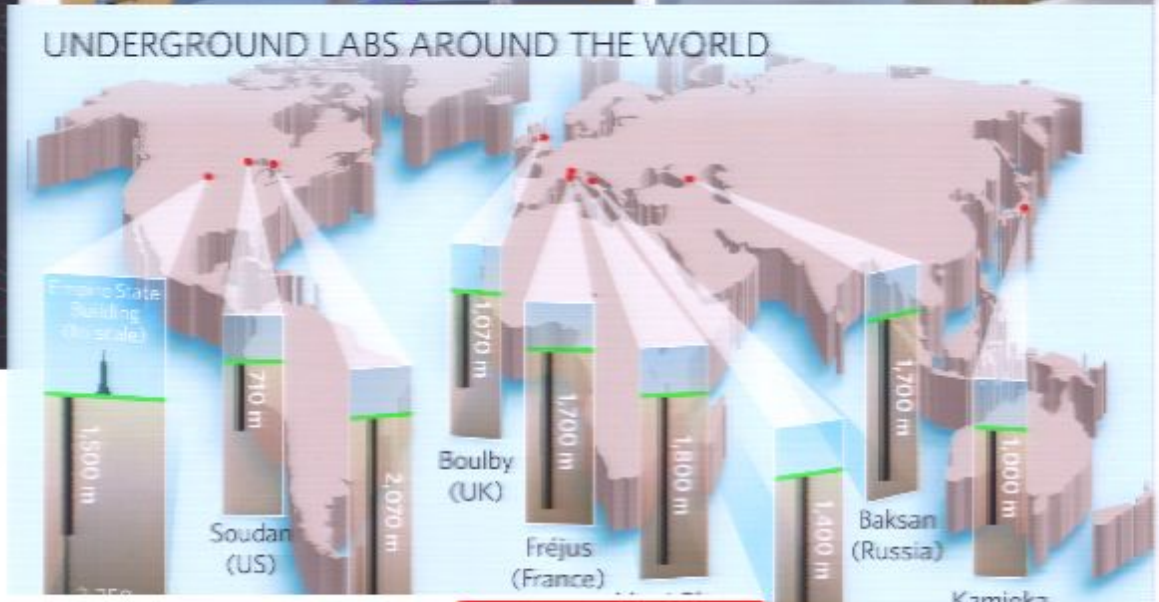

$$\frac{dR}{dE_R} = N_T M_N \frac{\rho_\chi \sigma_n}{2 m_\chi \mu_{ne}^2} \frac{(f_p Z + f_n (A - Z))^2}{f_n^2} F^2[E_R] \int_{\beta_{min}}^{\infty} \frac{f(v)}{v} dv$$

The Via Lactea Project

J. Diemand – M. Kuhlen – P. Madau

(& B. Moore, D. Potter, J. Stadel, M. Zemp)

GHALO
Stadel et al. (2009)
2.1 billion particles, 1,000 $M_\odot$

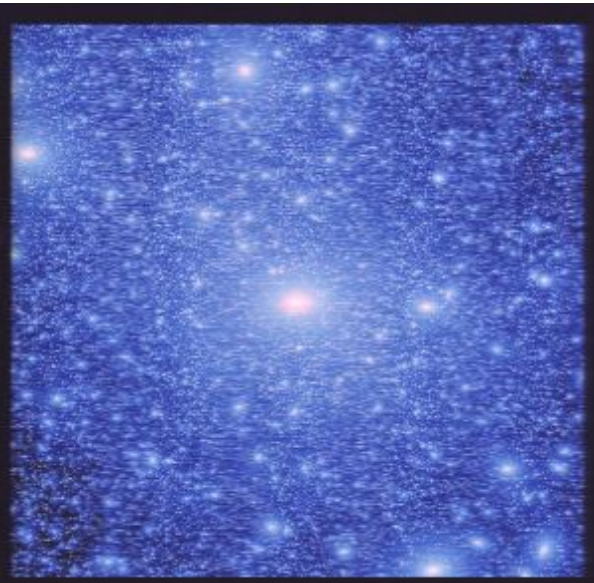

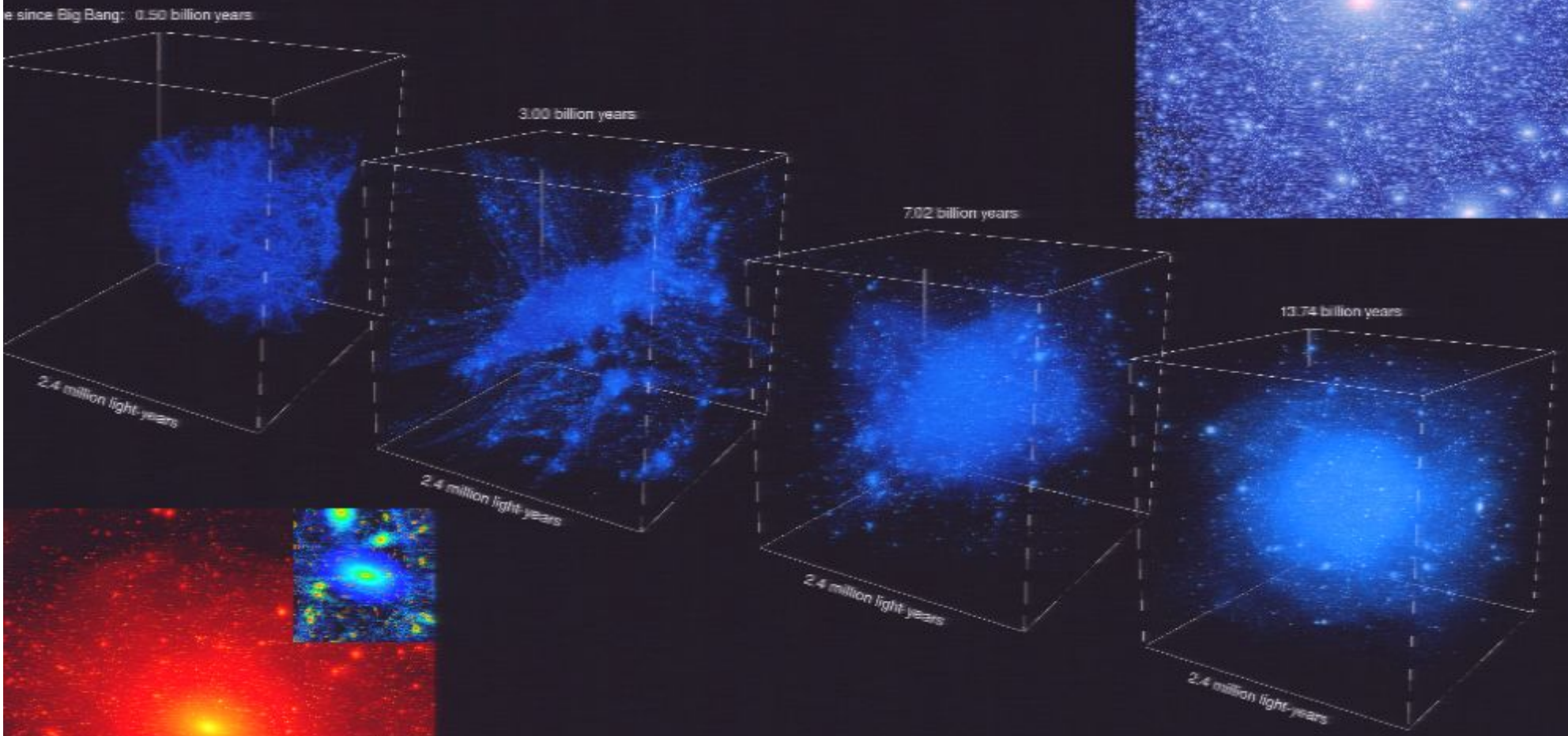

VIA LACTEA II
Diemand, Kuhlen et al. 2008
1.1 billion particles, 4,000 $M_\odot$

SciDAC
Scientific Discovery through Advanced Computing

Office of Science
INCITE
Advancing America's Science and Industrial Competitiveness

Velocity Space Substructure and Direct Detection

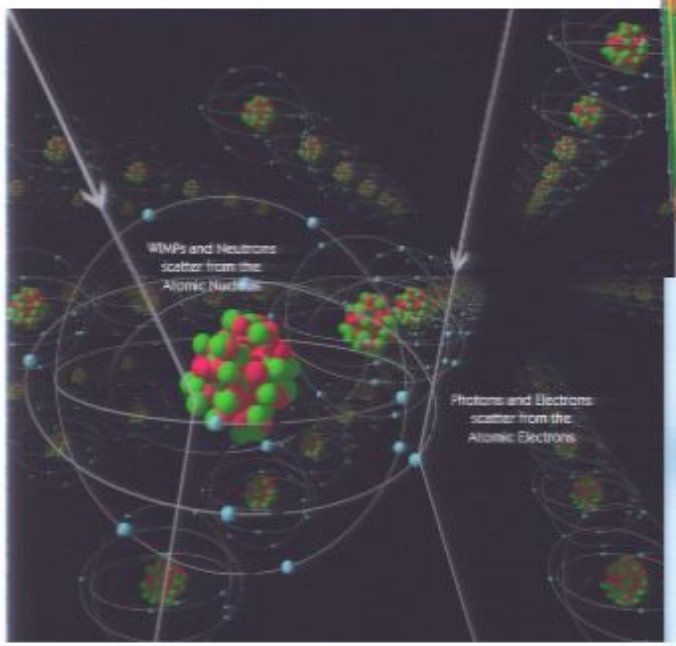

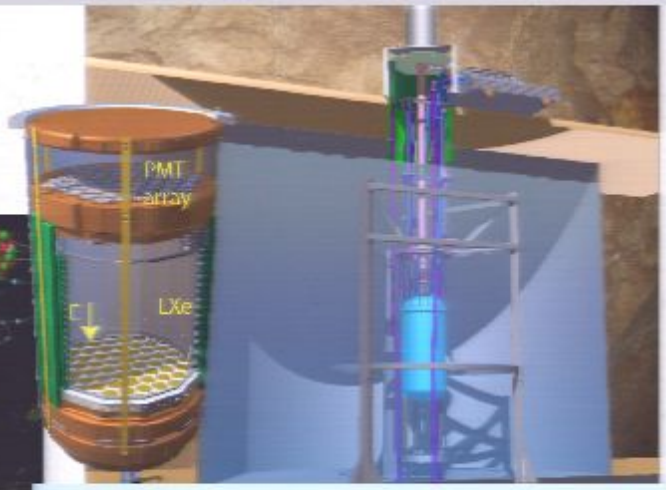

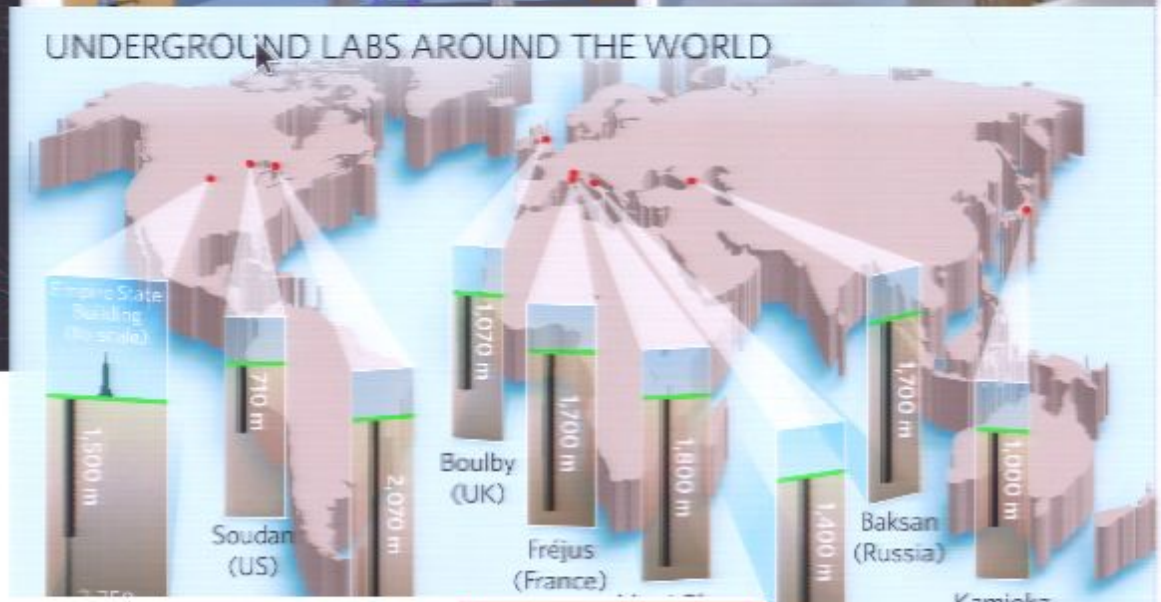

$$\frac{dR}{dE_R} = N_T M_N \frac{\rho_\chi \sigma_n}{2 m_\chi \mu_{ne}^2} \frac{(f_p Z + f_n (A - Z))^2}{f_n^2} F^2[E_R] \int_{\beta_{min}}^{\infty} \frac{f(v)}{v} dv$$

The Via Lactea Project

J. Diemand – M. Kuhlen – P. Madau

(& B. Moore, D. Potter, J. Stadel, M. Zemp)

GHALO
Stadel et al. (2009)
2.1 billion particles, 1,000 $M_\odot$

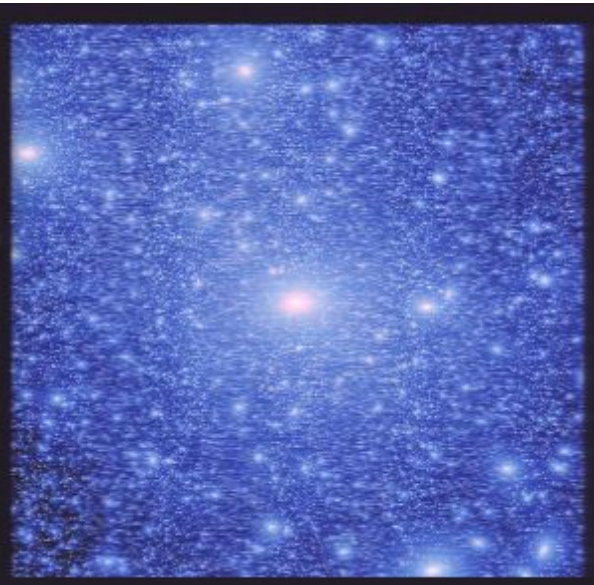

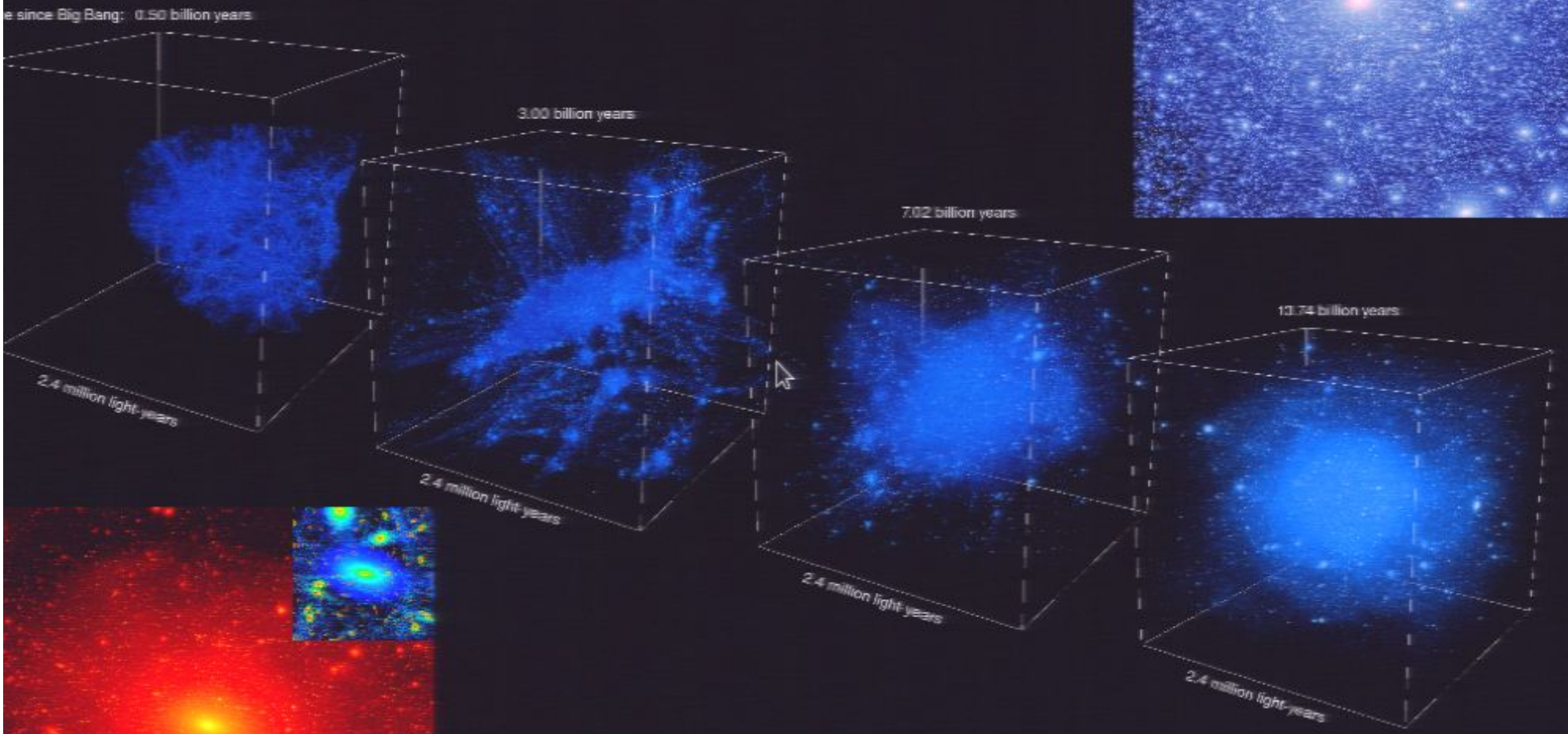

VIA LACTEA II
Diemand, Kuhlen et al. 2008
1.1 billion particles, 4,000 $M_\odot$

SciDAC
Scientific Discovery through Advanced Computing

Office of Science
INCITE
Advancing America's Science and Industrial Competitiveness

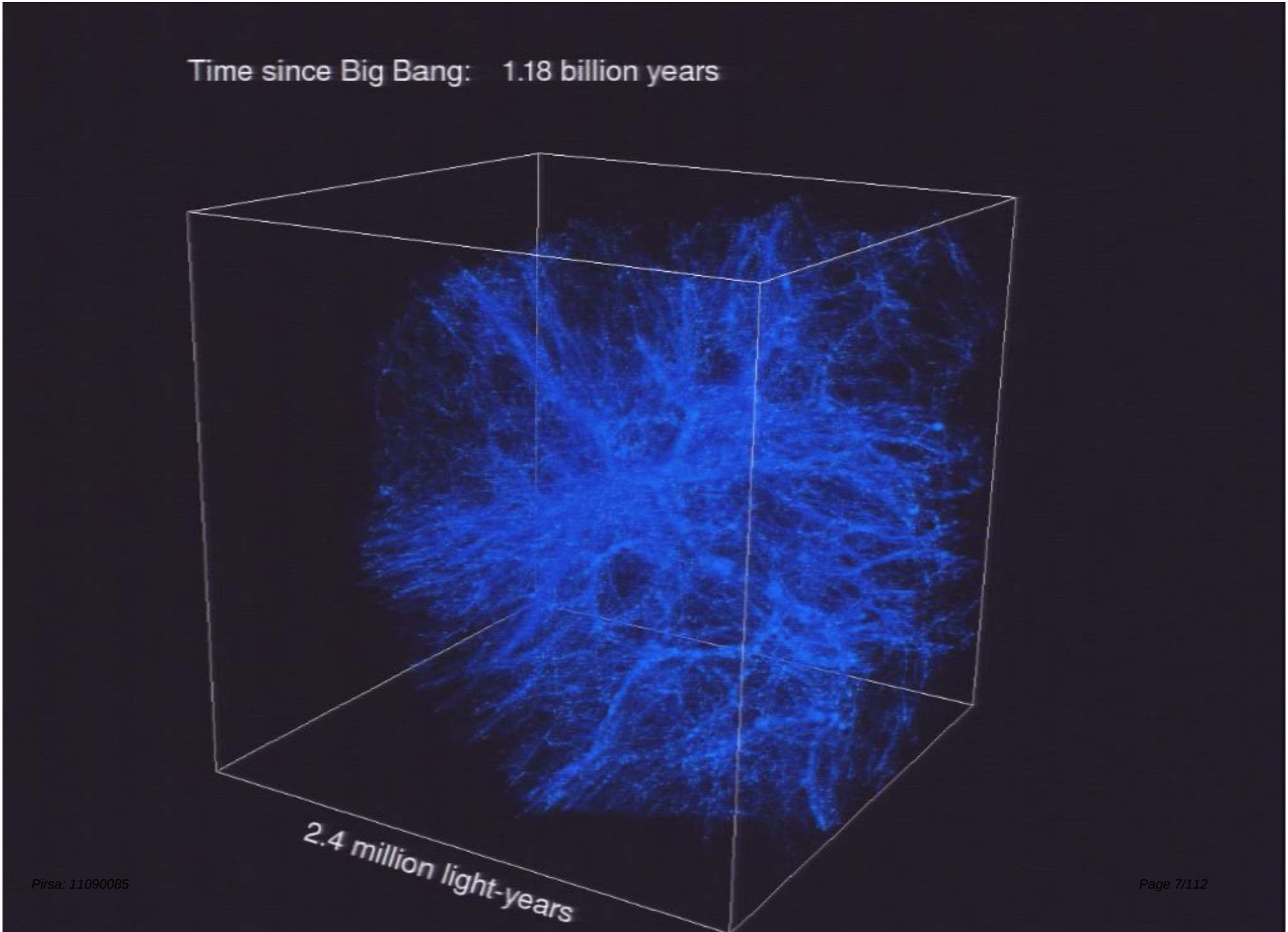
Time since Big Bang: 1.18 billion years
2.4 million light-years

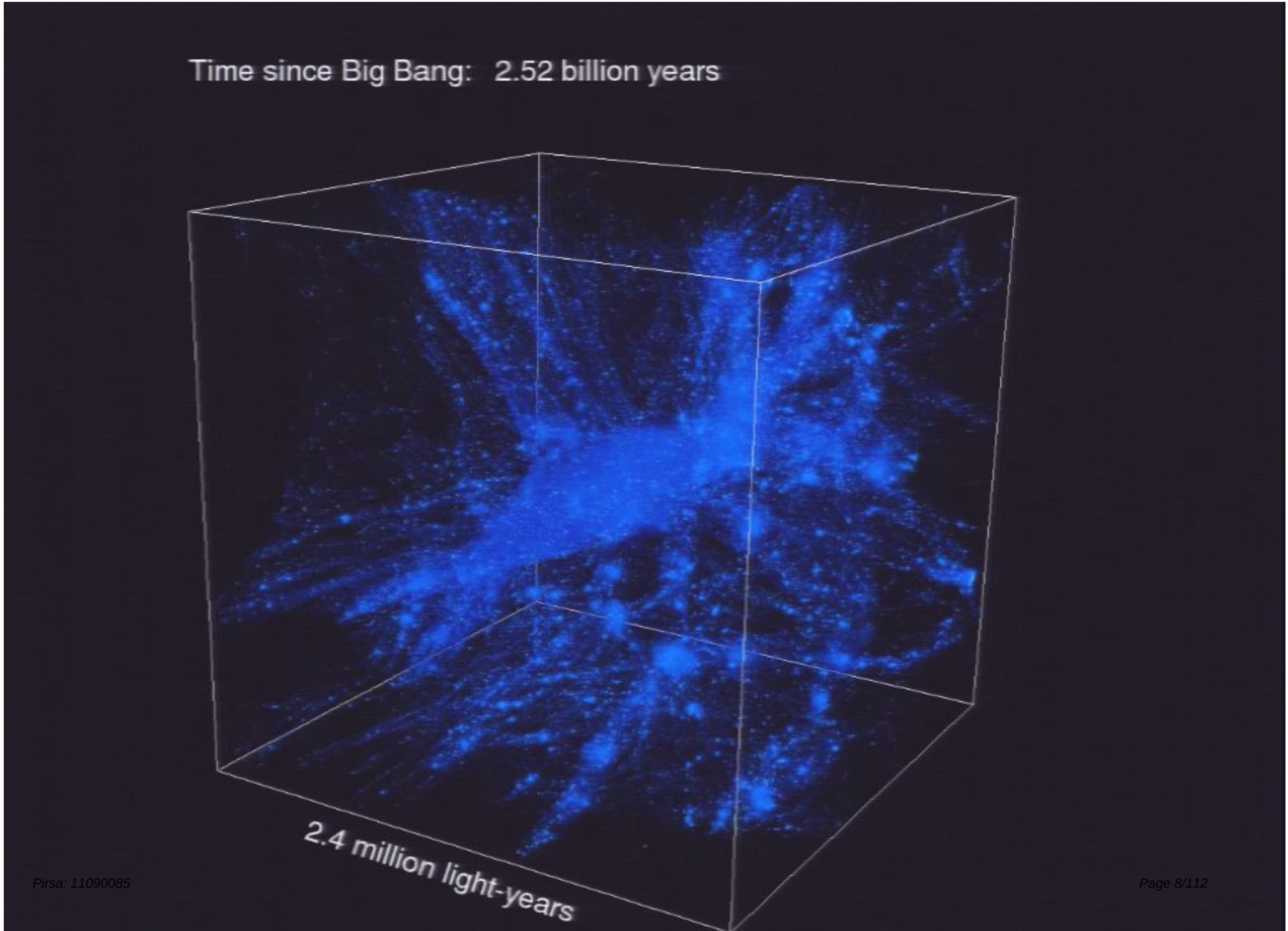
Time since Big Bang: 2.52 billion years
2.4 million light-years

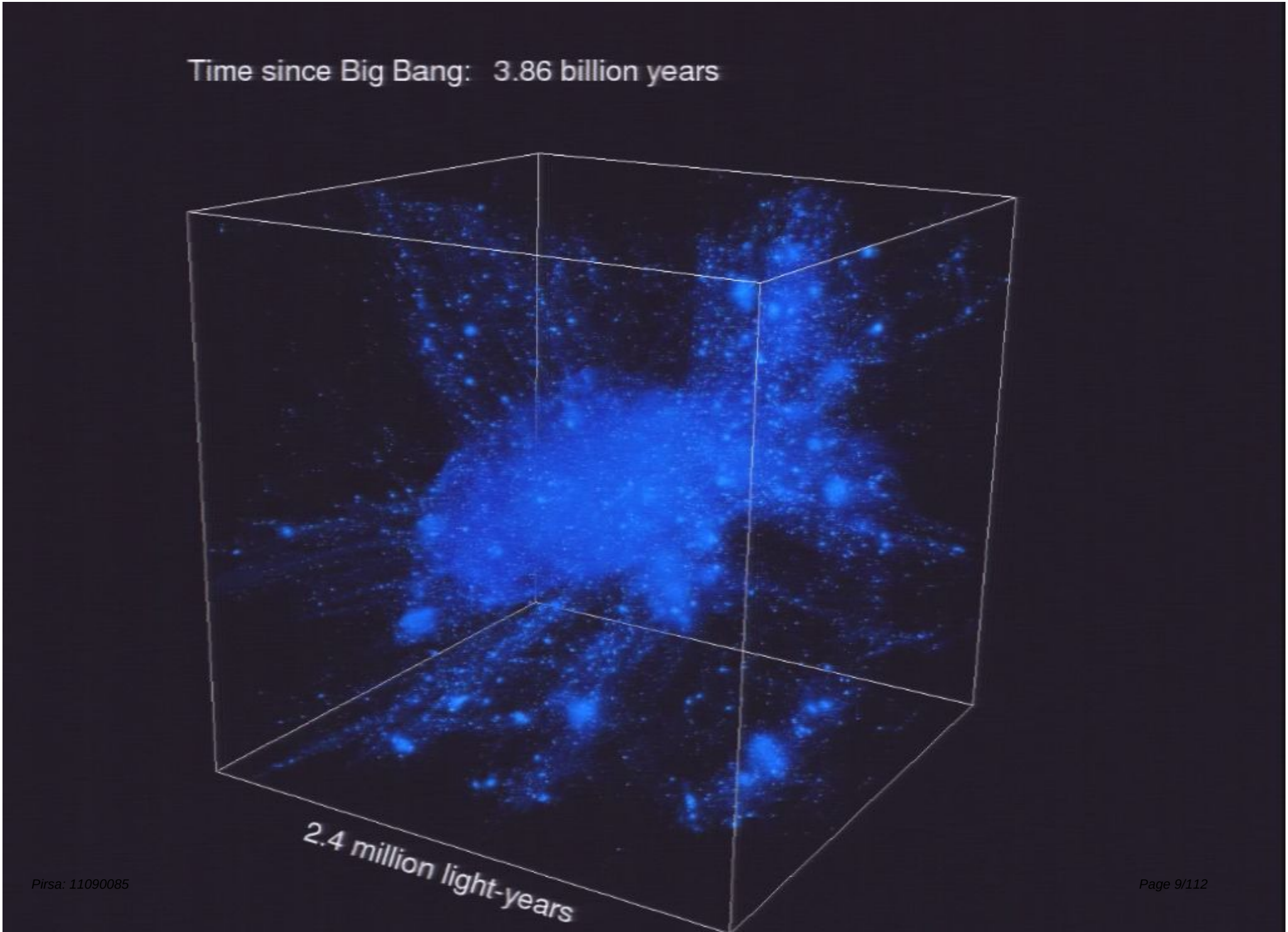
Time since Big Bang: 3.86 billion years
2.4 million light-years

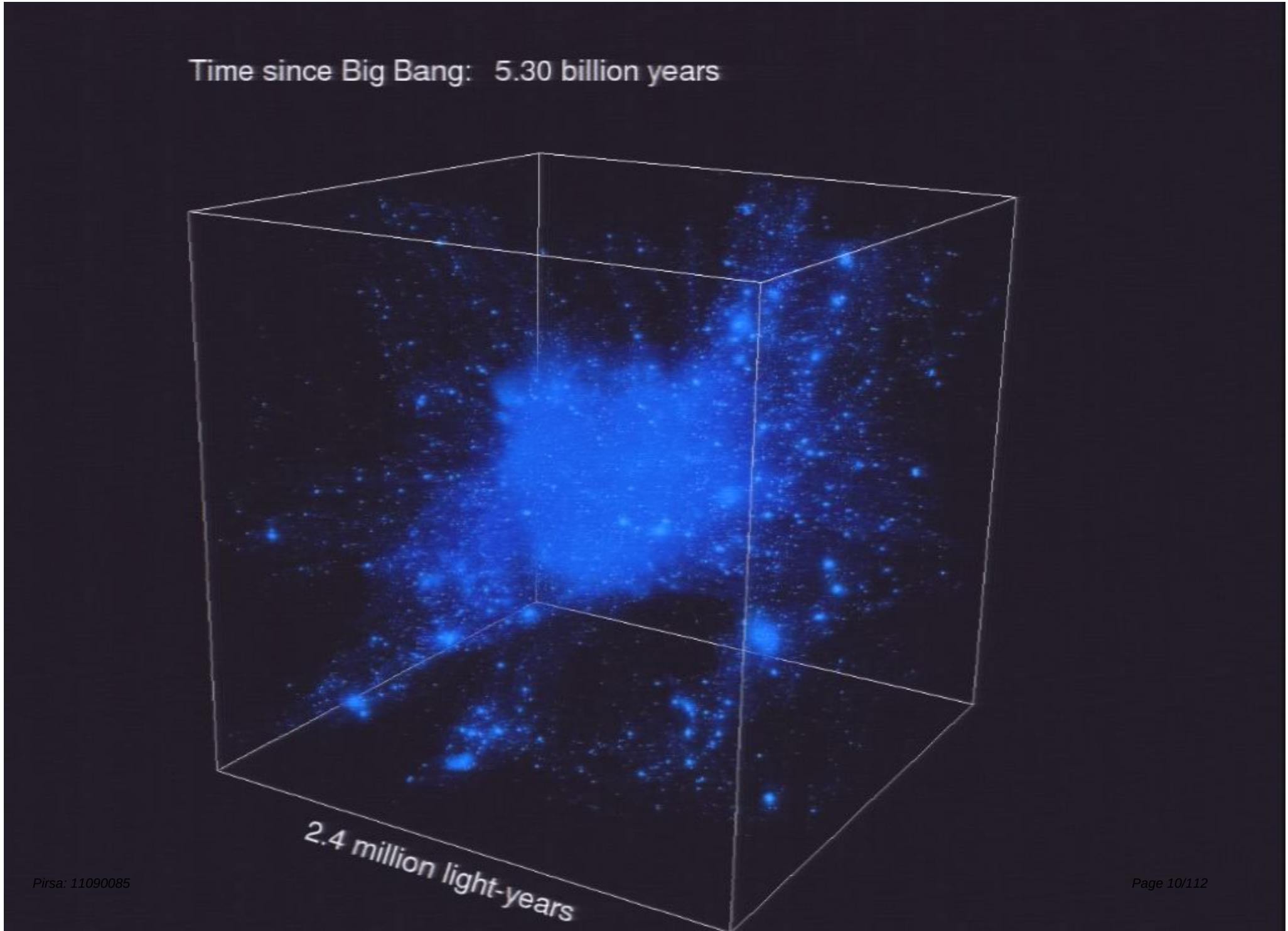
Time since Big Bang: 5.30 billion years
2.4 million light-years

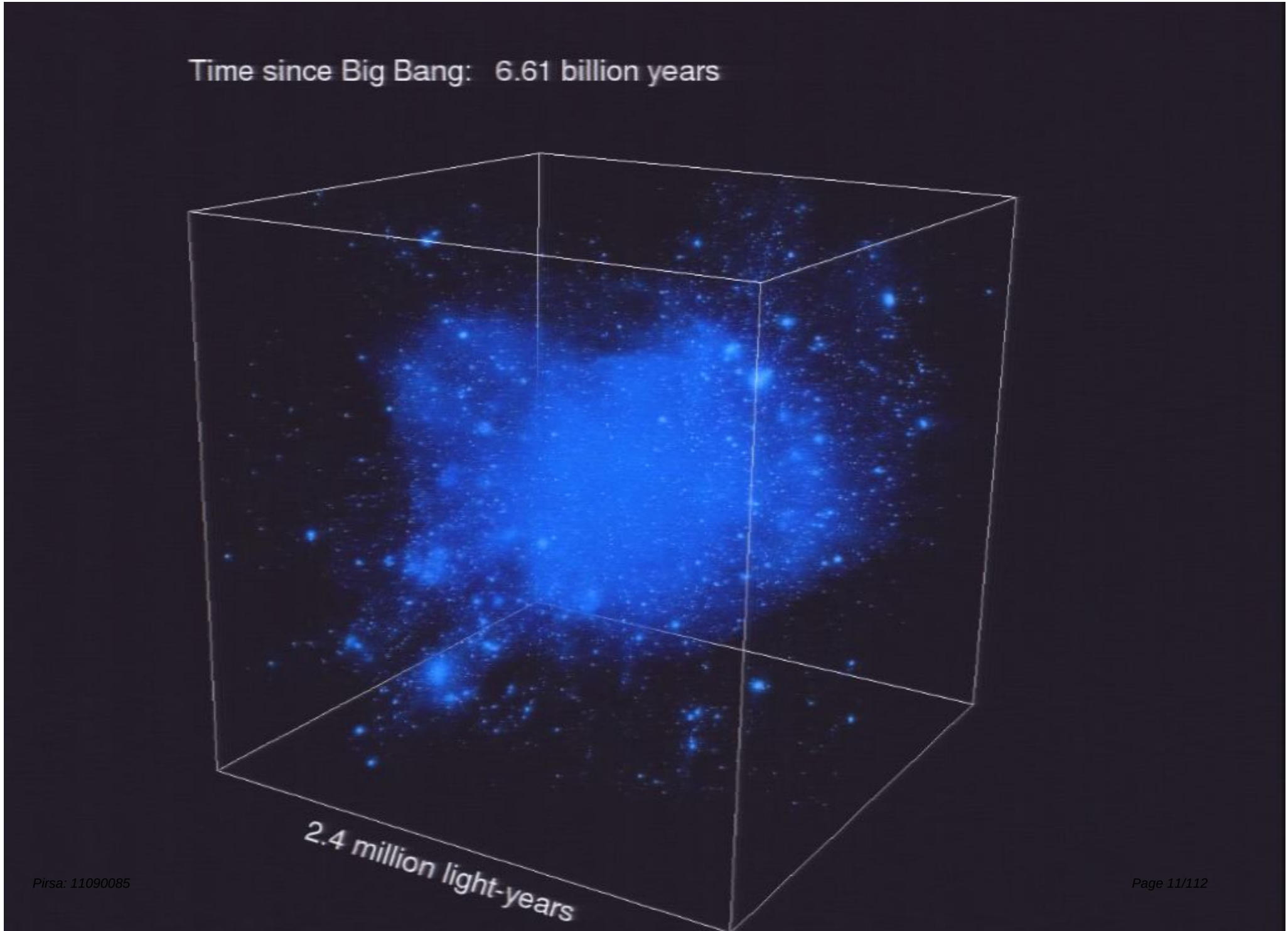
Time since Big Bang: 6.61 billion years
2.4 million light-years

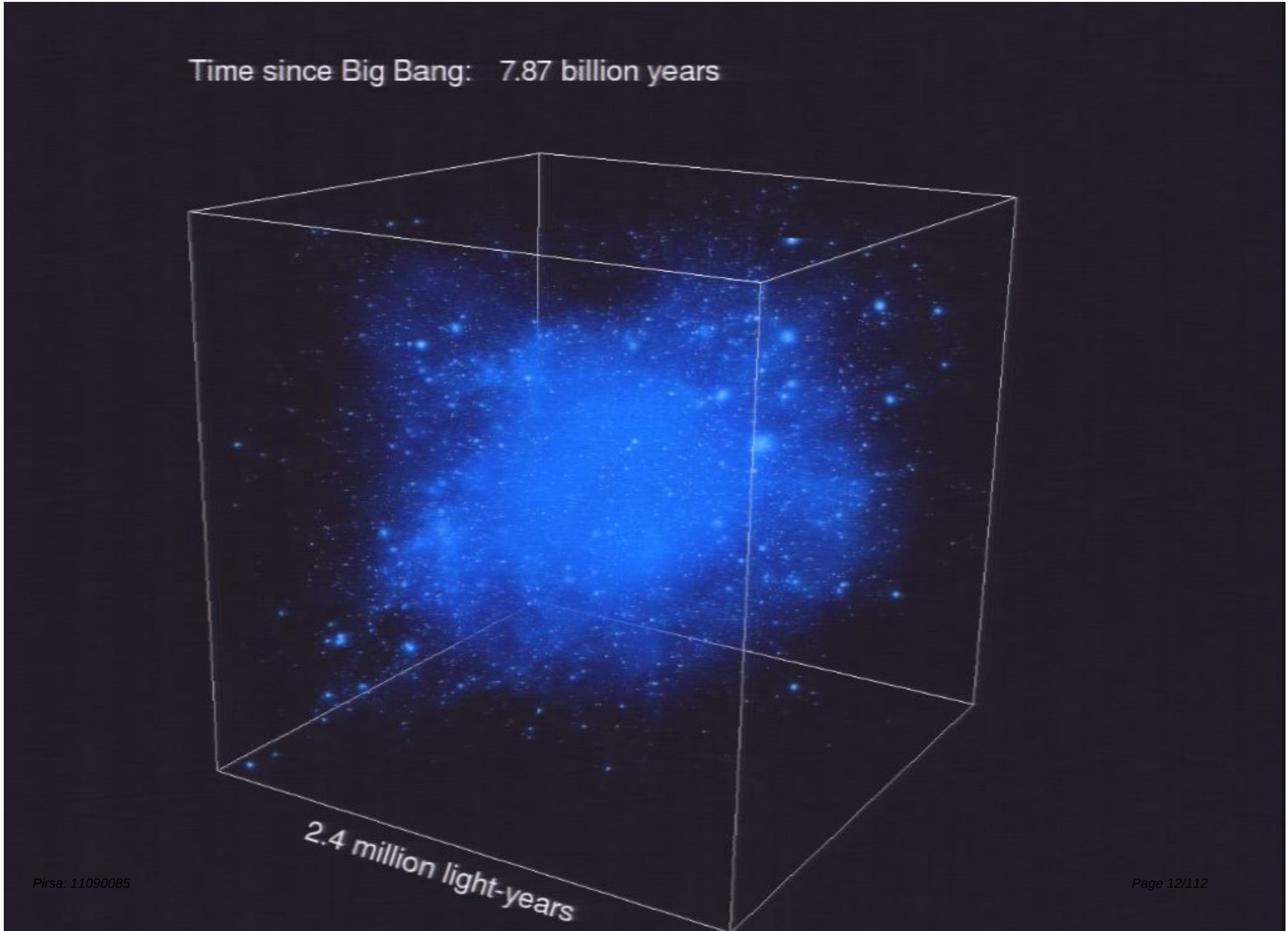
Time since Big Bang: 7.87 billion years
2.4 million light-years

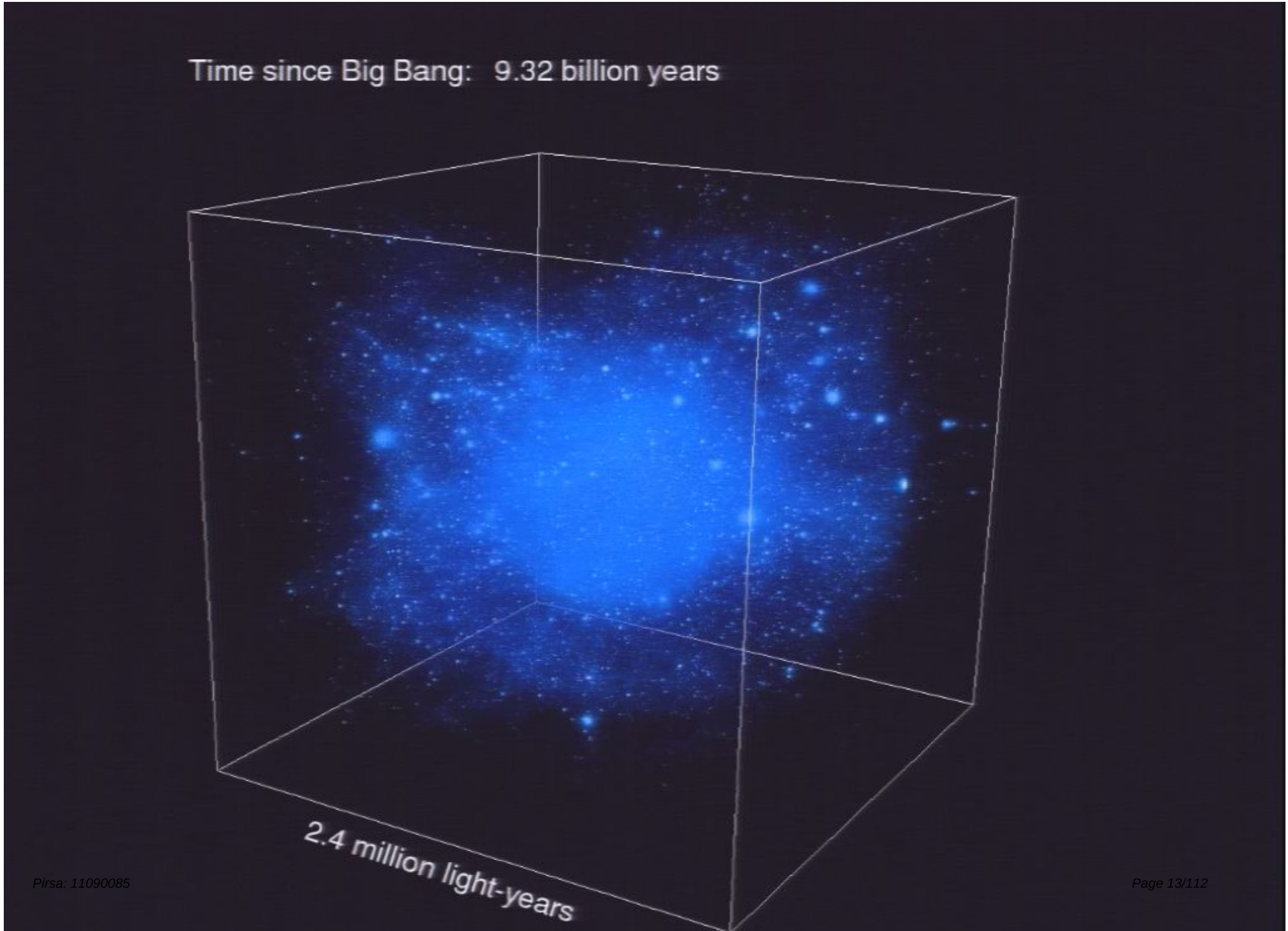
Time since Big Bang: 9.32 billion years
2.4 million light-years

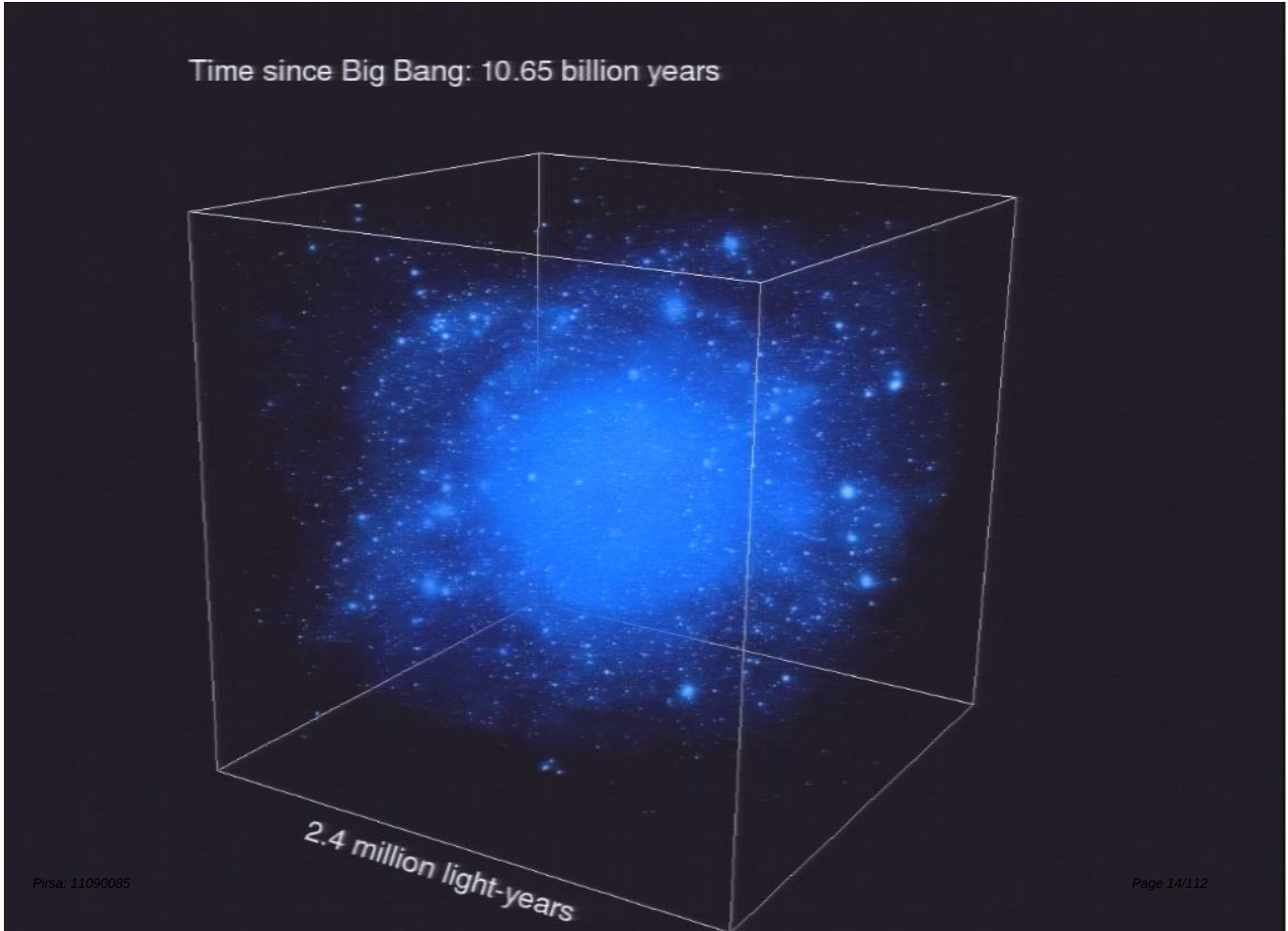
Time since Big Bang: 10.65 billion years
2.4 million light-years

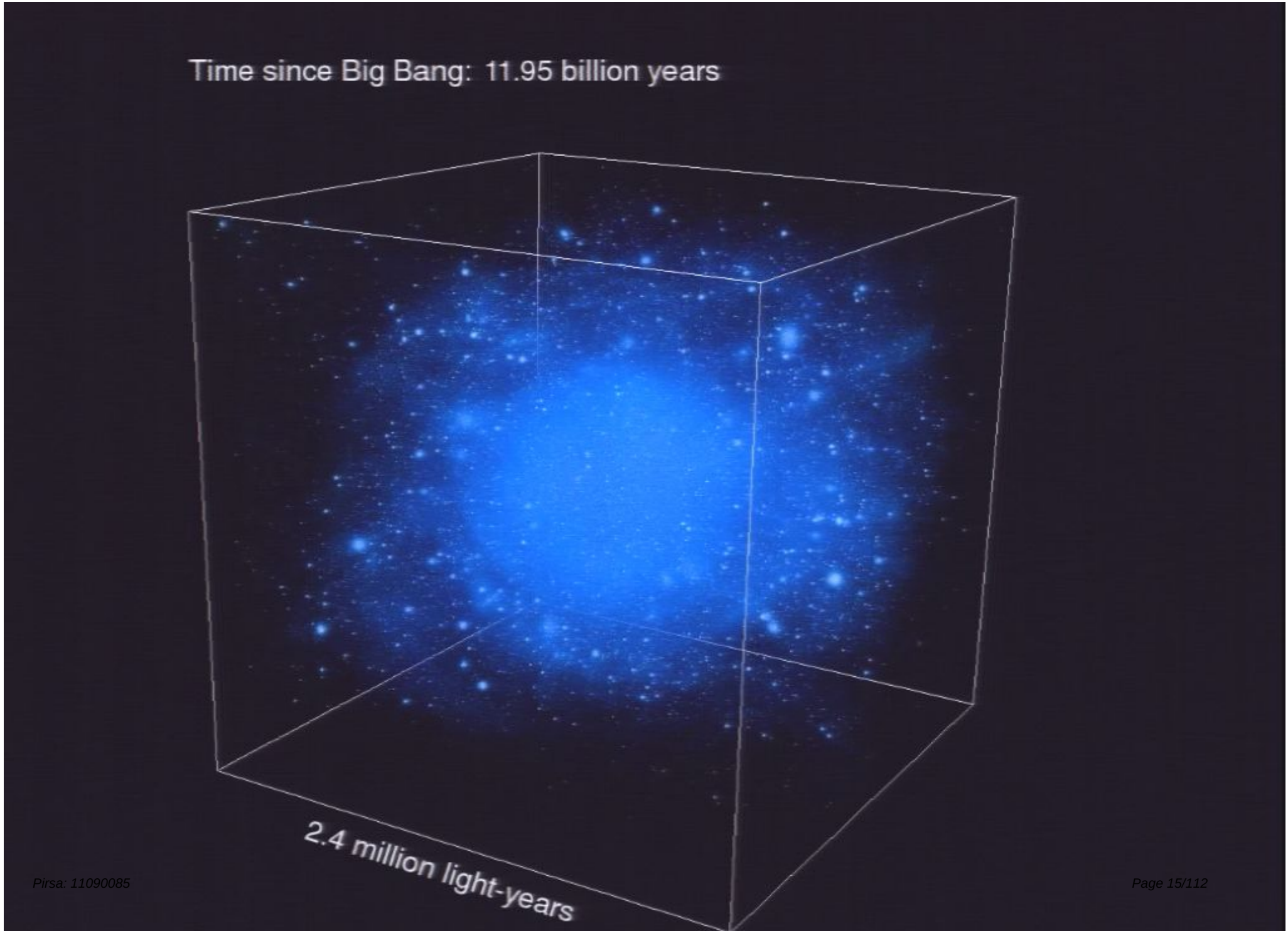
Time since Big Bang: 11.95 billion years
2.4 million light-years

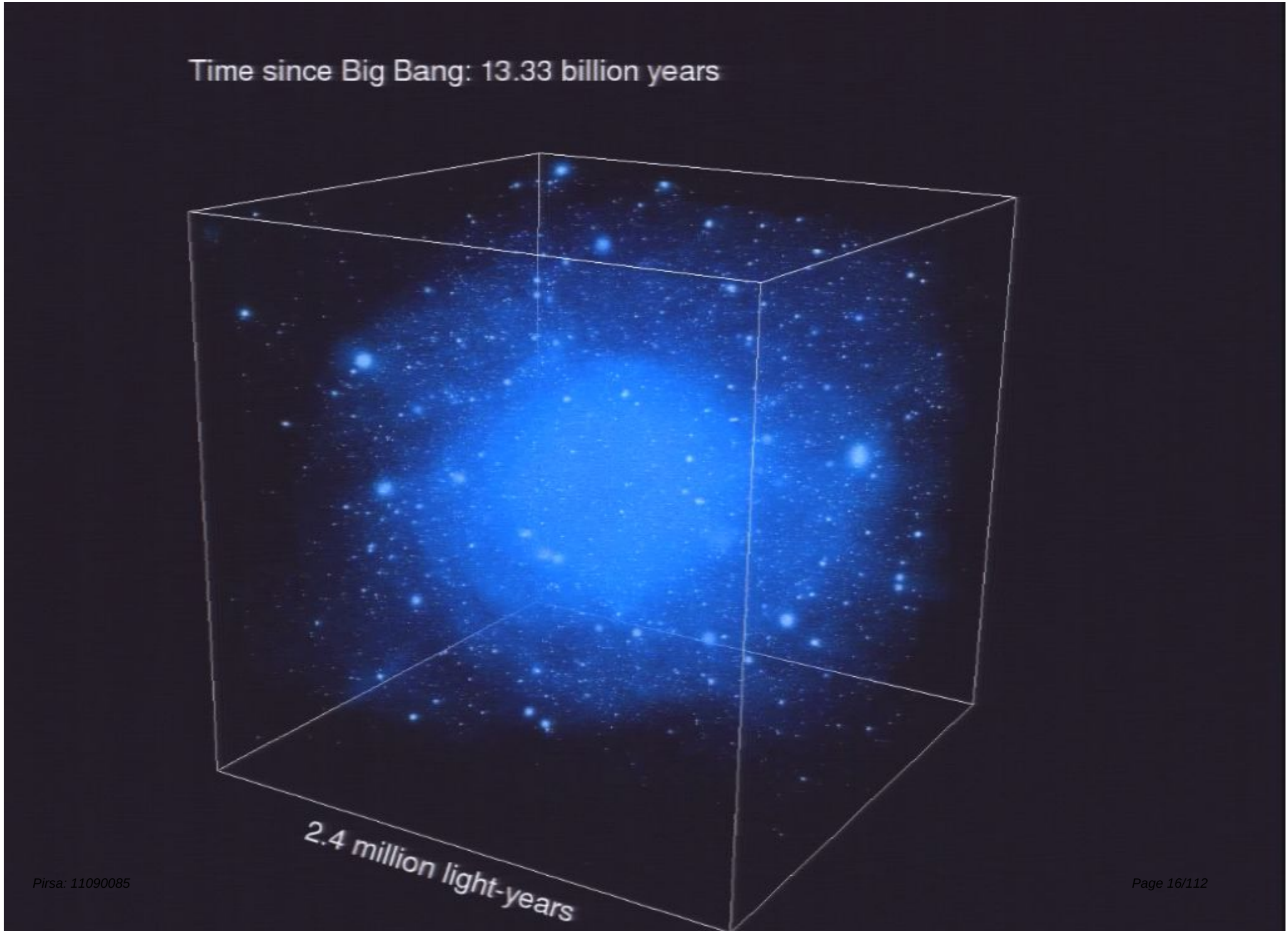
Time since Big Bang: 13.33 billion years
2.4 million light-years

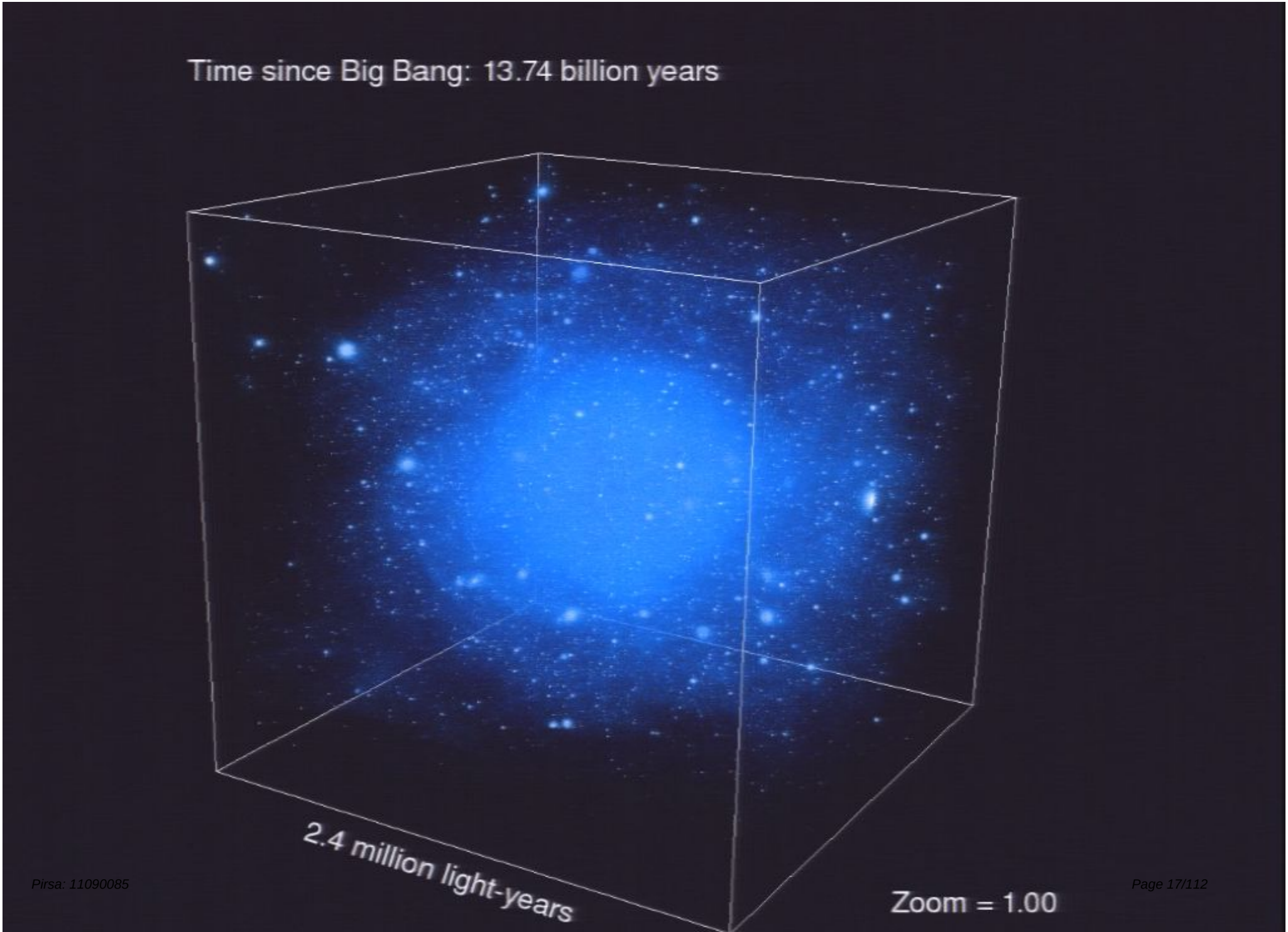
Time since Big Bang: 13.74 billion years
2.4 million light-years
Zoom = 1.00

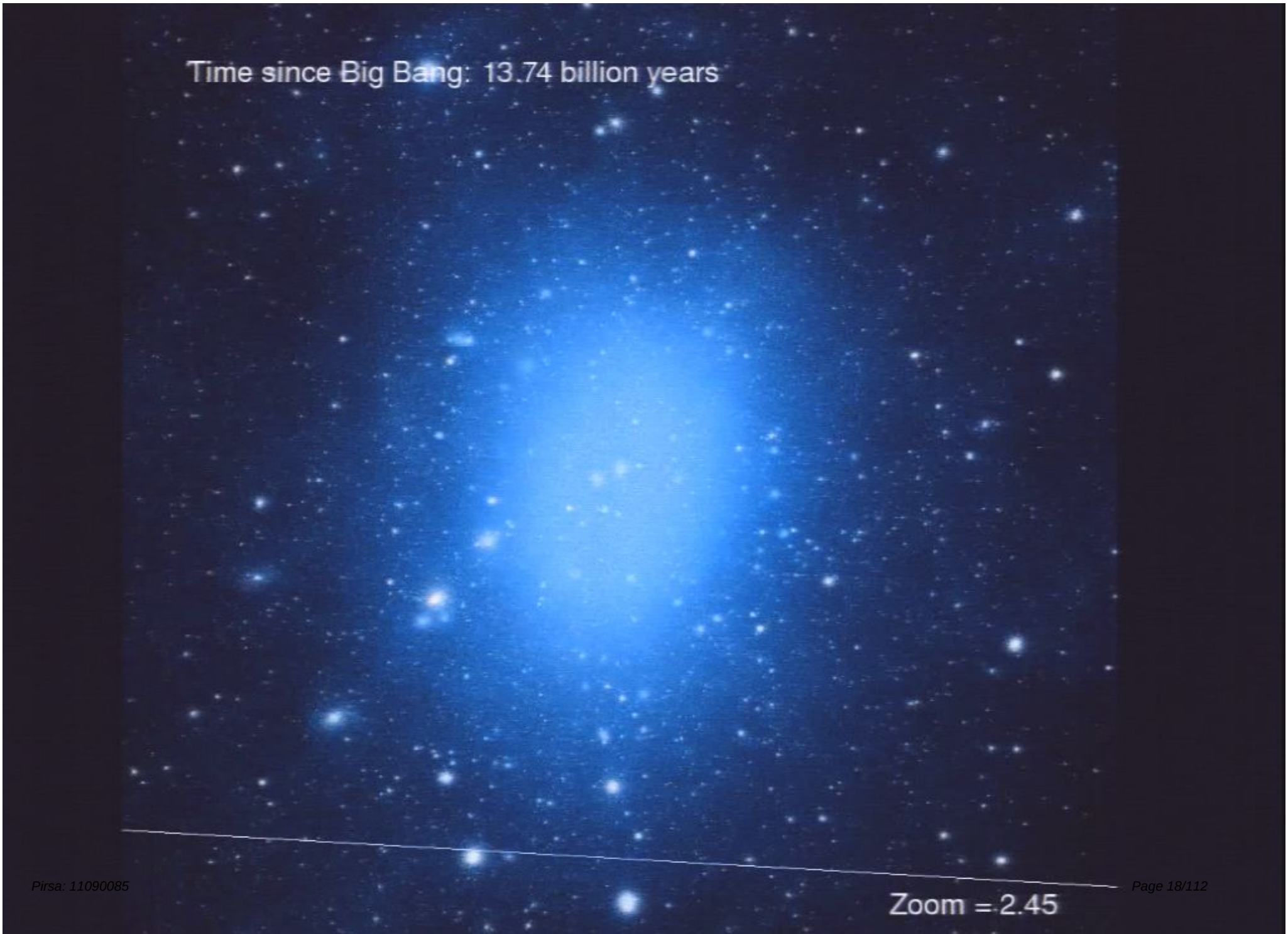
Time since Big Bang: 13.74 billion years
Zoom = 2.45

The Via Lactea Project

J. Diemand – M. Kuhlen – P. Madau

(& B. Moore, D. Potter, J. Stadel, M. Zemp)

GHALO
Stadel et al. (2009)
2.1 billion particles, 1,000 $M_\odot$

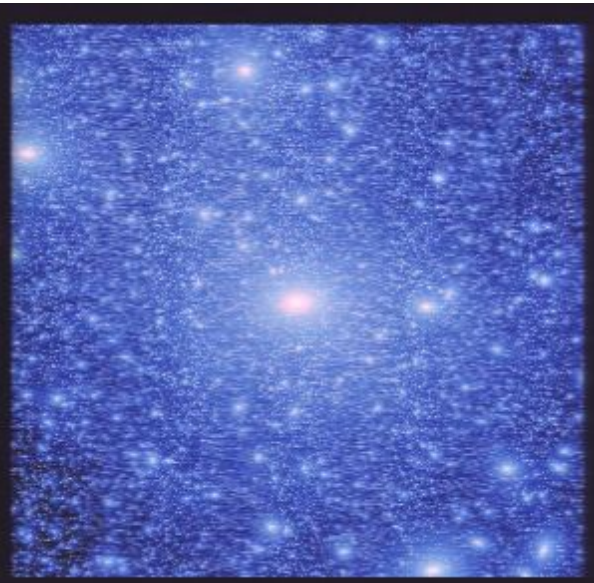

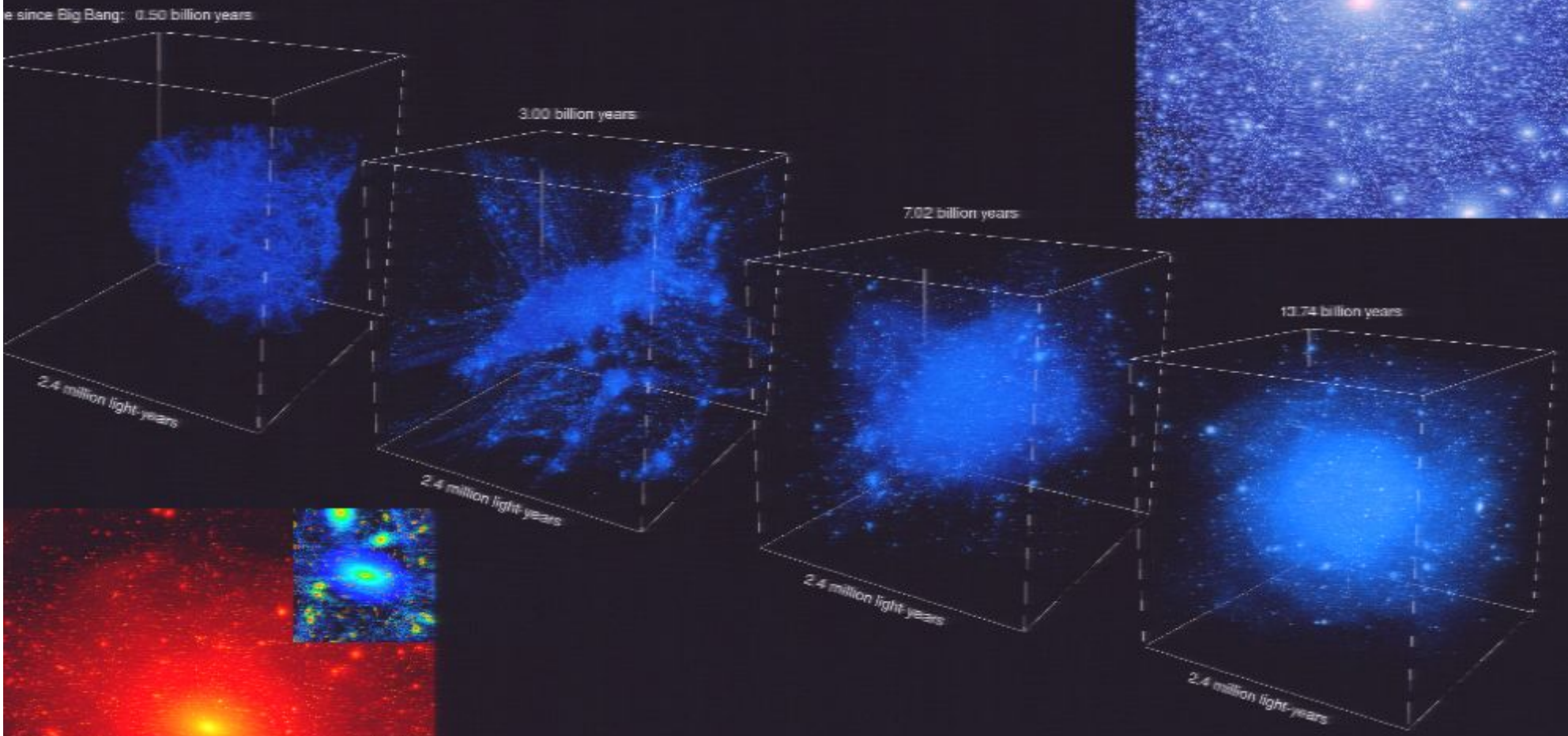

VIA LACTEA II
Diemand, Kuhlen et al. 2008
1.1 billion particles, 4,000 $M_\odot$

SciDAC
Scientific Discovery through Advanced Computing

Office of Science
INCITE
Advancing America's Science and Industrial Competitiveness

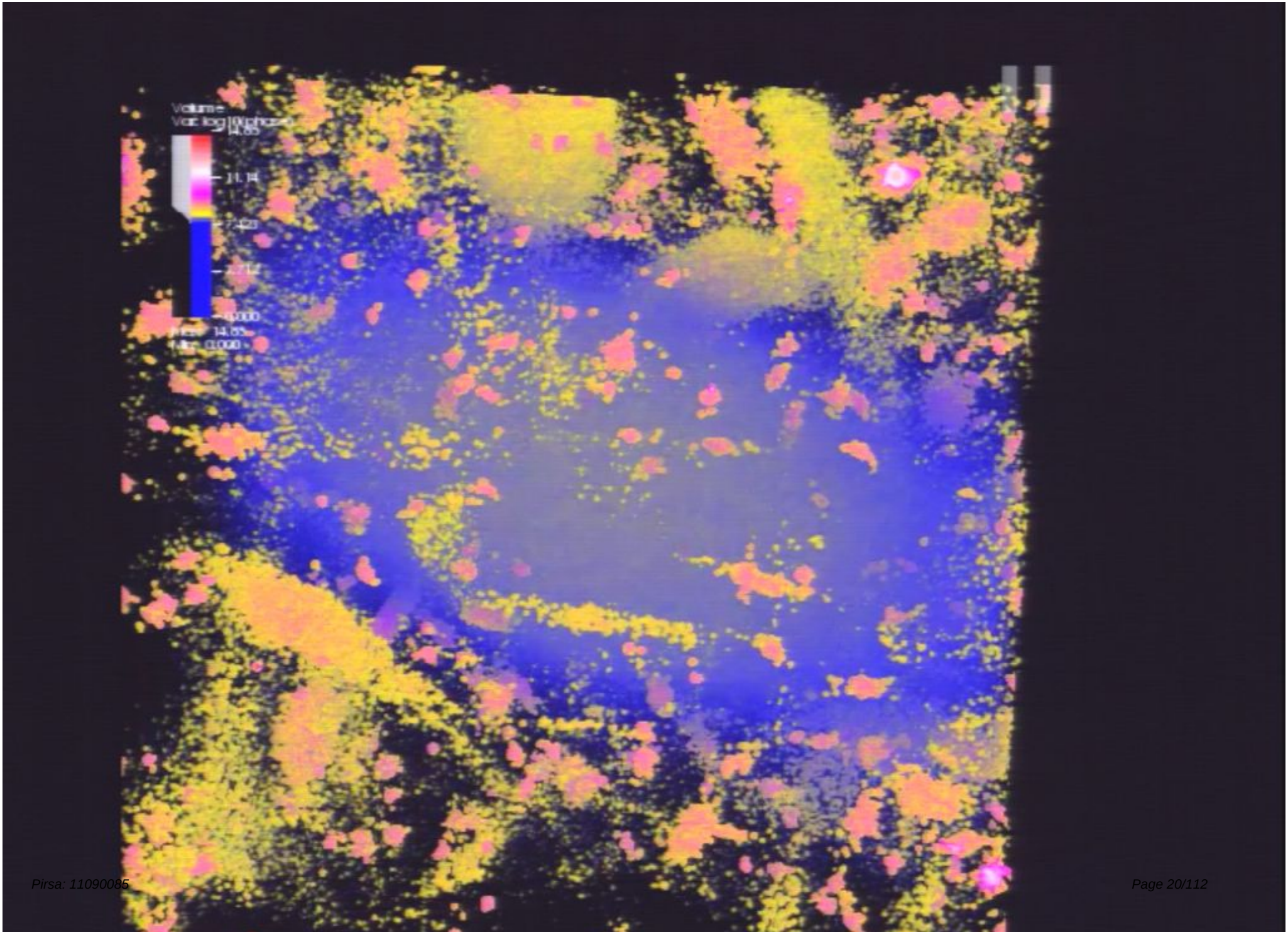
Volume
Var: log10(phase)
14.85
11.14
7.428
3.714
0.000
Min: 14.85
Max: 0.000

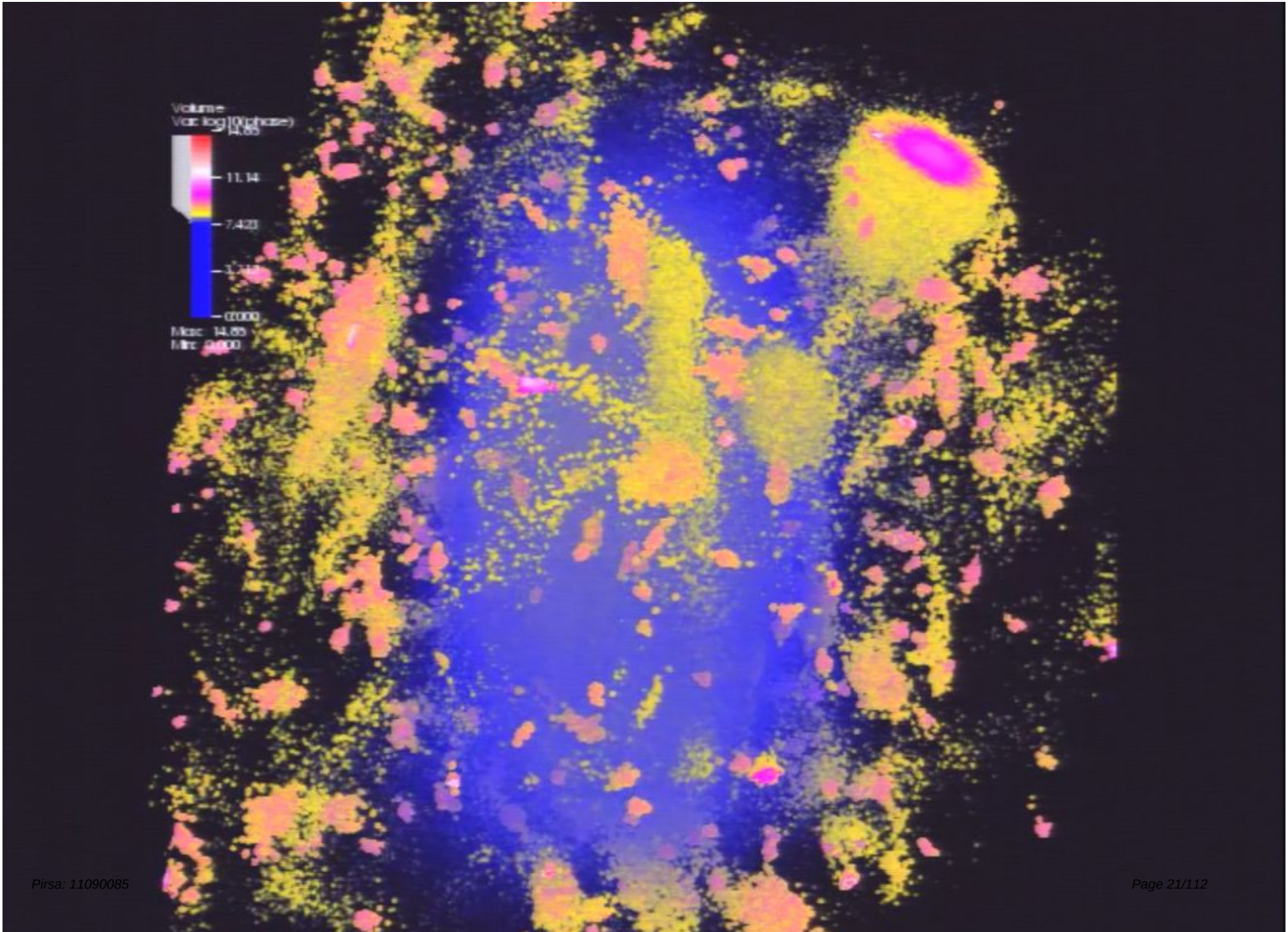
Volume
Var: log10(phase)
14.85
11.14
7.423
3.711
0.000
Max: 14.85
Min: 0.000

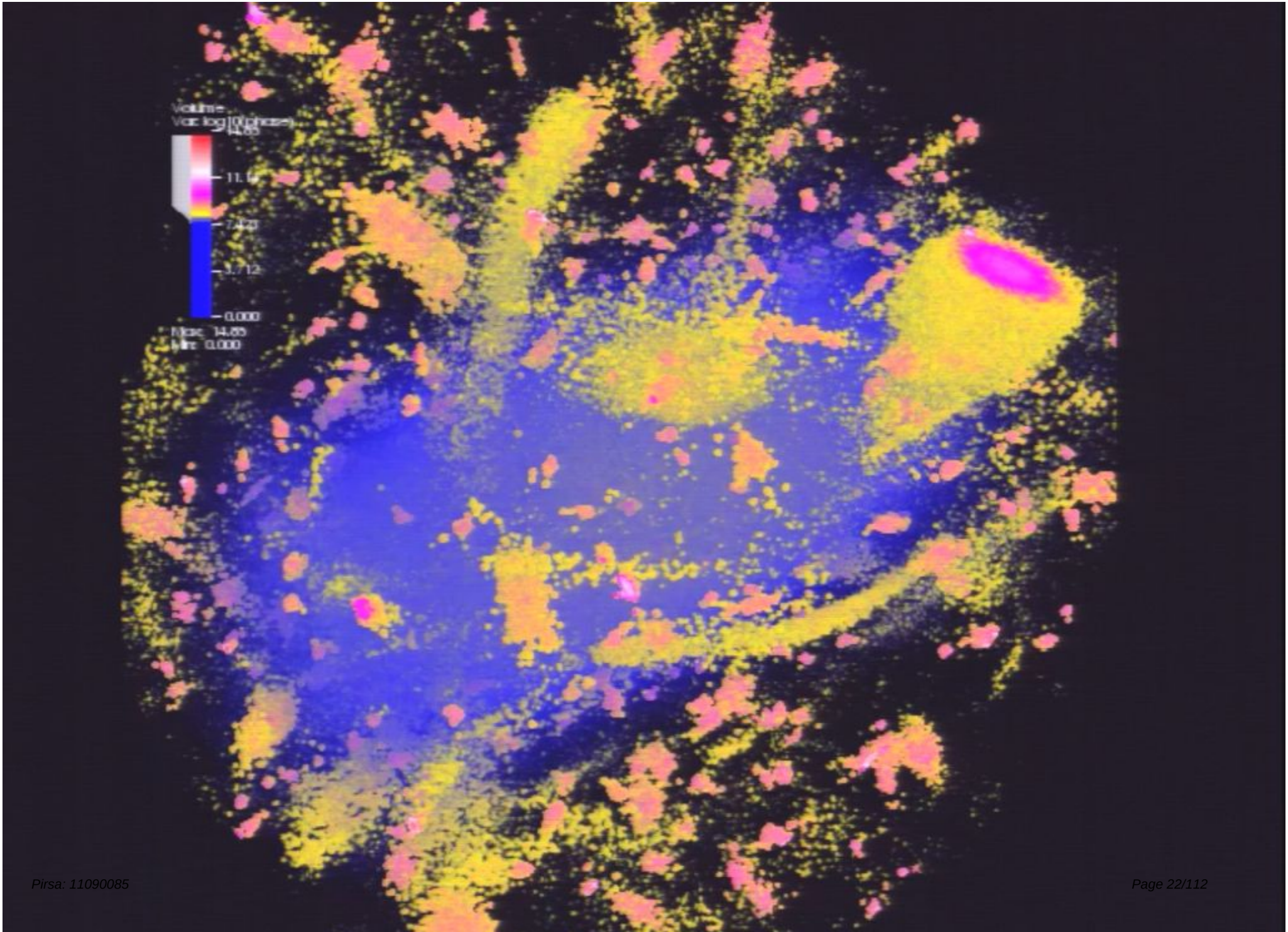
Volume
Var: log10(mass)
14.85
11.14
7.429
3.712
0.000
Max: 14.85
Min: 0.000

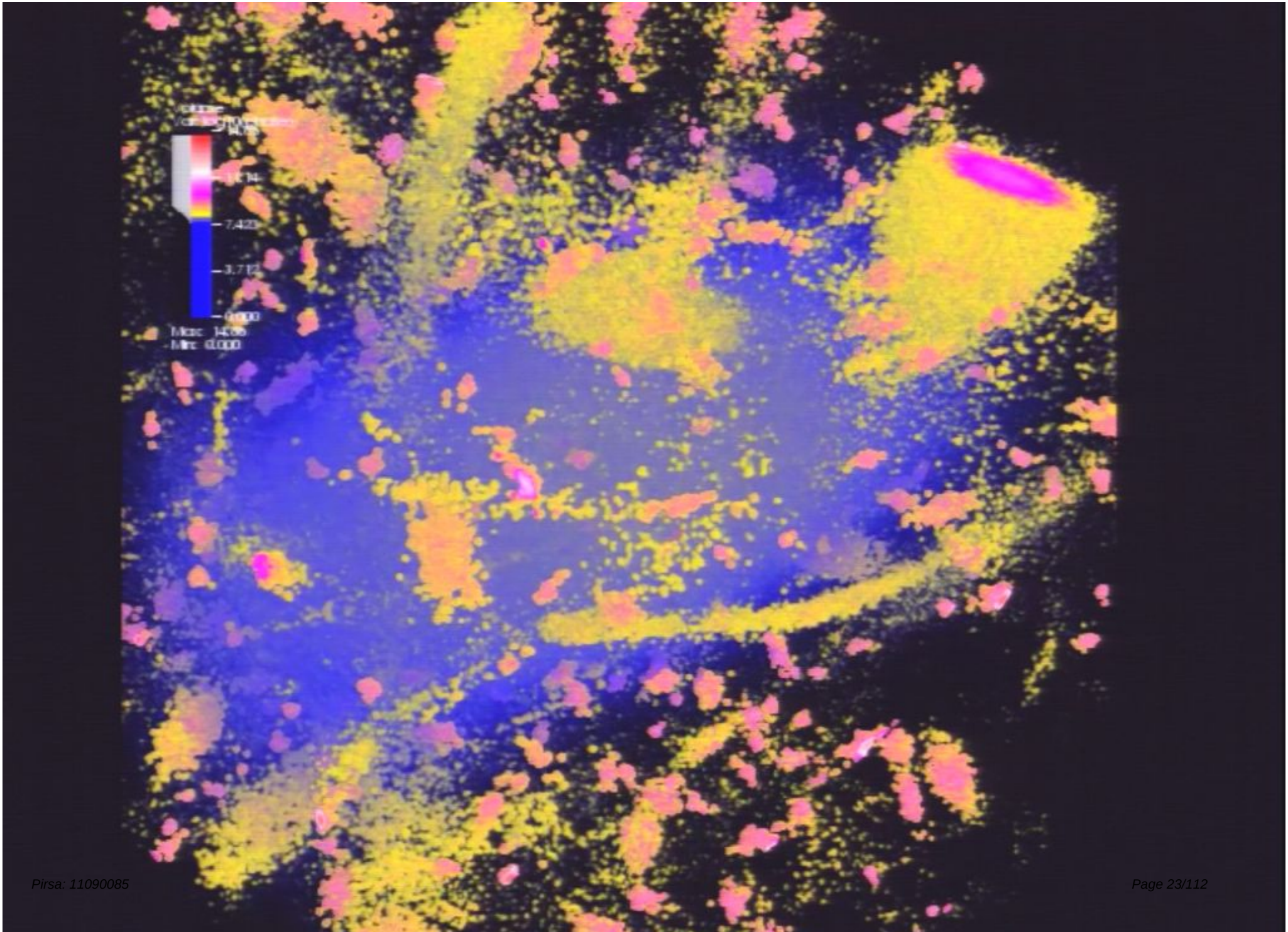
7.422
3.711
0.000
Max: 14.85
Min: 0.000

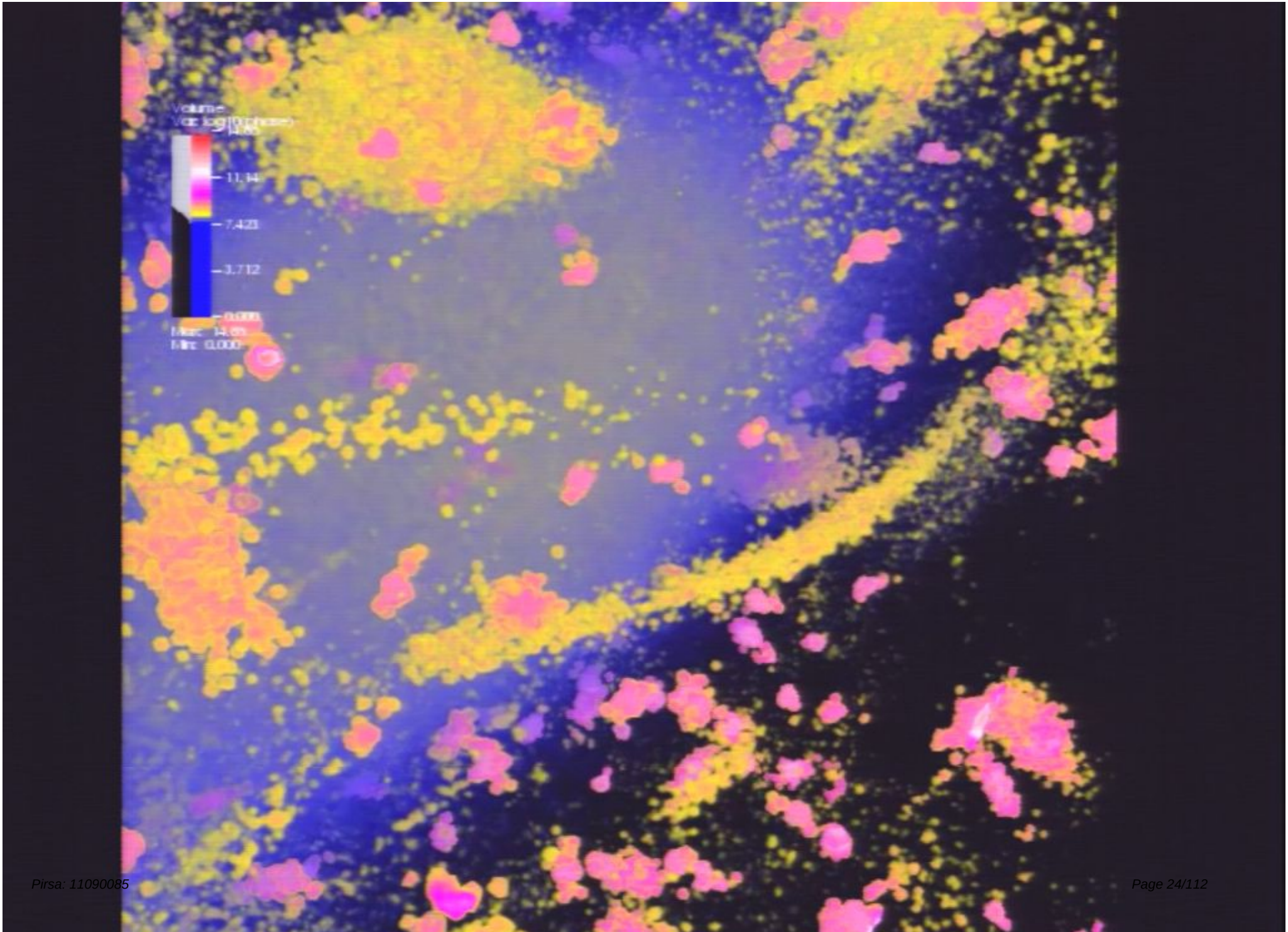
11.14
7.423
3.712

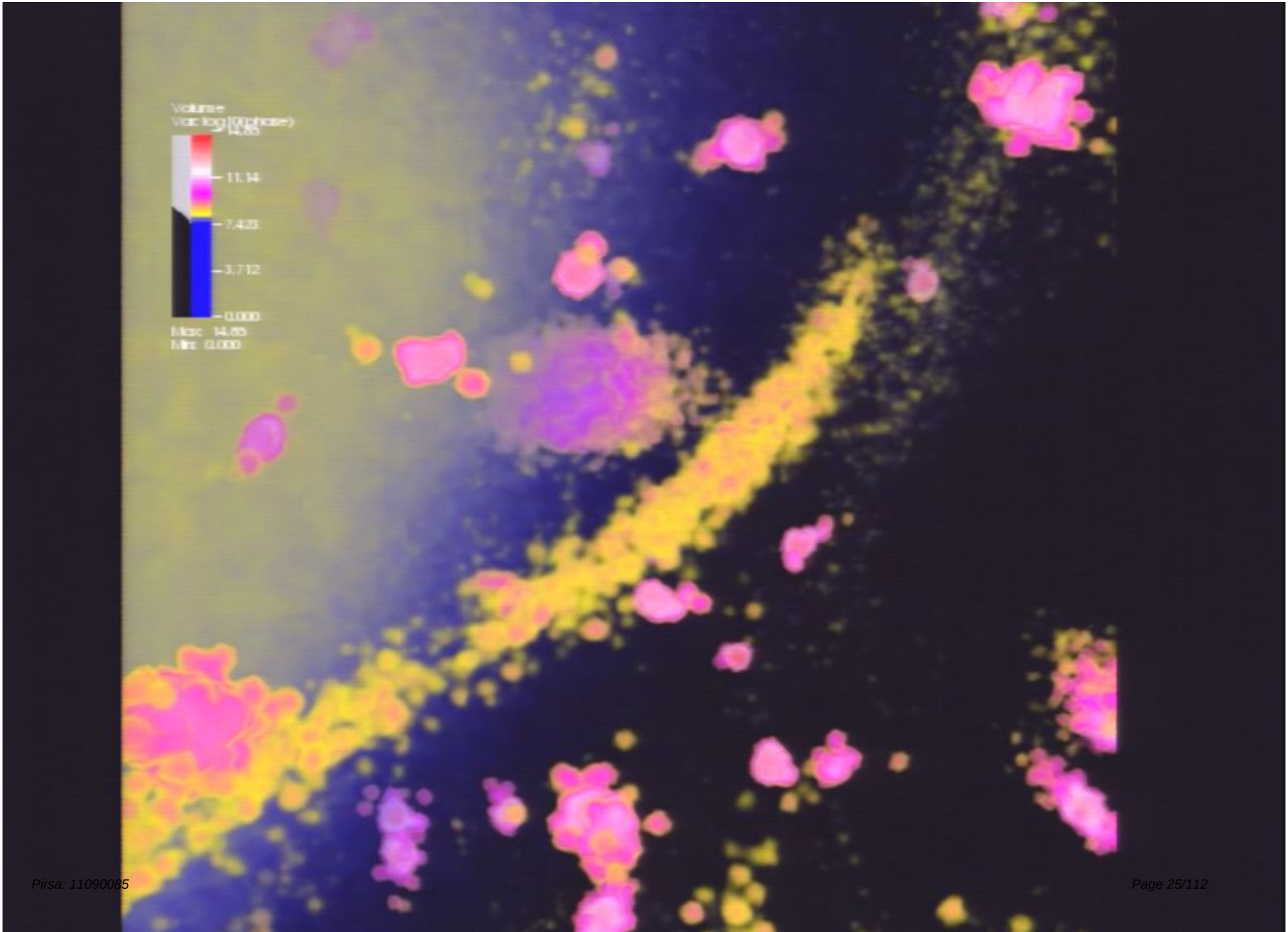
Volume
Vorticity (Magnitude)
14.85
11.14
7.423
3.712
0.000
Max: 14.85
Min: 0.000

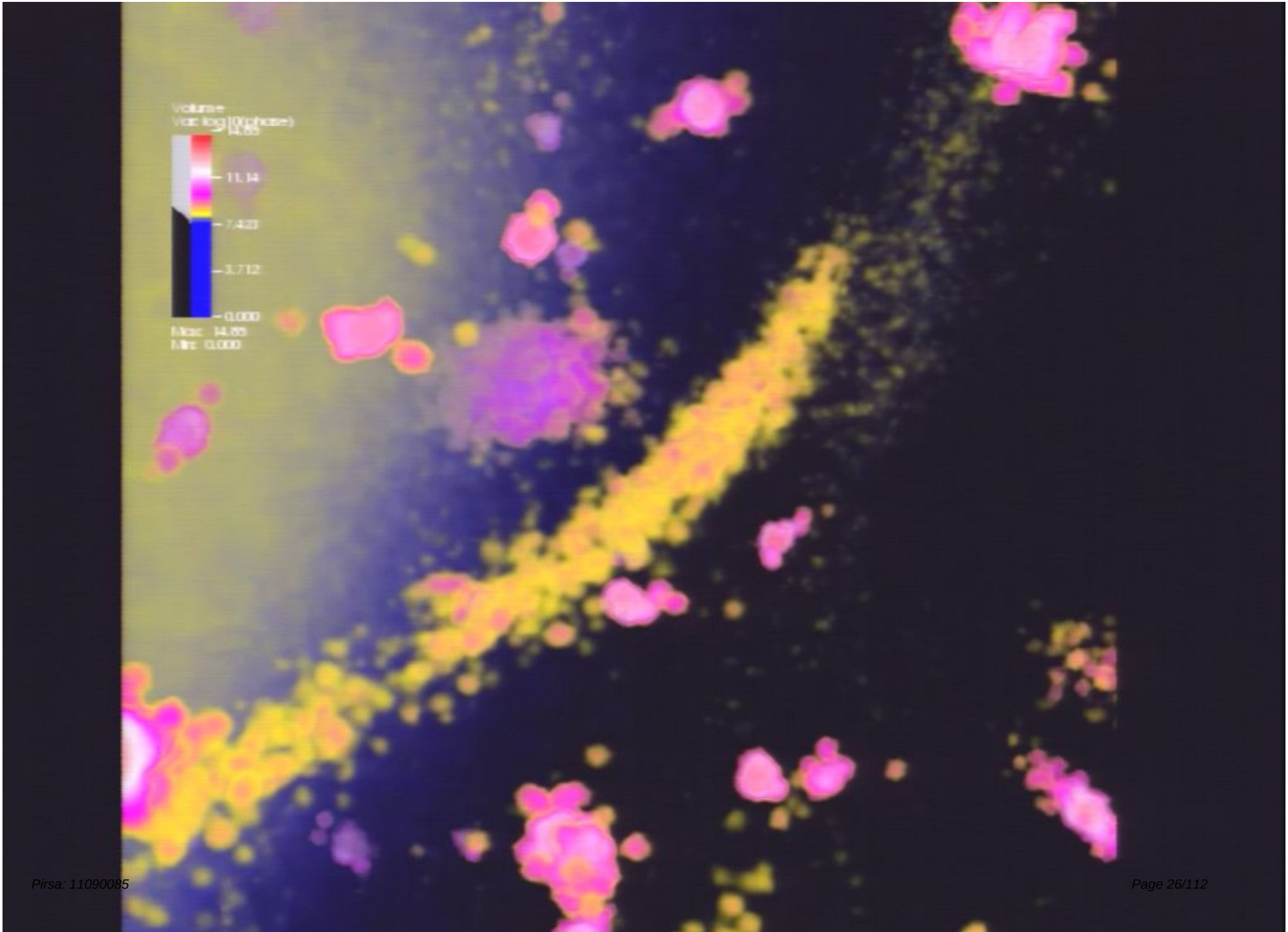
Volume
Vort.log(Orphase)
14.85
11.14
7.423
3.712
0.000
Max: 14.85
Min: 0.000

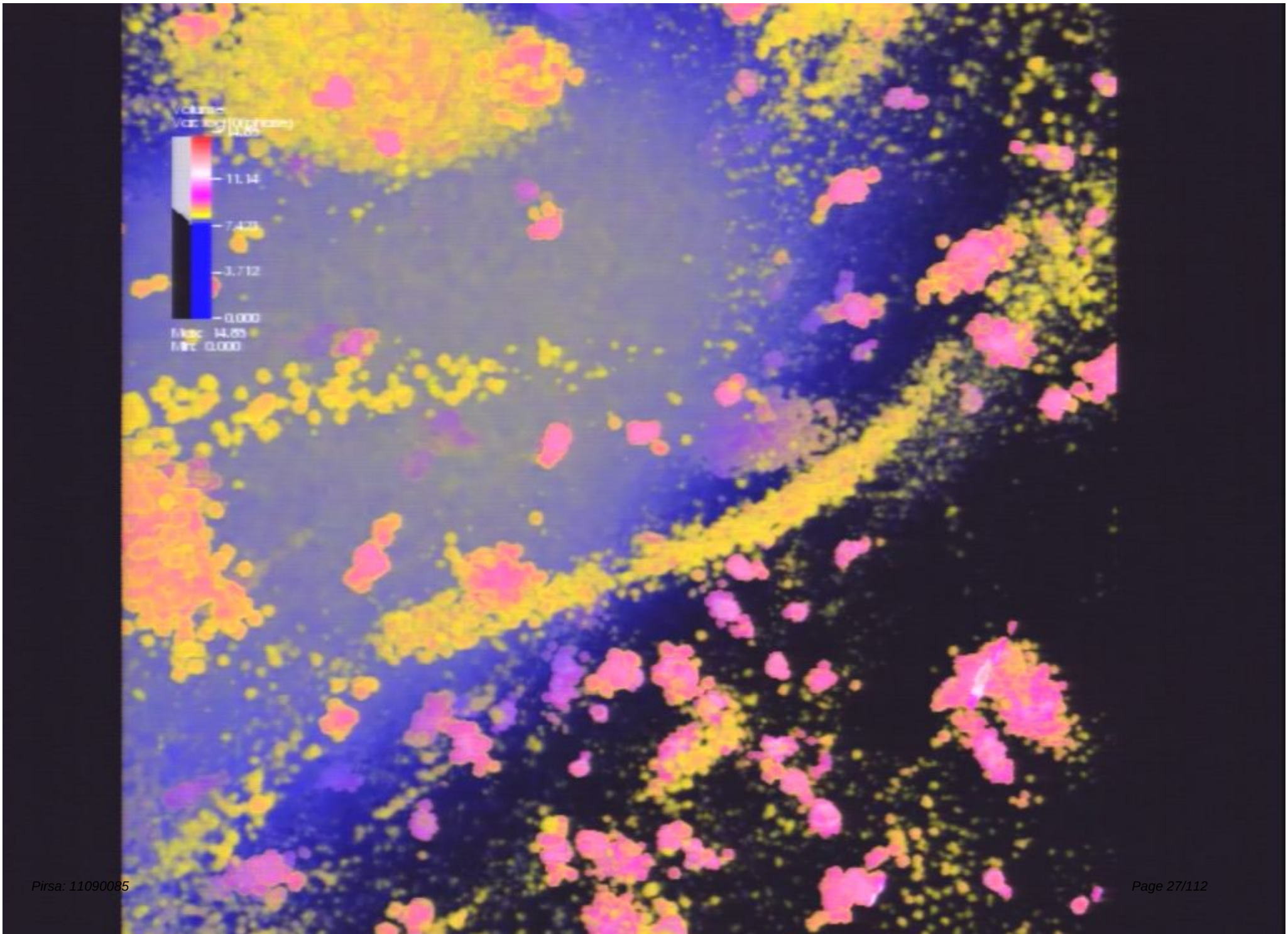
11.14
7.428
3.712
0.000

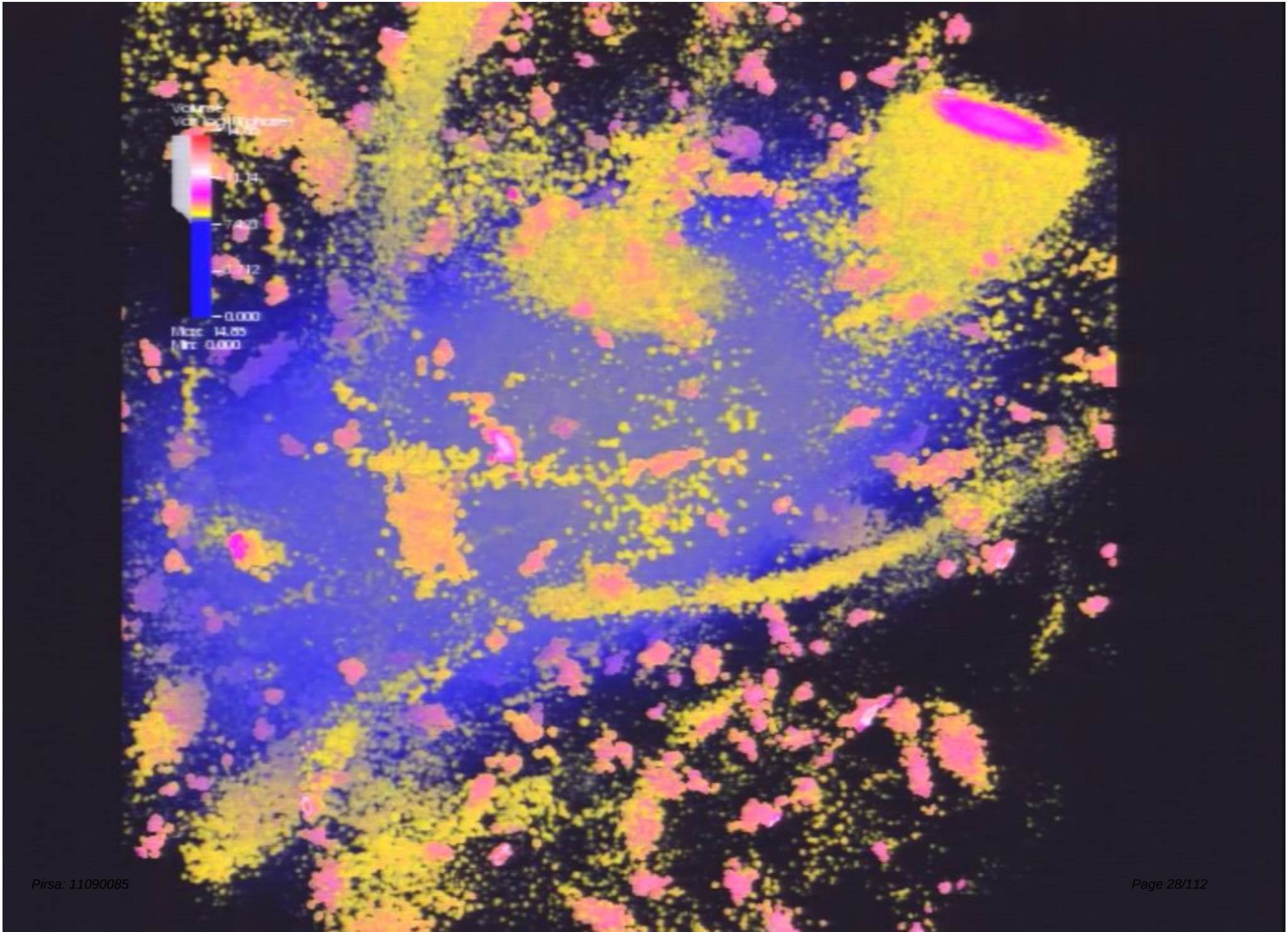
0.000
Max: 14.85
Min: 0.000

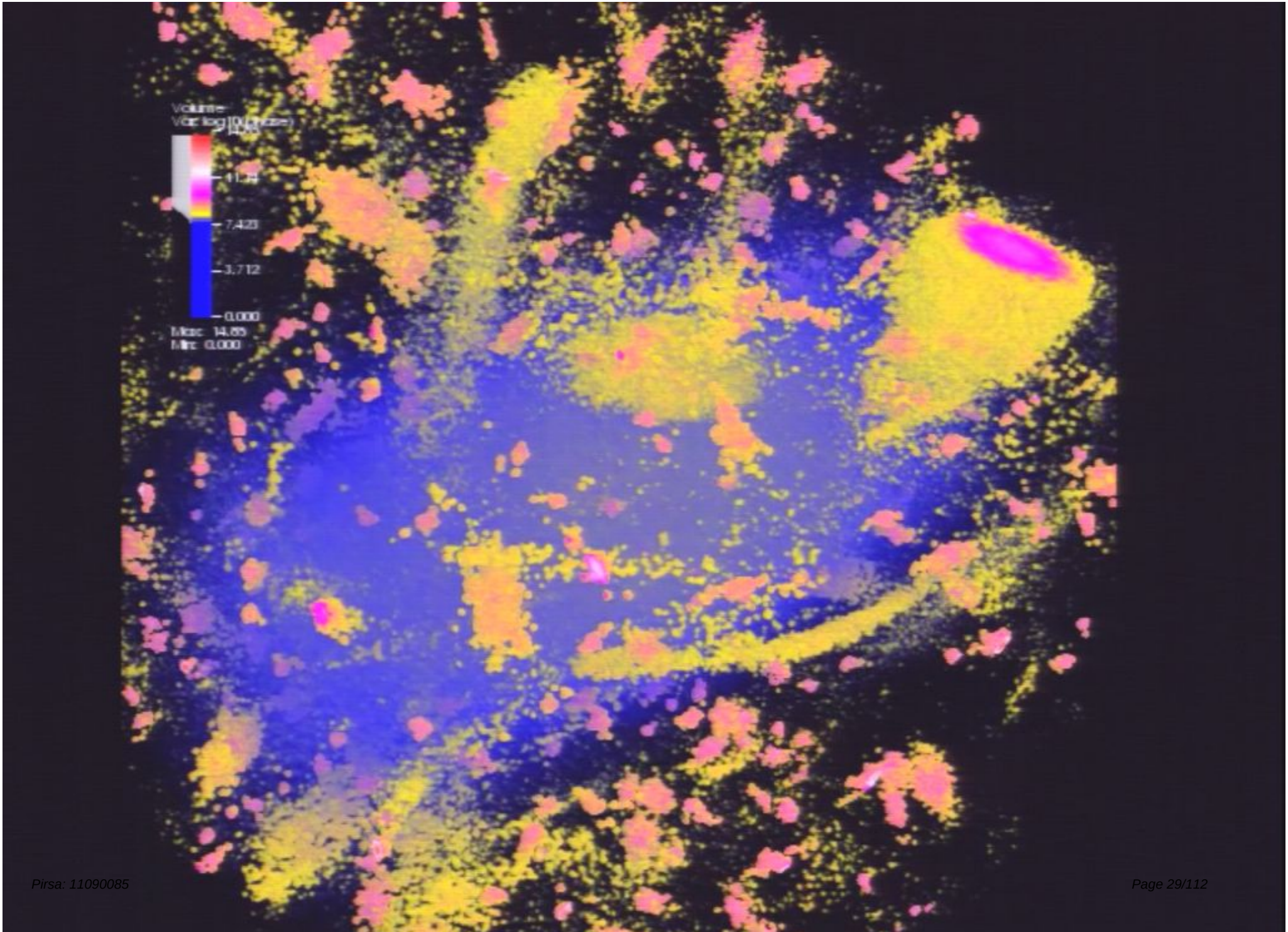
Volume
Vor log10(Vorm)
11.24
7.428
3.712
0.000
Max: 14.85
Min: 0.000

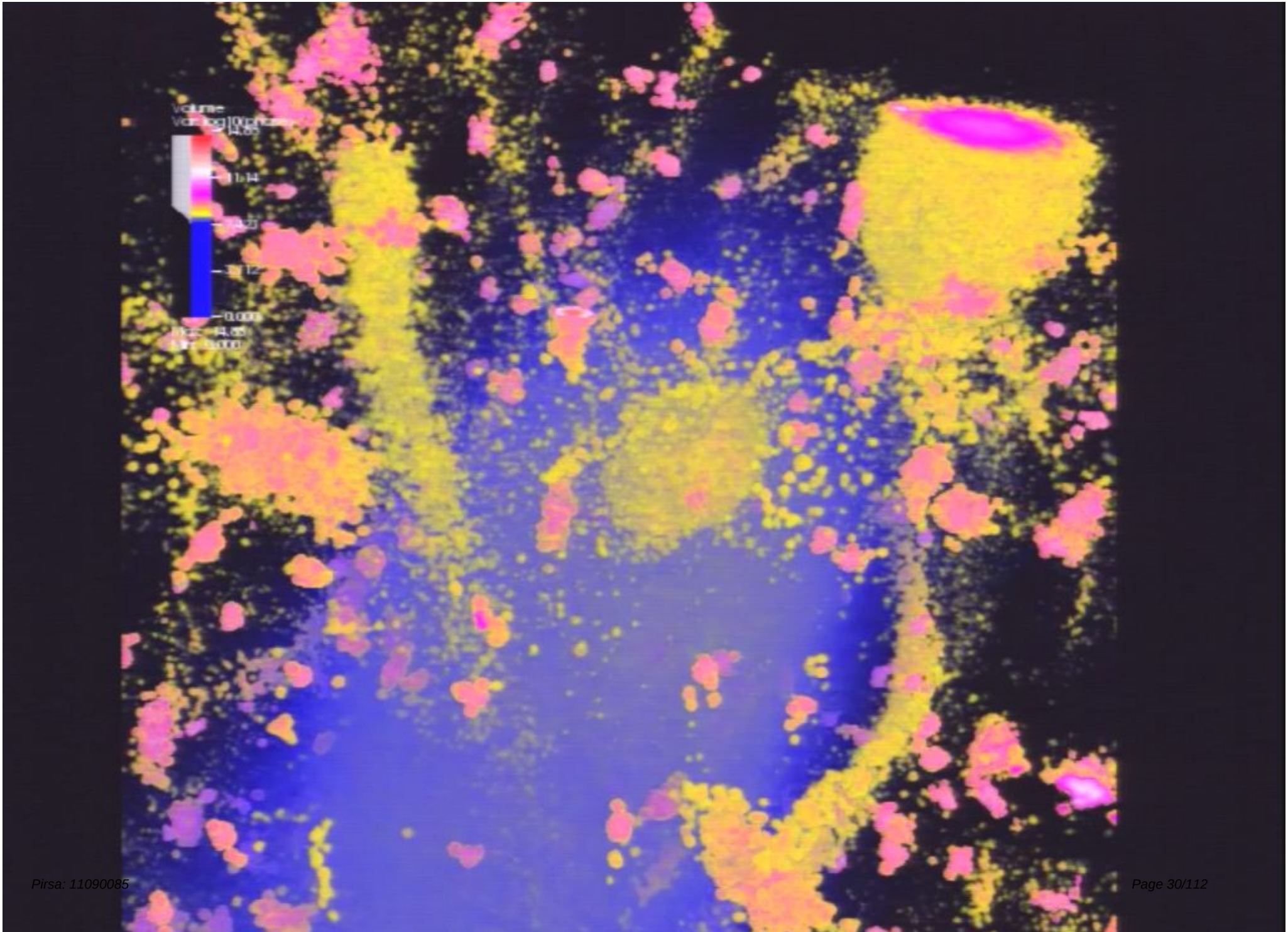

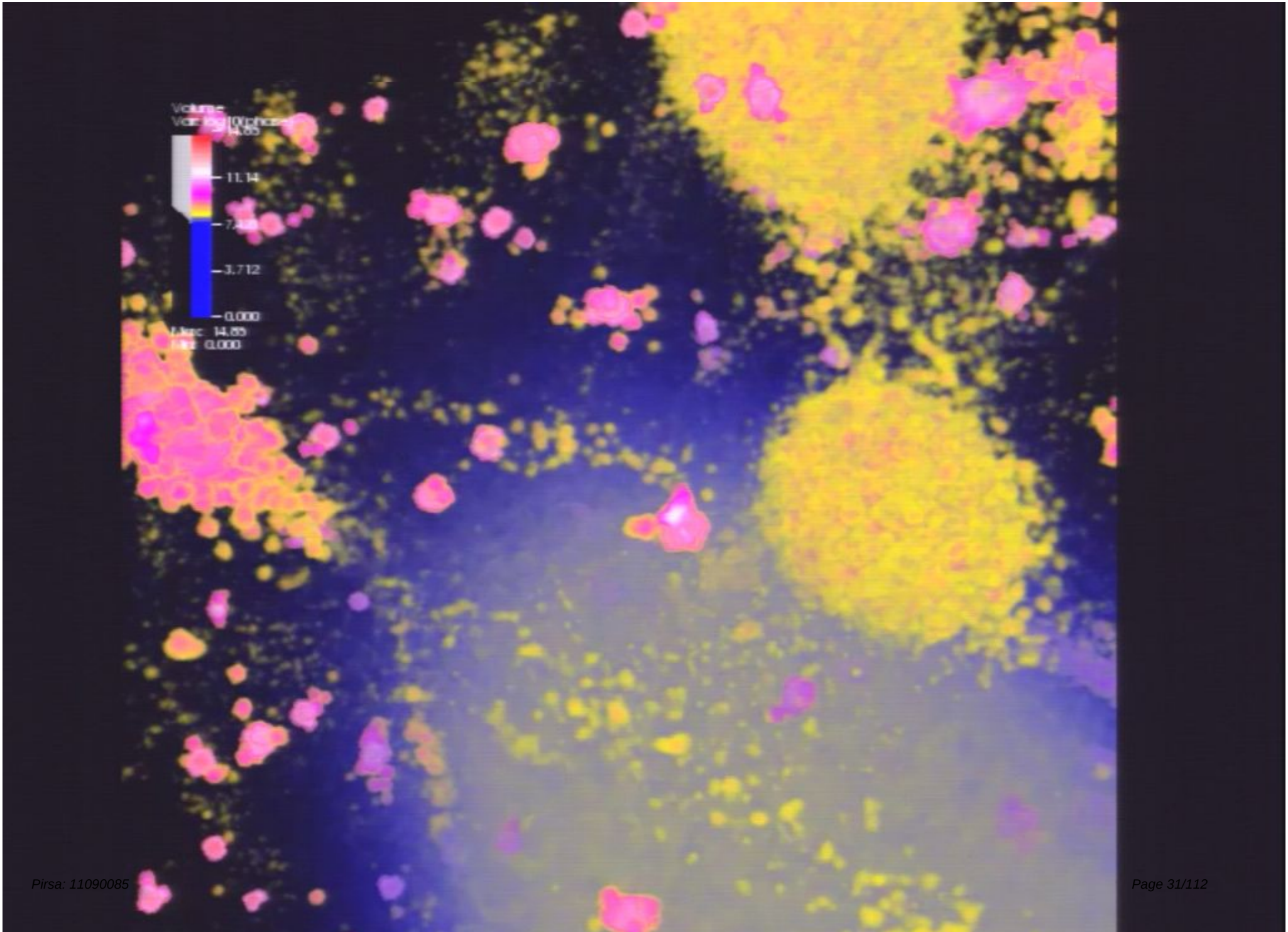
11.14
3.712
0.000

The Via Lactea Project

J. Diemand – M. Kuhlen – P. Madau

(& B. Moore, D. Potter, J. Stadel, M. Zemp)

GHALO
Stadel et al. (2009)
2.1 billion particles, 1,000 $M_\odot$

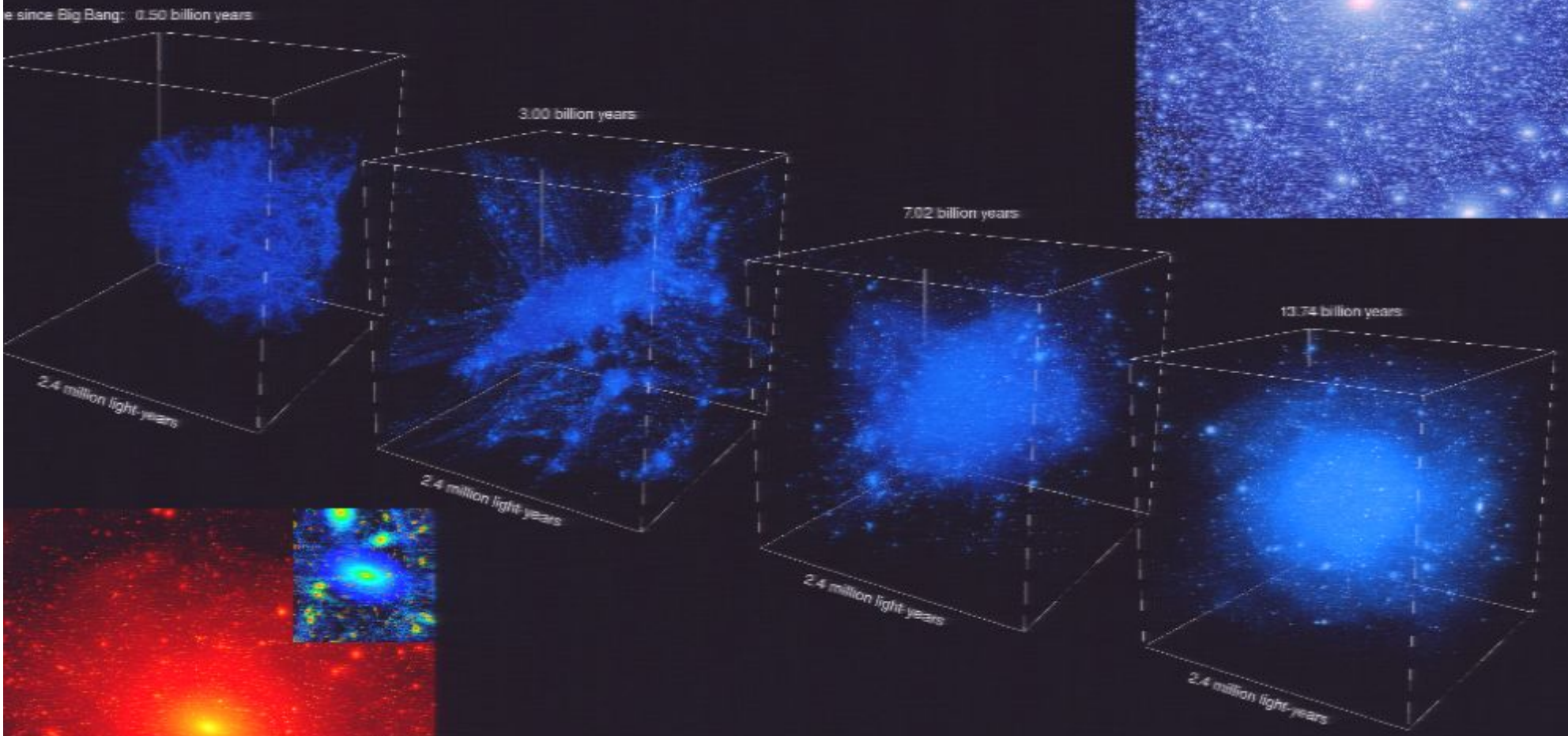

VIA LACTEA II
Diemand, Kuhlen et al. 2008
1.1 billion particles, 4,000 $M_\odot$

SciDAC
Scientific Discovery through Advanced Computing

Office of Science
INCITE
Advancing America's Science and Industrial Competitiveness

The Via Lactea Project

J. Diemand – M. Kuhlen – P. Madau

(& B. Moore, D. Potter, J. Stadel, M. Zemp)

GHALO
Stadel et al. (2009)
2.1 billion particles, 1,000 $M_\odot$

Via Lactea Series

Name	$N_{\rm hires}$	$M_{\rm hires}$	z_i	z_f	cosmology	r_{200}	M_{200}	$V_{\rm max}$	Nsub
VL-II	1.09×10^9	$4.1 \times 10^3 M_\odot$	104.3	0	WMAP-3	402 kpc	$1.93 \times 10^{12} M_\odot$	201 km/s	53,653
VL-I	2.34×10^8	$2.1 \times 10^4 M_\odot$	48.8	0	WMAP-3	389 kpc	$1.77 \times 10^{12} M_\odot$	181 km/s	9,224
1e8Ell	1.36×10^8	$1.8 \times 10^5 M_\odot$	59.5	0.49	WMAP-1	512 kpc	$1.34 \times 10^{13} M_\odot$	390 km/s	16,111
VL-IIm	2×10^7	$2.6 \times 10^5 M_\odot$	104.3	0	WMAP-3	402 kpc	$1.93 \times 10^{12} M_\odot$	201 km/s	$\sim 1,500$

GHALO Series

Name	$N_{\rm hires}$	$M_{\rm hires}$	z_i	z_f	cosmology	r_{200}	M_{200}	$V_{\rm max}$	Nsub
$\rm GHALO_2$	2.1×10^9	$1,000 M_\odot$	48.8	0	WMAP-3	347 kpc	$1.3 \times 10^{12} M_\odot$	153 km/s	$\sim 10^5$
$\rm GHALO_3$	$\sim 10^8$	$2.7 \times 10^4 M_\odot$	48.8	0	WMAP-3	347 kpc	$1.3 \times 10^{12} M_\odot$	150 km/s	$\sim 2,500$
$\rm GHALO_4$	$\sim 5 \times 10^6$	$7.3 \times 10^5 M_\odot$	48.8	0	WMAP-3	347 kpc	$1.3 \times 10^{12} M_\odot$	150 km/s	–

Silver River

Name	$N_{\rm hires}$	$M_{\rm hires}$	z_i	z_f	cosmology	r_{200}	M_{200}	$V_{\rm max}$	Nsub
SR1	50×10^9	$100 M_\odot$	180	currently at $z = 6.3$	WMAP-7	-	-	-	-

VIA LACTEA II
Diemand, Kuhlen et al. 2008
1.1 billion particles, 4,000 $M_\odot$

SciDAC
Scientific Discovery through Advanced Computing

Office of Science
INCITE
Advancing America's Science and Industrial Competitiveness

Tidal Interactions with the Host Halo

Hayashi et al.(2003), Kravtsov et al. (2004), etc., etc.

- Subhalos orbit through host halo and are subject to tidal interactions.
- Strongest during peri-center passage.
- Tidal mass loss from outside in.
- Diverse amount of tidal mass loss.

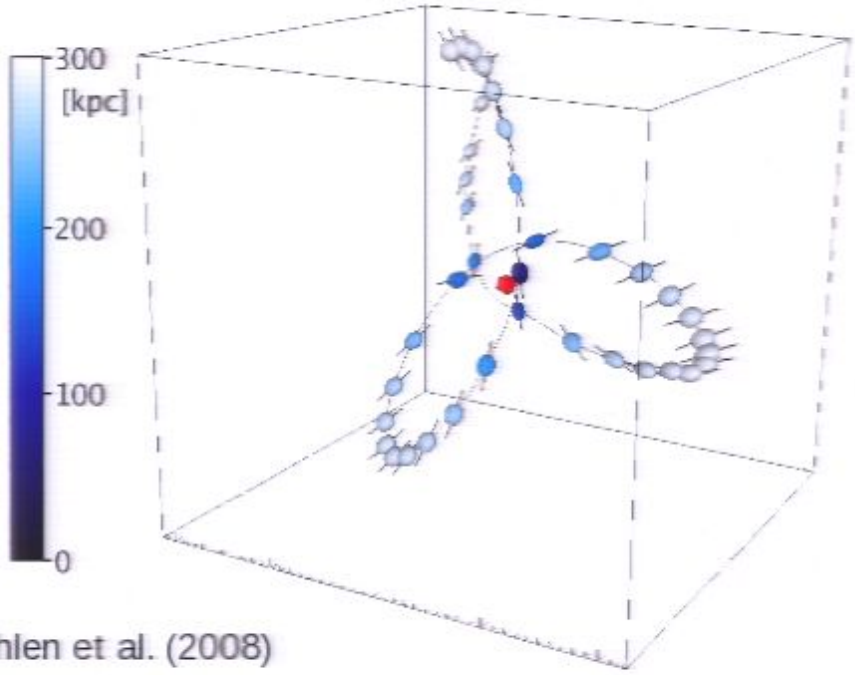

Kuhlen et al. (2008)

Diemand, Kuhlen, et al. (2008)

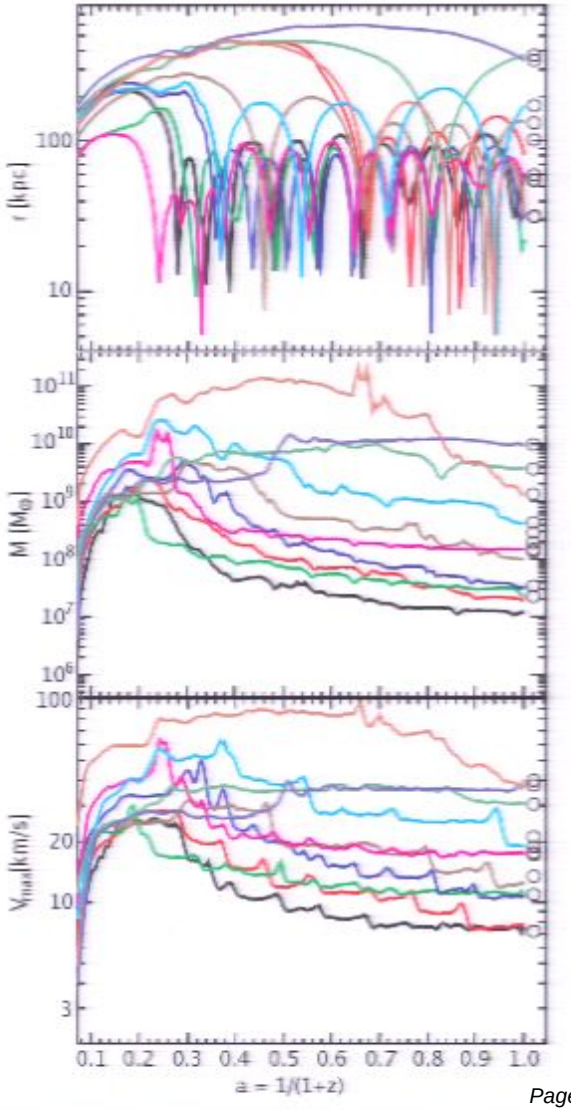

Velocity Space Substructure and Direct Detection

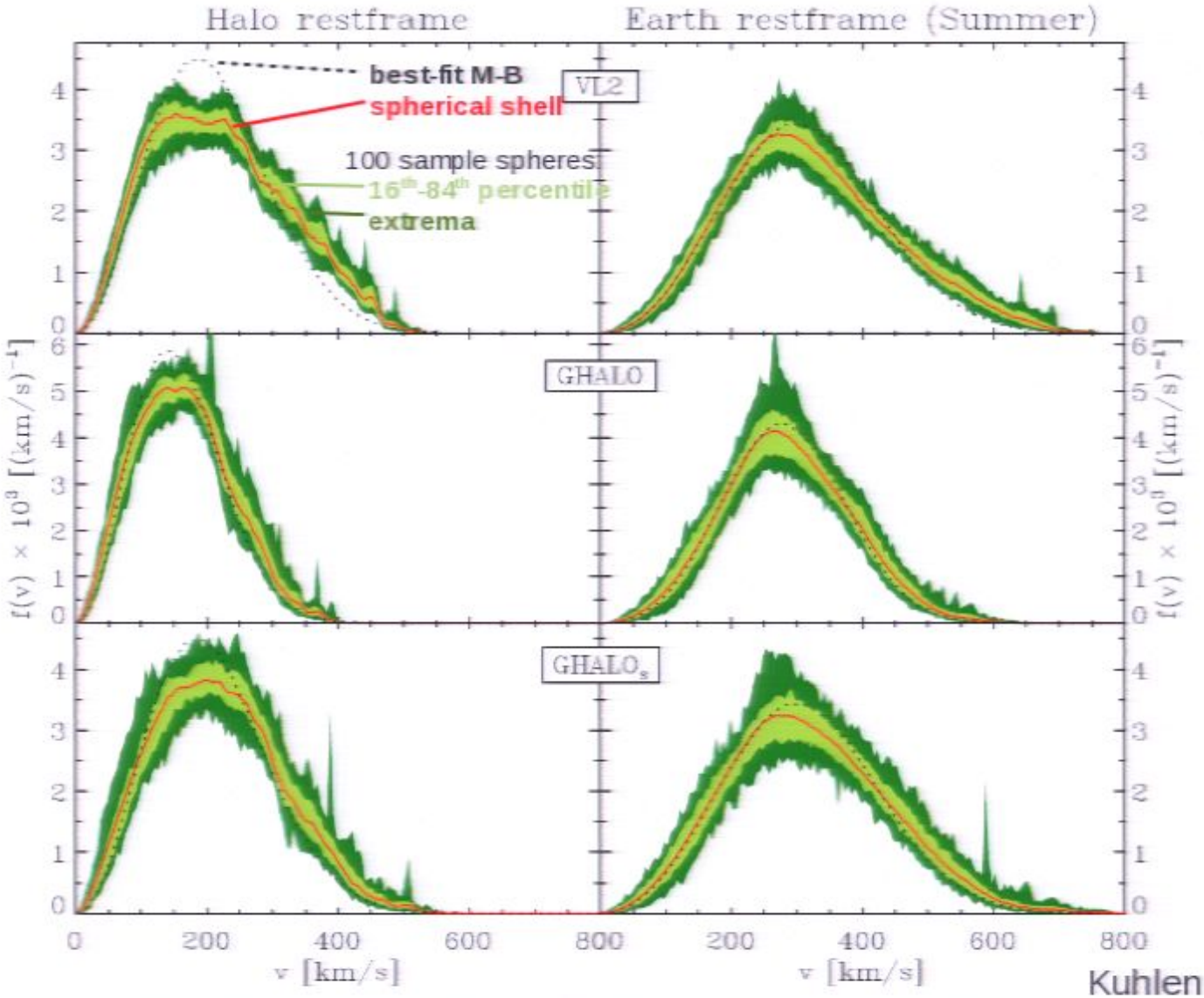

Kuhlen et al. (2010)

See also: Hansen et al. (2005), Vogelsberger et al. (2009)

Experimental Benchmarks

Name	Experiment	Element	(Z, A)	m_χ [GeV]	E_{recoil} [keV_{nr}]	v_{min} [km s^{-1}]	Reference	Comments
CDMS_Ge_50GeV	CDMS-II	Ge	(32, 73)	50.0	[10.0, 100.0]	[193.1, 610.8]	0912.3592	
CDMS_Ge_100GeV	—	—	—	100.0	—	[135.8, 429.5]	—	
CDMS_Ge_500GeV	—	—	—	500.0	—	[89.98, 284.5]	—	
CDMS_Si_50GeV	CDMS-II	Si	(14, 28)	50.0	[10.0, 100.0]	[197.8, 625.4]	0912.3592	
CDMS_Si_100GeV	—	—	8—	100.0	—	[162.3, 513.1]	—	
CDMS_Si_500GeV	—	—	—	500.0	—	[133.9, 423.3]	—	
CDMS_Ge_lowE	CDMS-II	Ge	(32, 73)	7.0	[2.3, 11.6]	[430.3, 966.4]	1107.0717	matched to CoGeNT
CDMS_Si_lowE	—	Si	(14, 28)	7.0	[4.5, 22.8]	[425.2, 957.1]	—	matched to CoGeNT
Xenon_50GeV	Xenon100	Xe	(54, 131)	50.0	[8.4, 44.6]	[194.5, 448.1]	1005.0380	
Xenon_100GeV	—	—	—	100.0	—	[124.1, 285.9]	—	
Xenon_500GeV	—	—	—	500.0	—	[67.89, 156.2]	—	
Xenon_lowE	Xenon100	Xe	(54, 131)	7.0	[1.4, 7.0]	[431.3, 966.7]	1107.0717	matched to CoGeNT
DAMA_Na_10GeV	DAMA	Na	(11, 23)	10.0	[6.7, 20.0]	[377.8, 652.8]	1002.1028	Q(Na) = 0.3
DAMA_I_100GeV	—	I	(53, 127)	100.0	[25.0, 75.0]	[213.6, 370.1]	—	Q(I) = 0.08
DAMA_Na_lowE	DAMA	Na	(11, 23)	7.0	[5.0, 25.3]	[423.9, 954.1]	1107.0717	matched to CoGeNT
CoGeNT_7GeV	CoGeNT	Ge	(32, 73)	7.0	[2.3, 11.6]	[430.3, 966.4]	1106.0650	
CRESST_O_10GeV	CRESST	O	(8, 16)	10.0	[12.0, 40.0]	[477.7, 872.1]	1109.0702	
CRESST_Ca_15GeV	—	Ca	(20, 40)	15.0	—	[426.0, 777.8]	—	
CRESST_W_50GeV	—	W	(74, 184)	50.0	—	[253.5, 462.9]	—	
CRESST_O_lowE	CRESST	O	(8, 16)	7.0	[5.8, 29.8]	[419.7, 951.2]	1107.0717	matched to CoGeNT

Velocity Space Substructure and Direct Detection

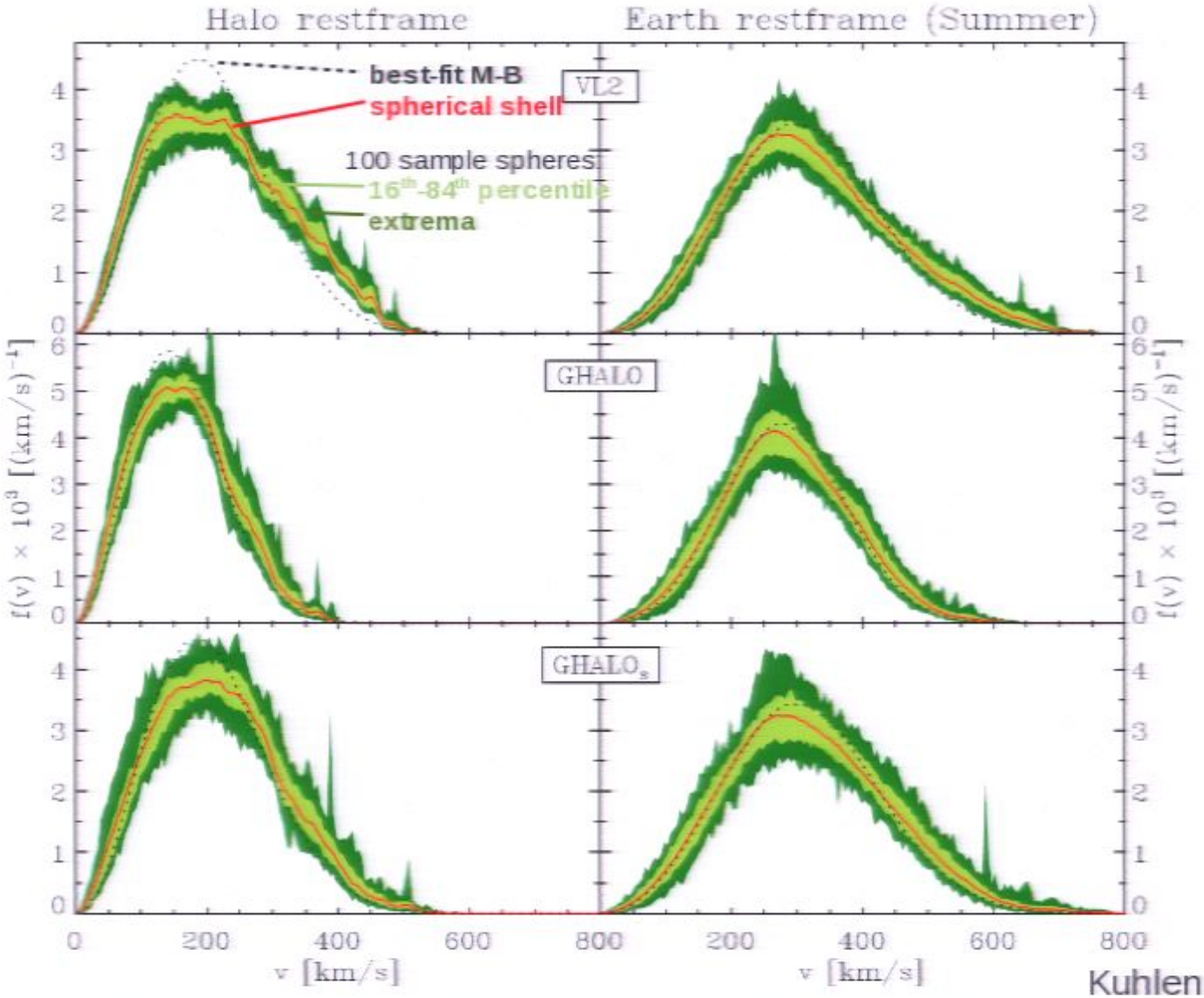

Kuhlen et al. (2010)

See also: Hansen et al. (2005), Vogelsberger et al. (2009)

Experimental Benchmarks

Name	Experiment	Element	(Z, A)	m_χ [GeV]	E_{recoil} [keV_{nr}]	v_{min} [km s^{-1}]	Reference	Comments
CDMS_Ge_50GeV	CDMS-II	Ge	(32, 73)	50.0	[10.0, 100.0]	[193.1, 610.8]	0912.3592	
CDMS_Ge_100GeV	—	—	—	100.0	—	[135.8, 429.5]	—	
CDMS_Ge_500GeV	—	—	—	500.0	—	[89.98, 284.5]	—	
CDMS_Si_50GeV	CDMS-II	Si	(14, 28)	50.0	[10.0, 100.0]	[197.8, 625.4]	0912.3592	
CDMS_Si_100GeV	—	—	8—	100.0	—	[162.3, 513.1]	—	
CDMS_Si_500GeV	—	—	—	500.0	—	[133.9, 423.3]	—	
CDMS_Ge_lowE	CDMS-II	Ge	(32, 73)	7.0	[2.3, 11.6]	[430.3, 966.4]	1107.0717	matched to CoGeNT
CDMS_Si_lowE	—	Si	(14, 28)	7.0	[4.5, 22.8]	[425.2, 957.1]	—	matched to CoGeNT
Xenon_50GeV	Xenon100	Xe	(54, 131)	50.0	[8.4, 44.6]	[194.5, 448.1]	1005.0380	
Xenon_100GeV	—	—	—	100.0	—	[124.1, 285.9]	—	
Xenon_500GeV	—	—	—	500.0	—	[67.89, 156.2]	—	
Xenon_lowE	Xenon100	Xe	(54, 131)	7.0	[1.4, 7.0]	[431.3, 966.7]	1107.0717	matched to CoGeNT
DAMA_Na_10GeV	DAMA	Na	(11, 23)	10.0	[6.7, 20.0]	[377.8, 652.8]	1002.1028	Q(Na) = 0.3
DAMA_I_100GeV	—	I	(53, 127)	100.0	[25.0, 75.0]	[213.6, 370.1]	—	Q(I) = 0.08
DAMA_Na_lowE	DAMA	Na	(11, 23)	7.0	[5.0, 25.3]	[423.9, 954.1]	1107.0717	matched to CoGeNT
CoGeNT_7GeV	CoGeNT	Ge	(32, 73)	7.0	[2.3, 11.6]	[430.3, 966.4]	1106.0650	
CRESST_O_10GeV	CRESST	O	(8, 16)	10.0	[12.0, 40.0]	[477.7, 872.1]	1109.0702	
CRESST_Ca_15GeV	—	Ca	(20, 40)	15.0	—	[426.0, 777.8]	—	
CRESST_W_50GeV	—	W	(74, 184)	50.0	—	[253.5, 462.9]	—	
CRESST_O_lowE	CRESST	O	(8, 16)	7.0	[5.8, 29.8]	[419.7, 951.2]	1107.0717	matched to CoGeNT

Velocity Space Substructure and Direct Detection

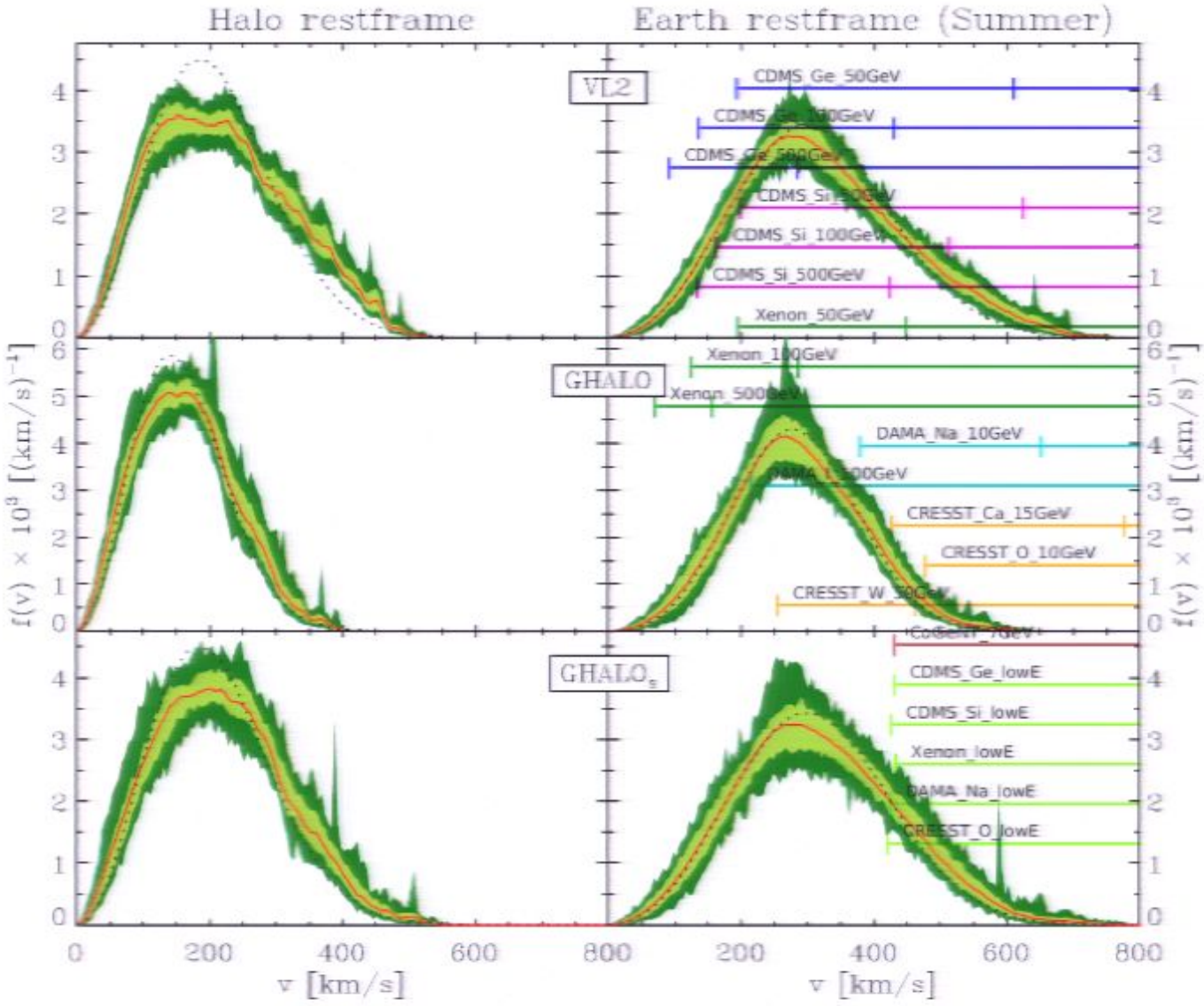

et al. (2010)

See also: Hansen et al. (2005), Vogelsberger et al. (2009)

Velocity Space Substructure and Direct Detection

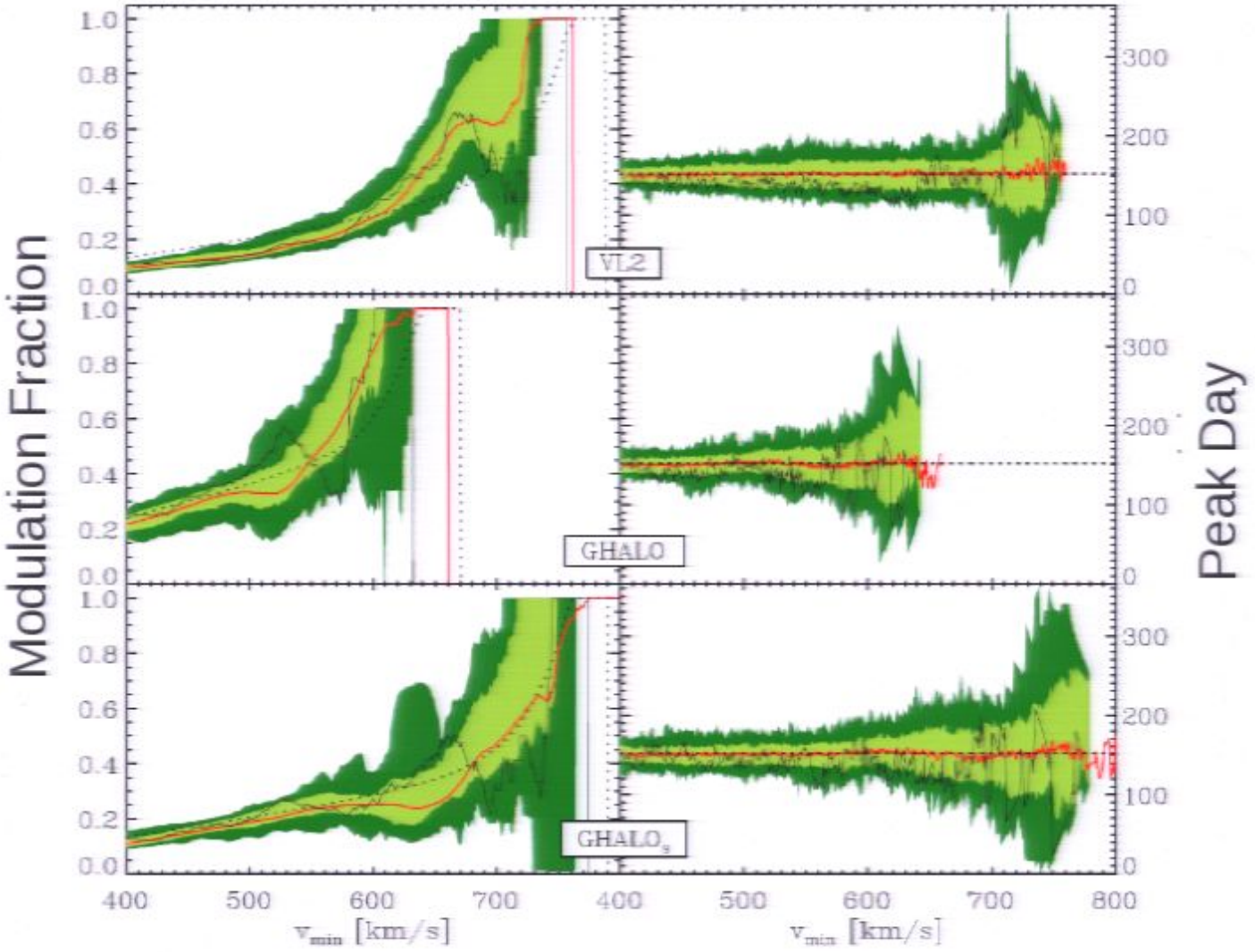

Kuhlen et al. (2010)

Velocity Space Substructure and Direct Detection

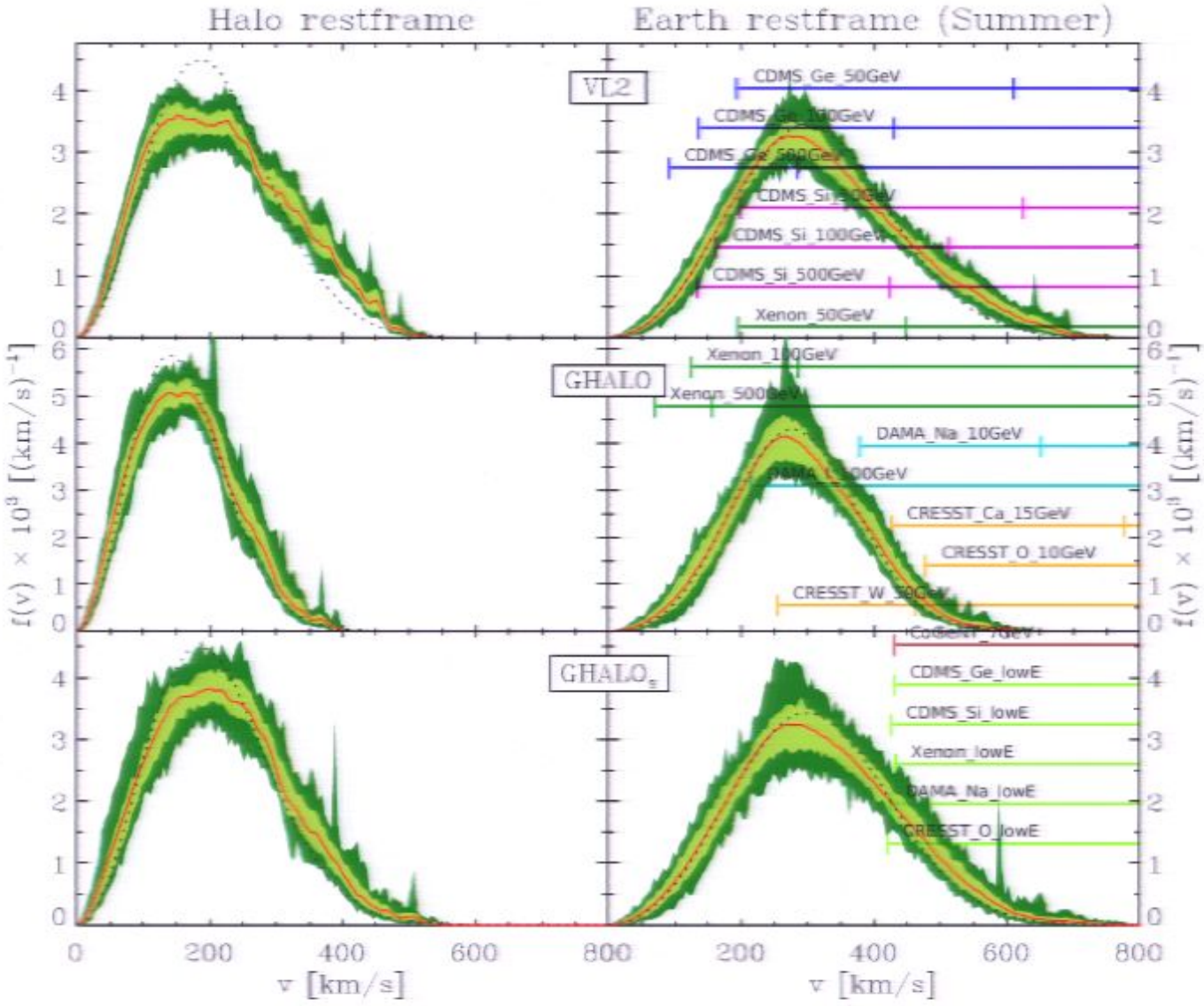

et al. (2010)

See also: Hansen et al. (2005), Vogelsberger et al. (2009)

Velocity Space Substructure and Direct Detection

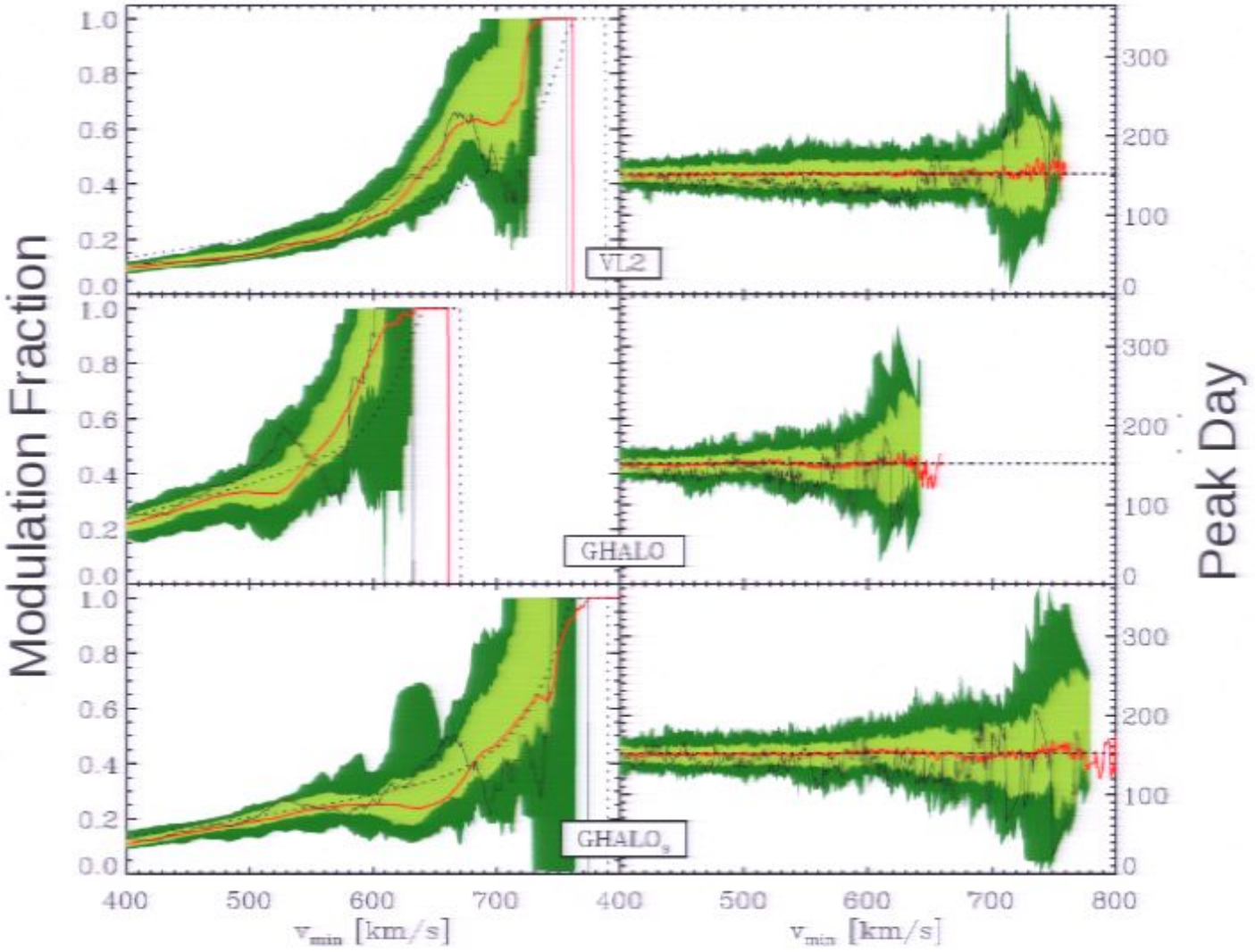

Kuhlen et al. (2010)

In Halo Restframe (v_{min} = 0 km/s)

Maxwell-Boltzmann (isotropic)

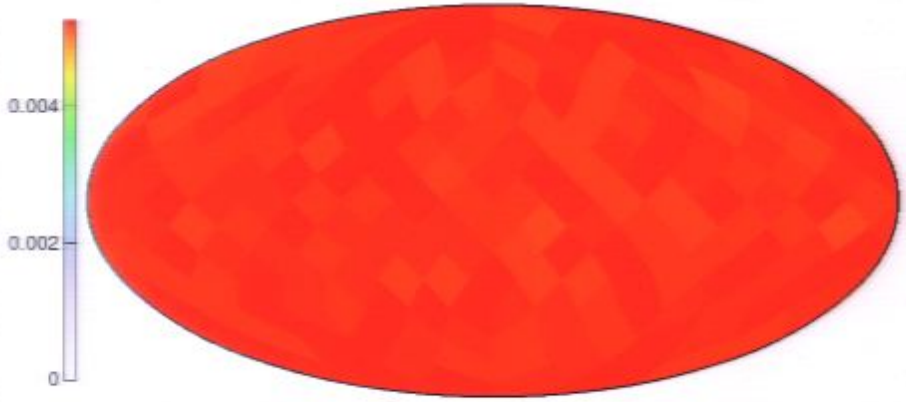

Spherical Shell (8 kpc < R < 9 kpc)

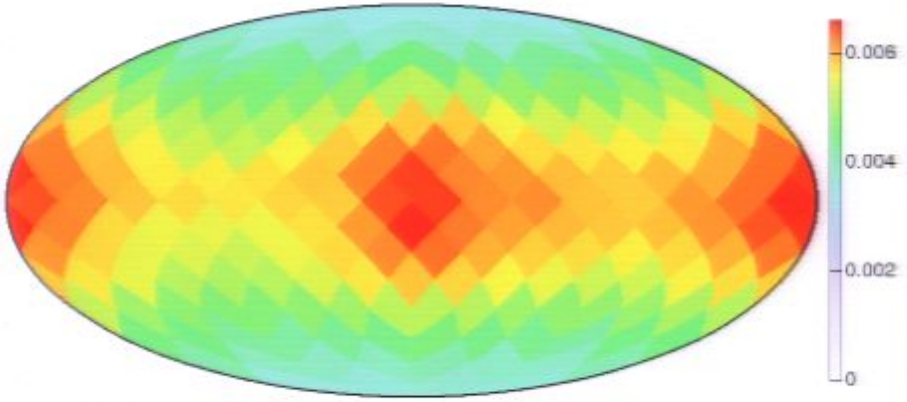

Sample Sphere #001

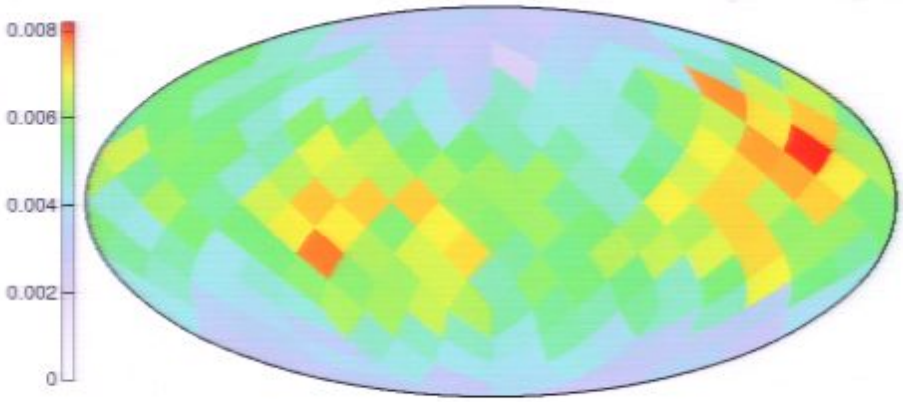

Sample Sphere #004 (containing a subhalo)

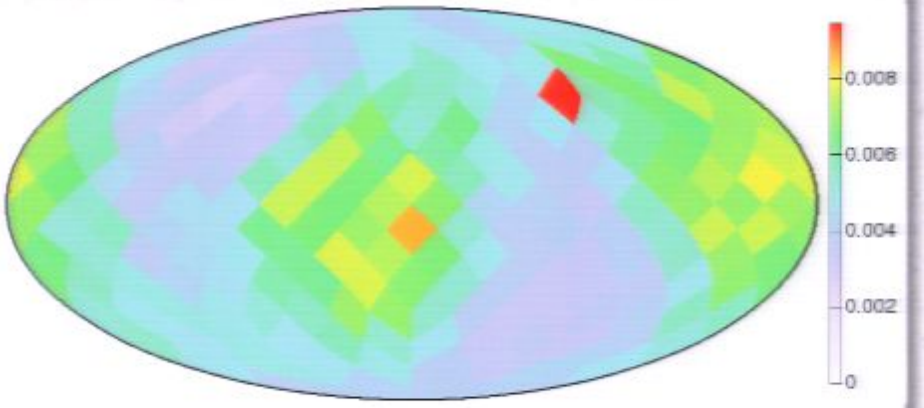

Velocity Space Substructure and Direct Detection

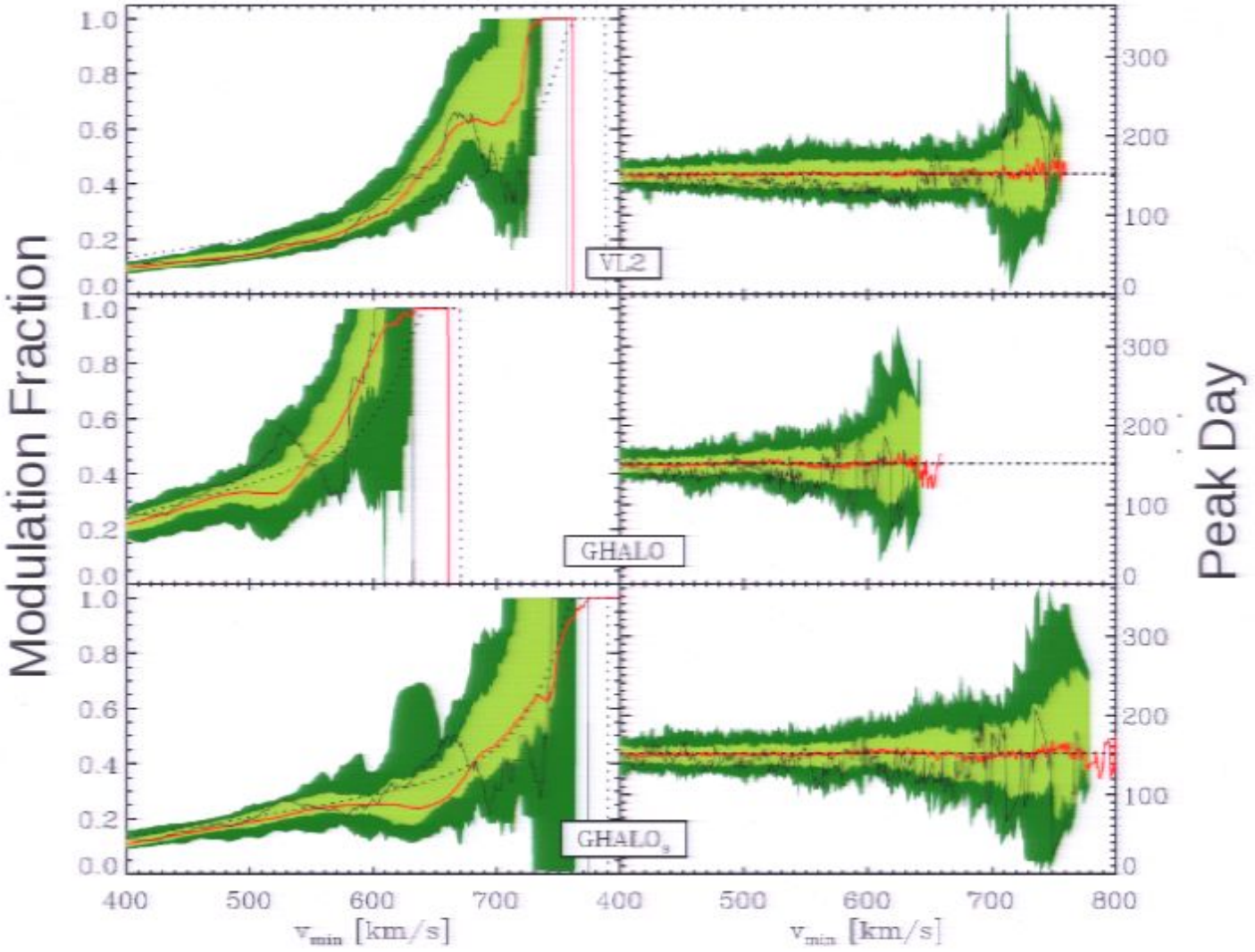

Kuhlen et al. (2010)

In Halo Restframe (v_{min} = 0 km/s)

Maxwell-Boltzmann (isotropic)

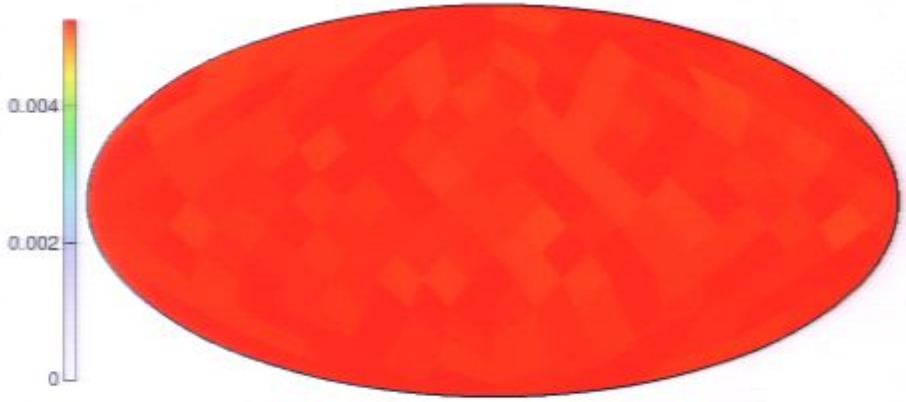

Spherical Shell (8 kpc < R < 9 kpc)

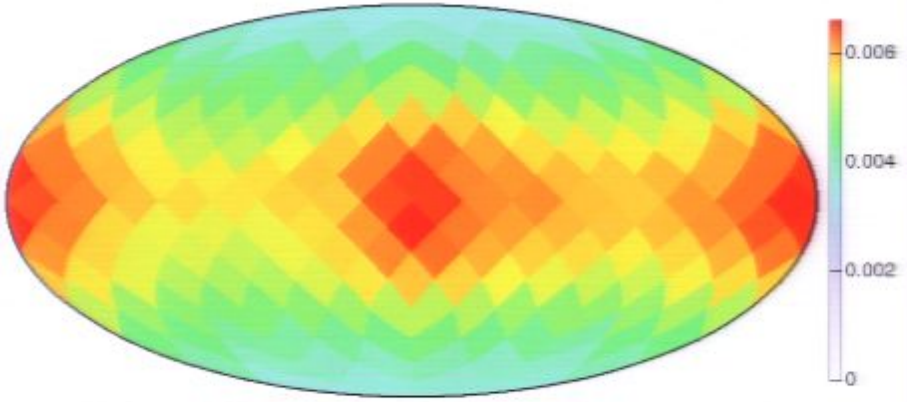

Sample Sphere #001

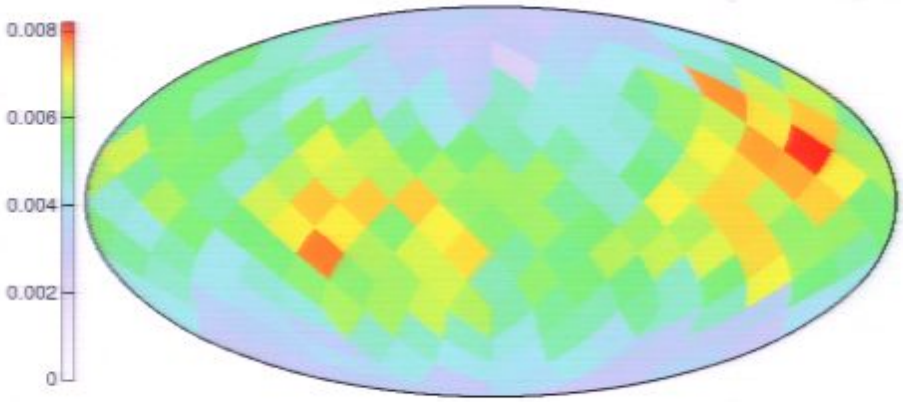

Sample Sphere #004 (containing a subhalo)

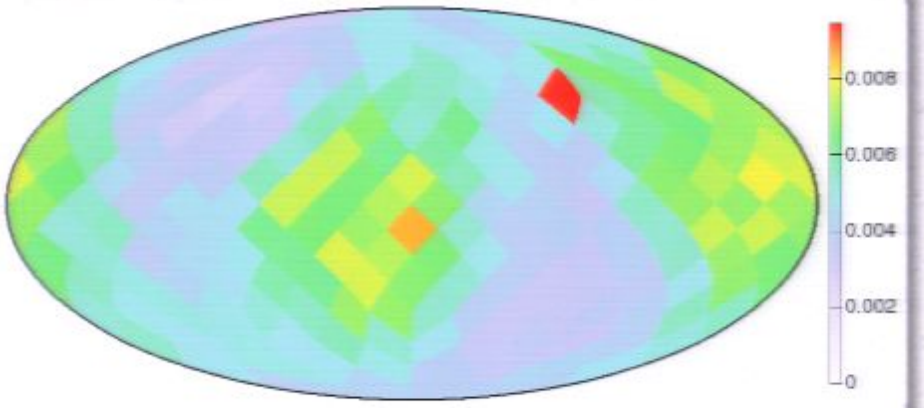

In Earth Restframe (v_{min} = 0 km/s)

Maxwell-Boltzmann (isotropic)

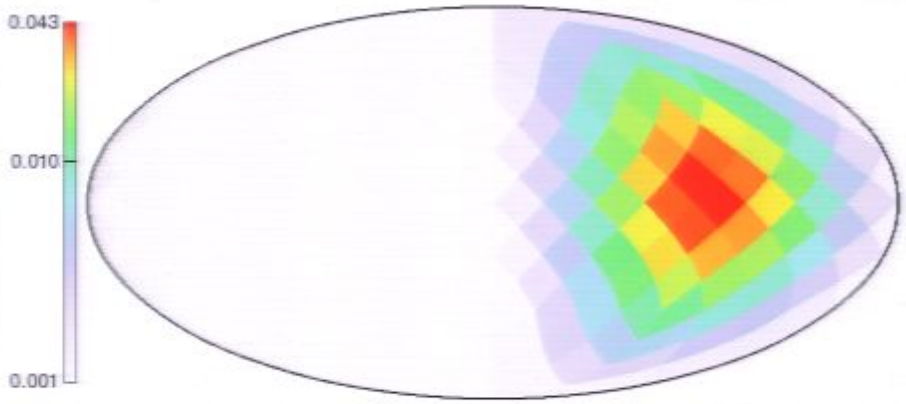

Spherical Shell (8 kpc < R < 9 kpc)

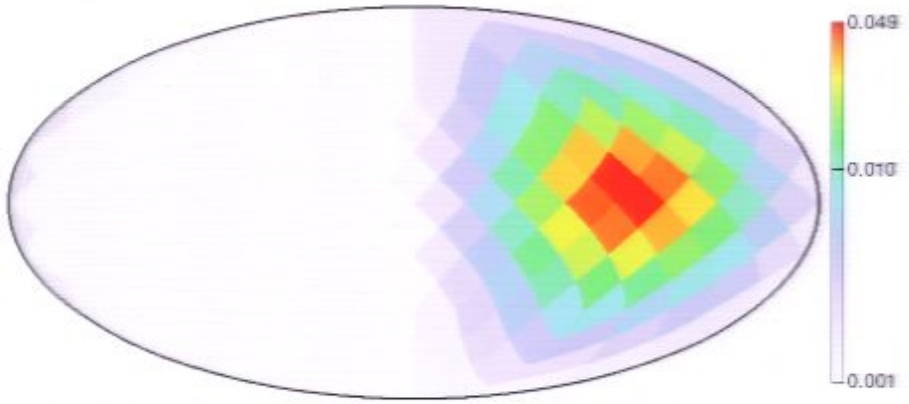

Sample Sphere #001

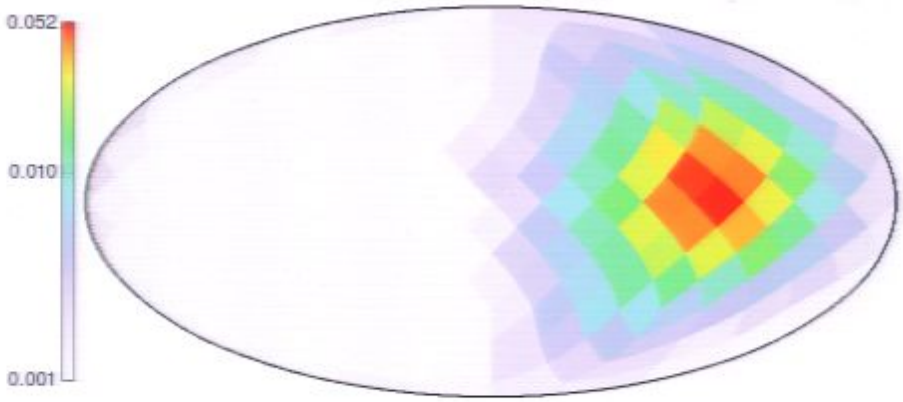

Sample Sphere #004 (containing a subhalo)

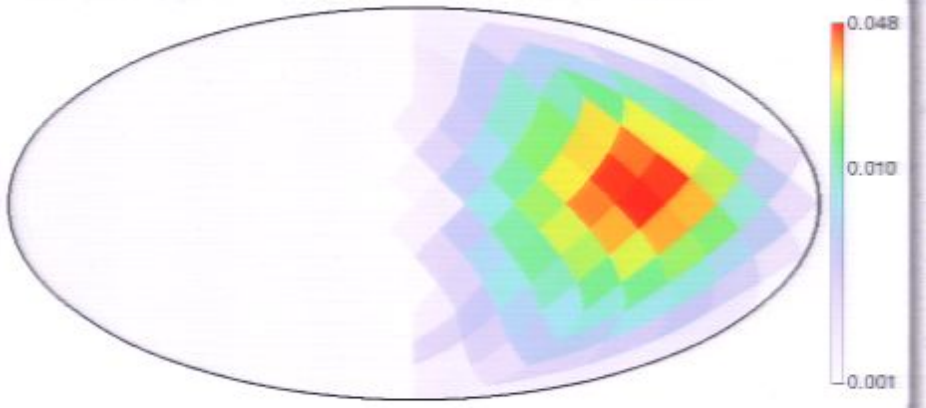

In Earth Restframe (v_{min} = 500 km/s)

Maxwell-Boltzmann (isotropic)

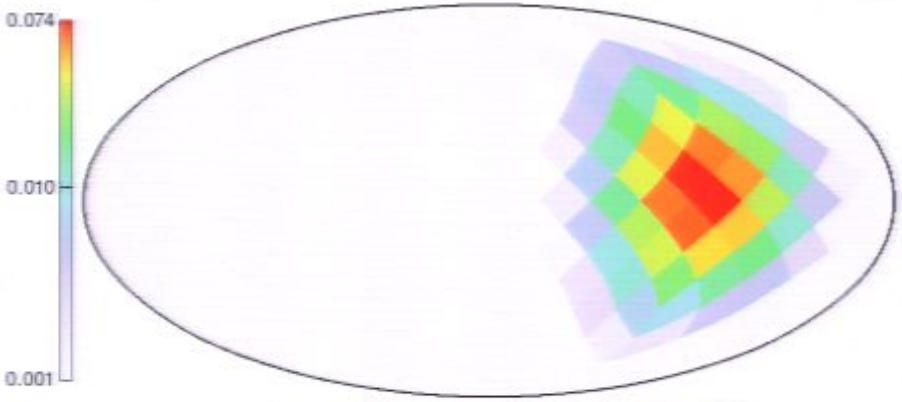

Spherical Shell (8 kpc < R < 9 kpc)

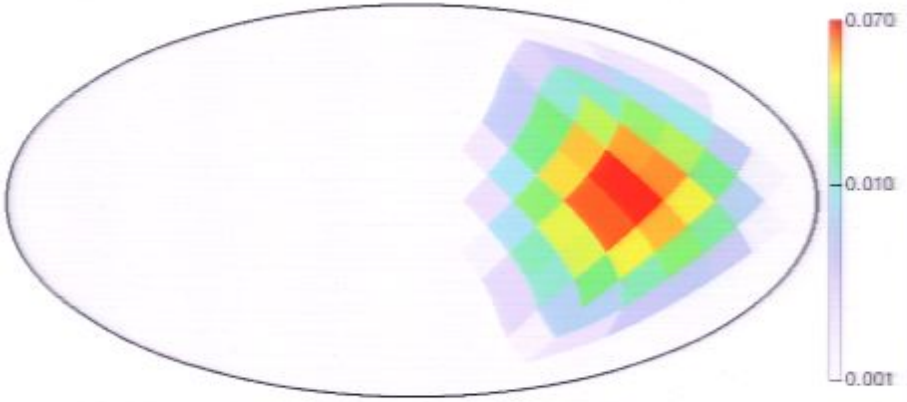

Sample Sphere #001

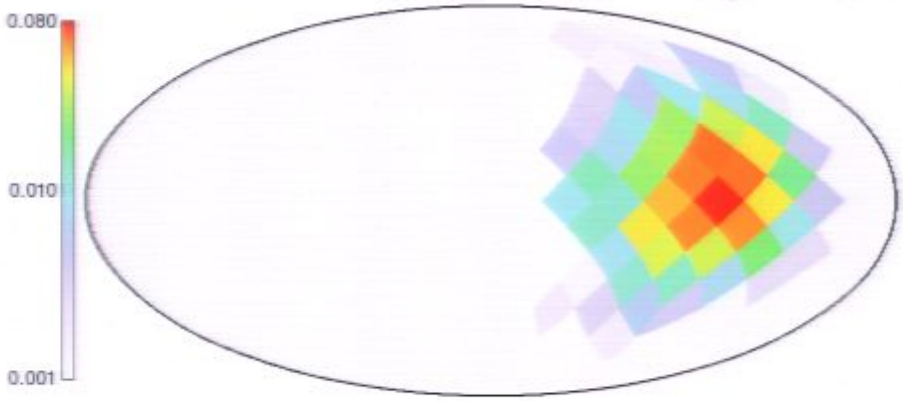

Sample Sphere #004 (containing a subhalo)

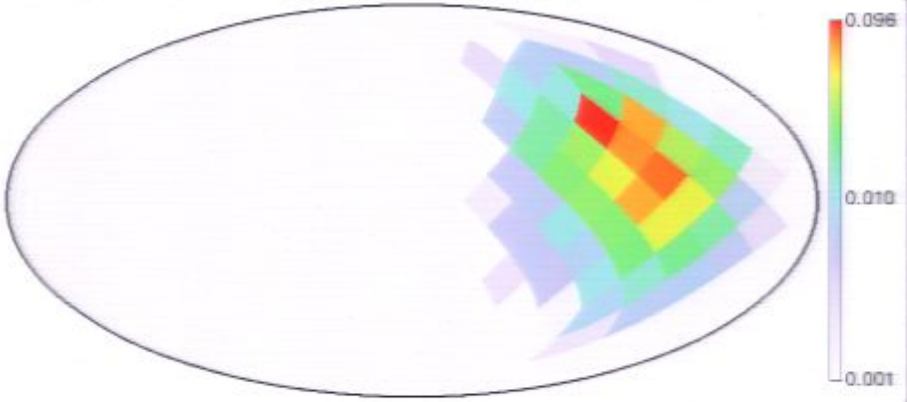

Hotspot Direction

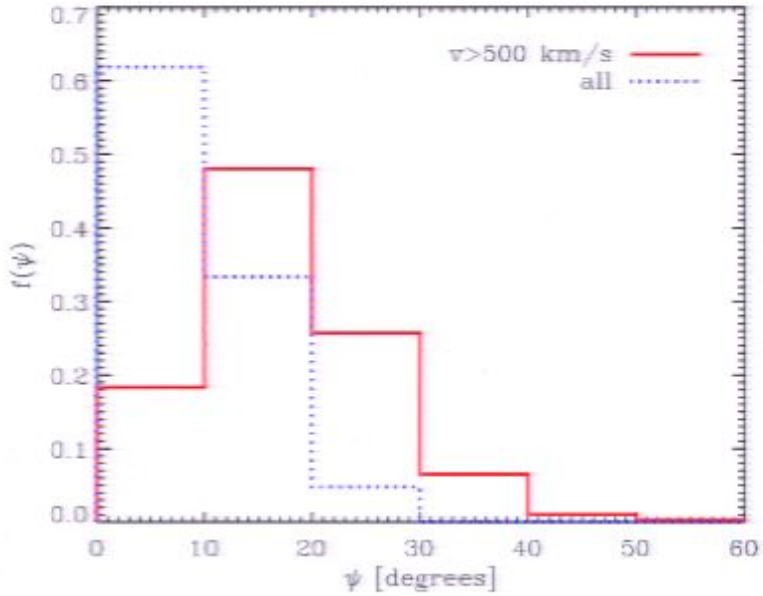

Sample Sphere #004 (containing a subhalo)

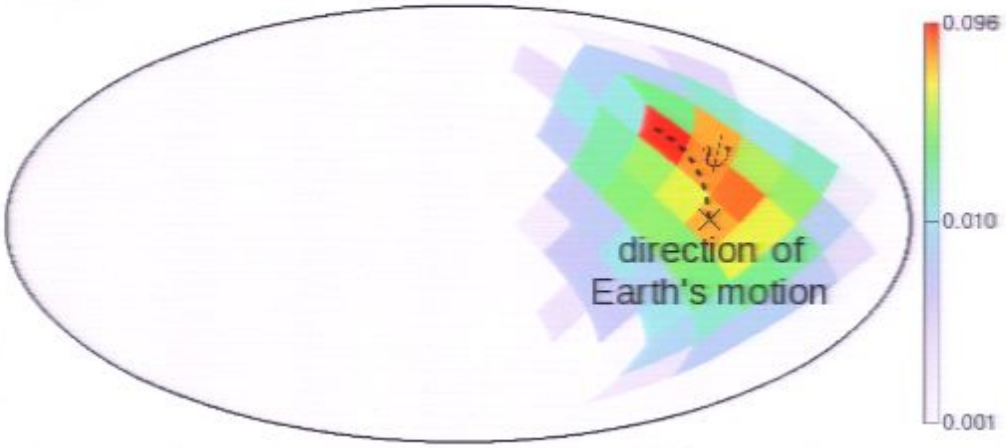

At v_{min}=500 km/s the hotspot is more than 10° away from the direction of Earth's motion in ~80% of all cases!

Velocity Space Substructure: Debris Flow

Recent work with M. Lisanti – **Work in Progress!**

Study of the origin of the velocity space structure by tracking (sub)halo particles though time in the simulation.

Debris ≡ particles that were at some earlier time bound to a subhalo but are unbound at z=0.

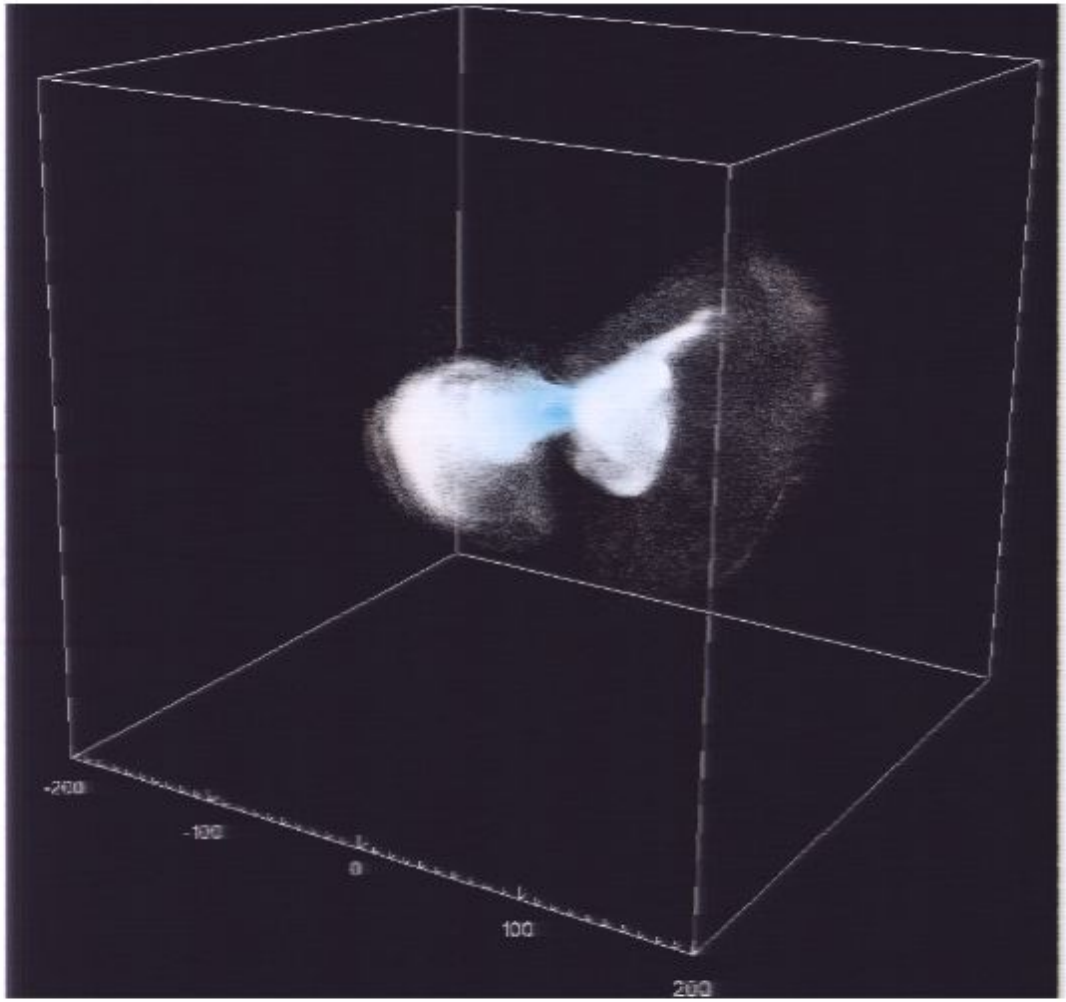

[First pointed out in Lisanti & Spergel 2011 (arXiv:1105.4166)]

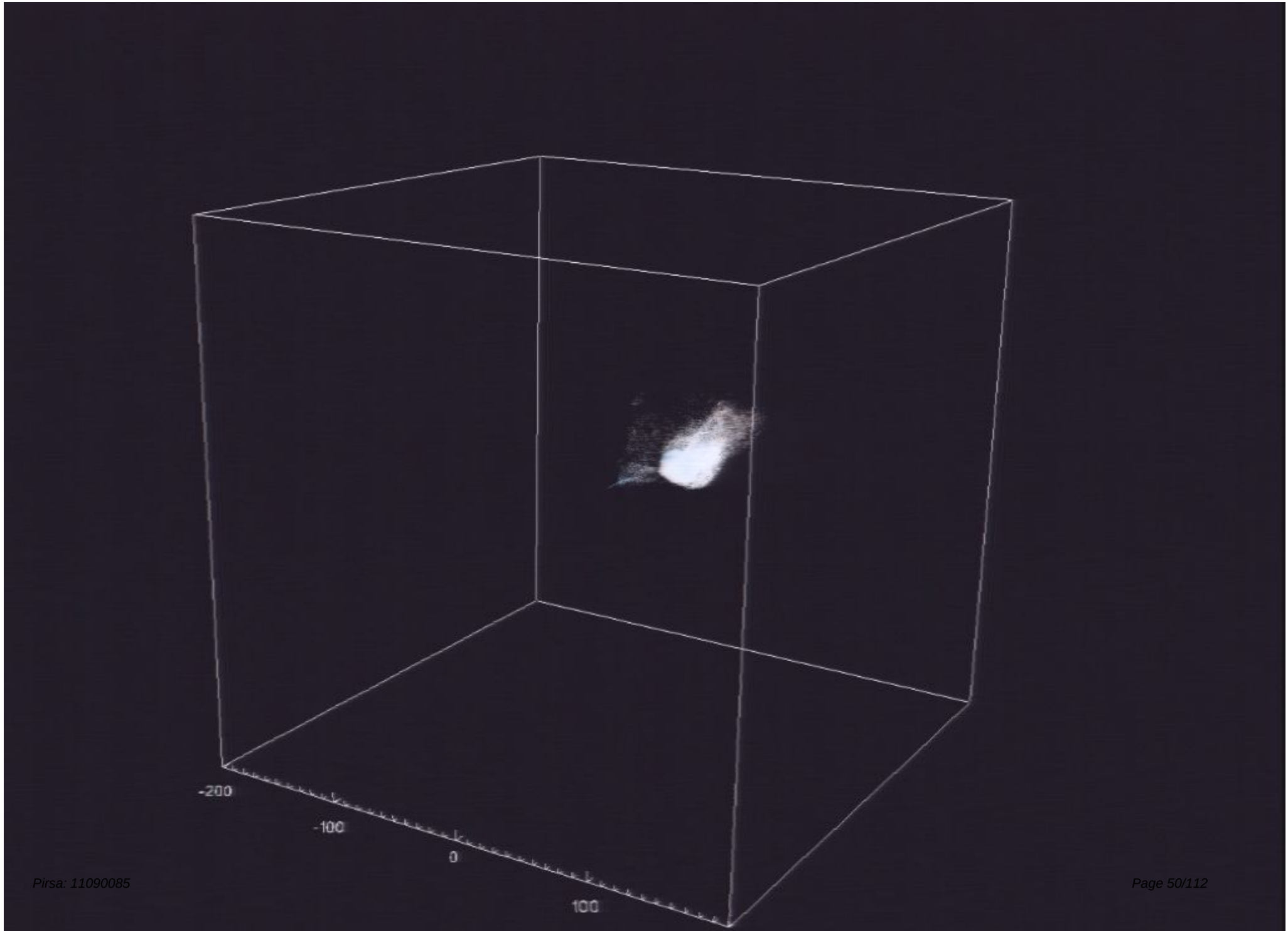
-200
-100
0
100

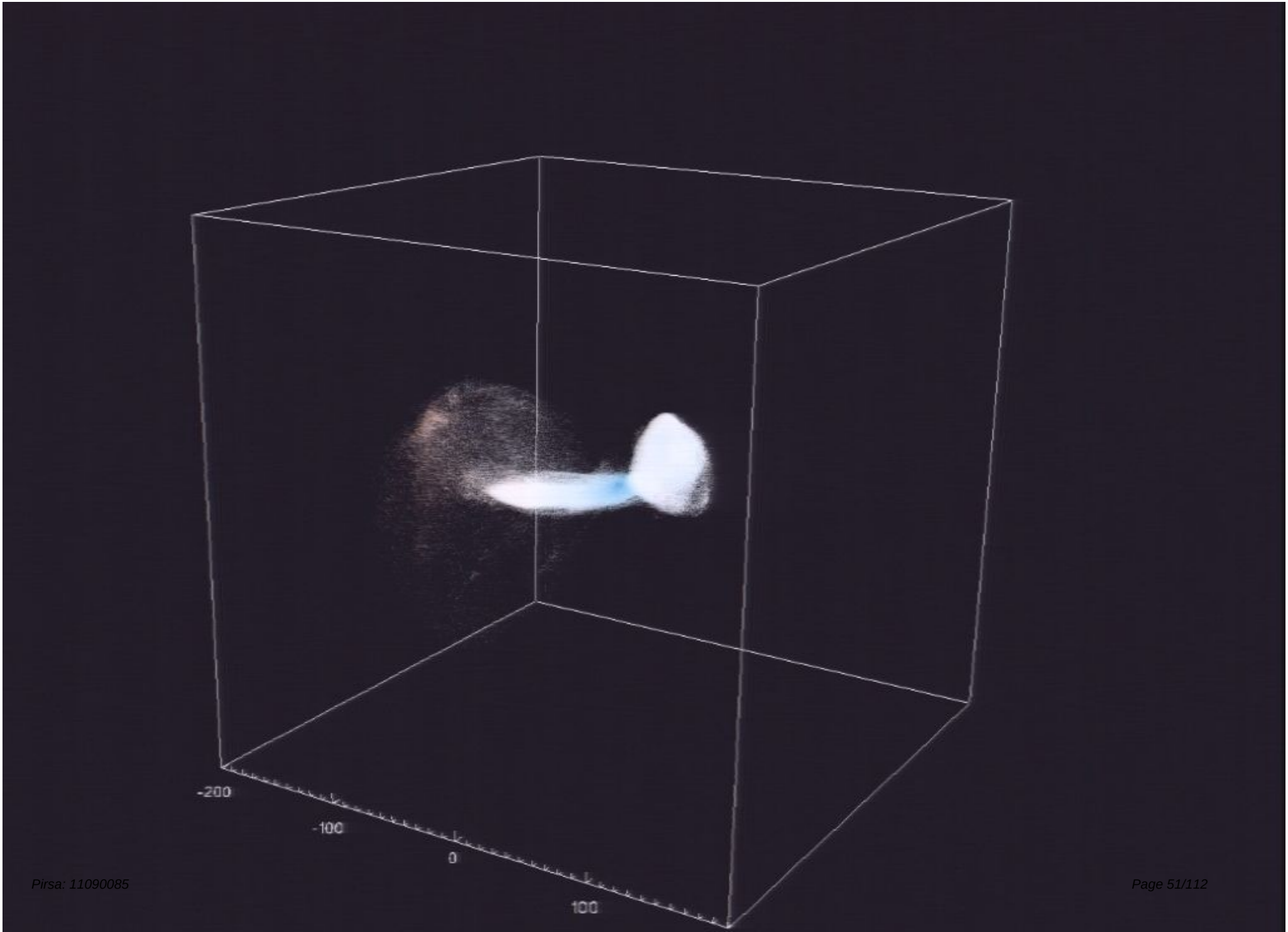
-200
-100
0
100

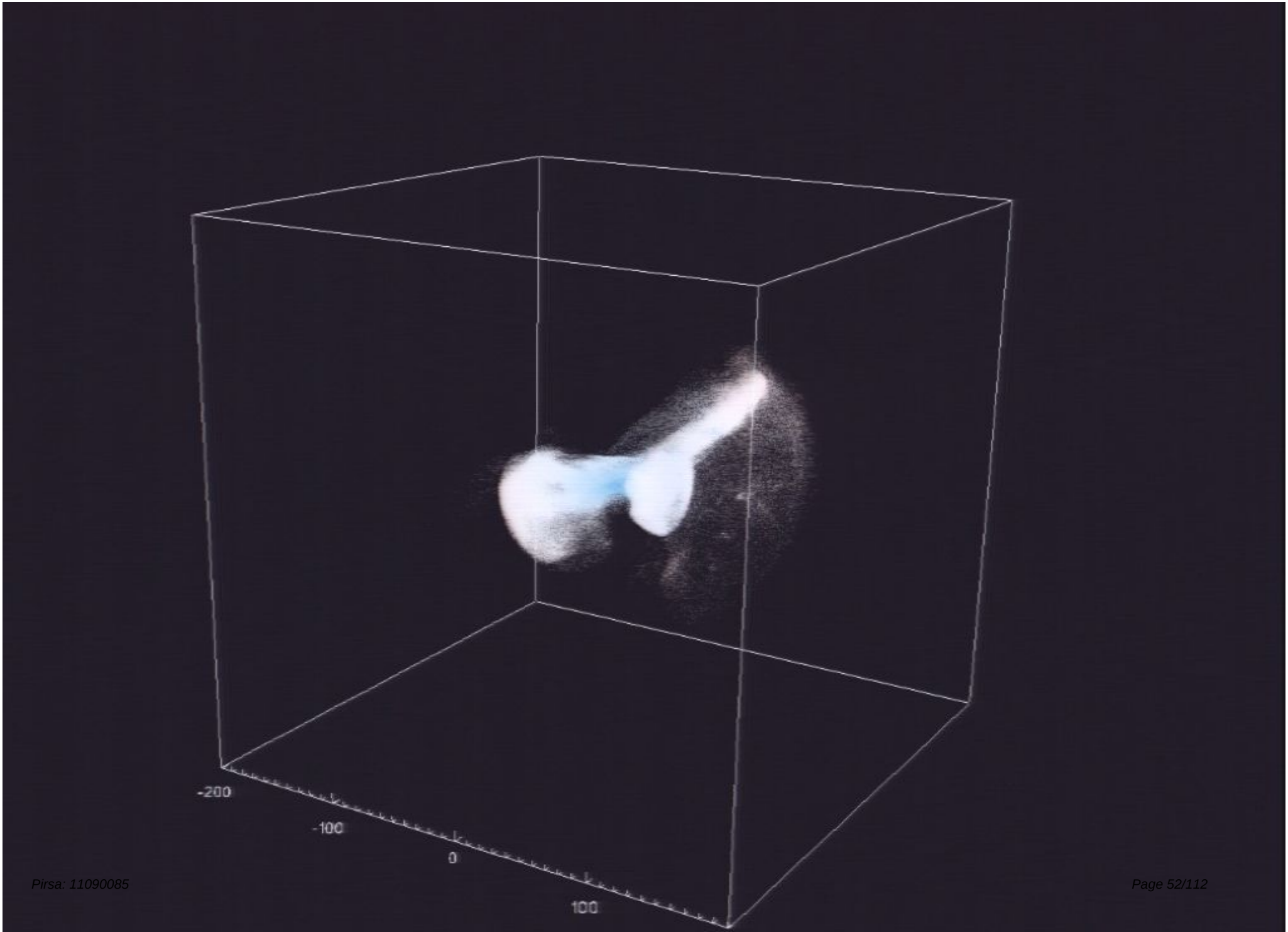
-200
-100
0
100

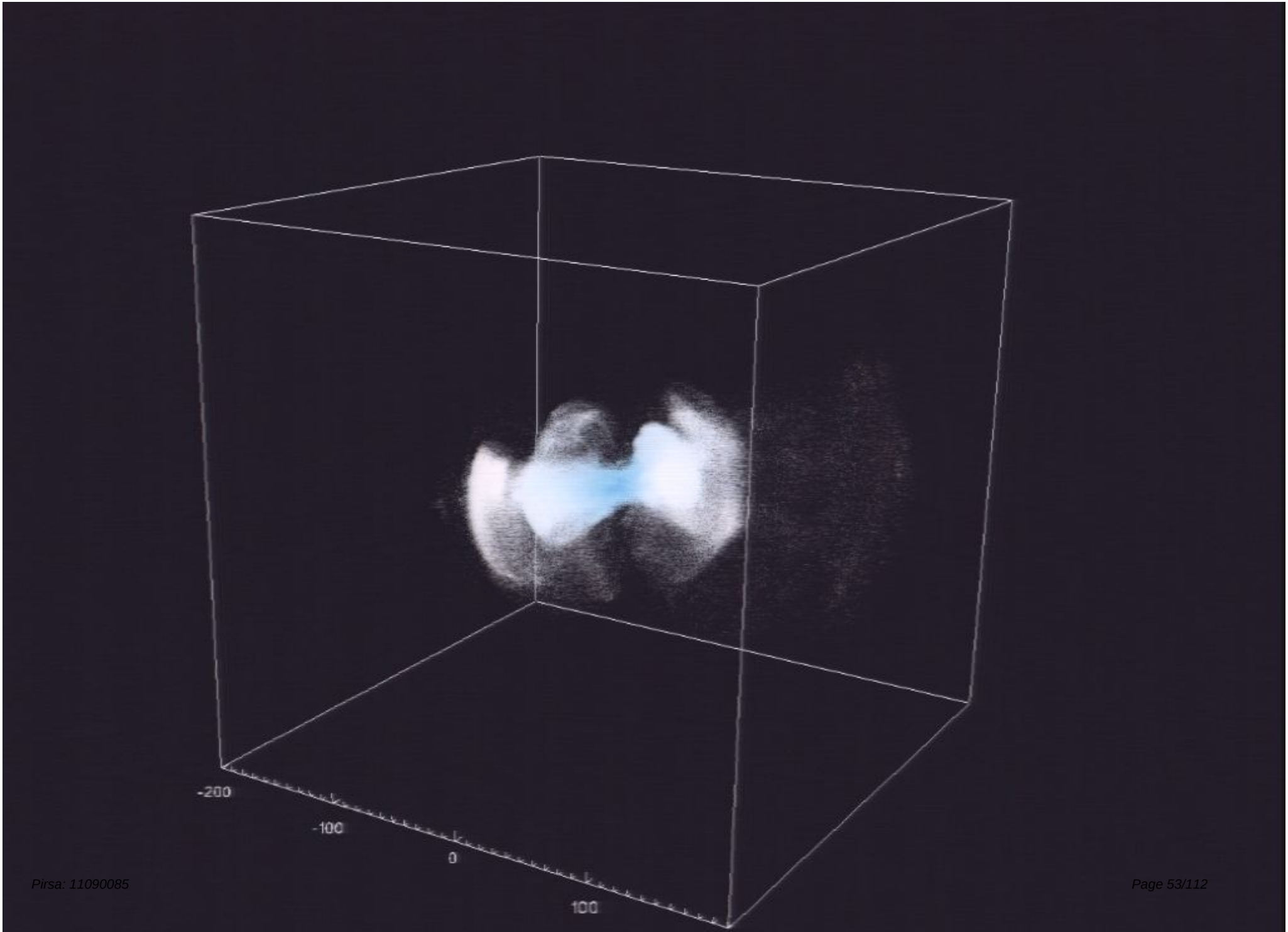
-200
-100
0
100

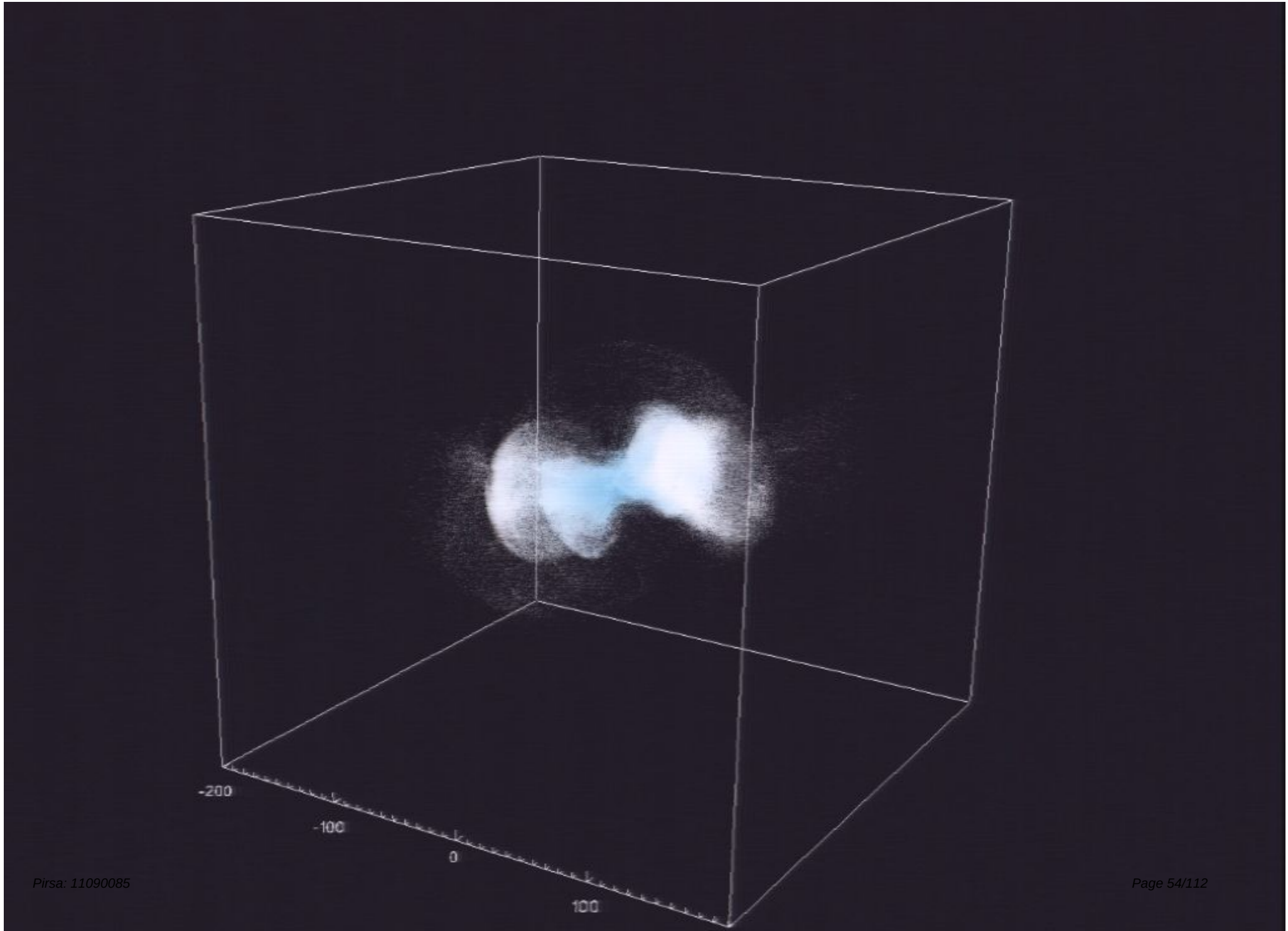
-200
-100
0
100

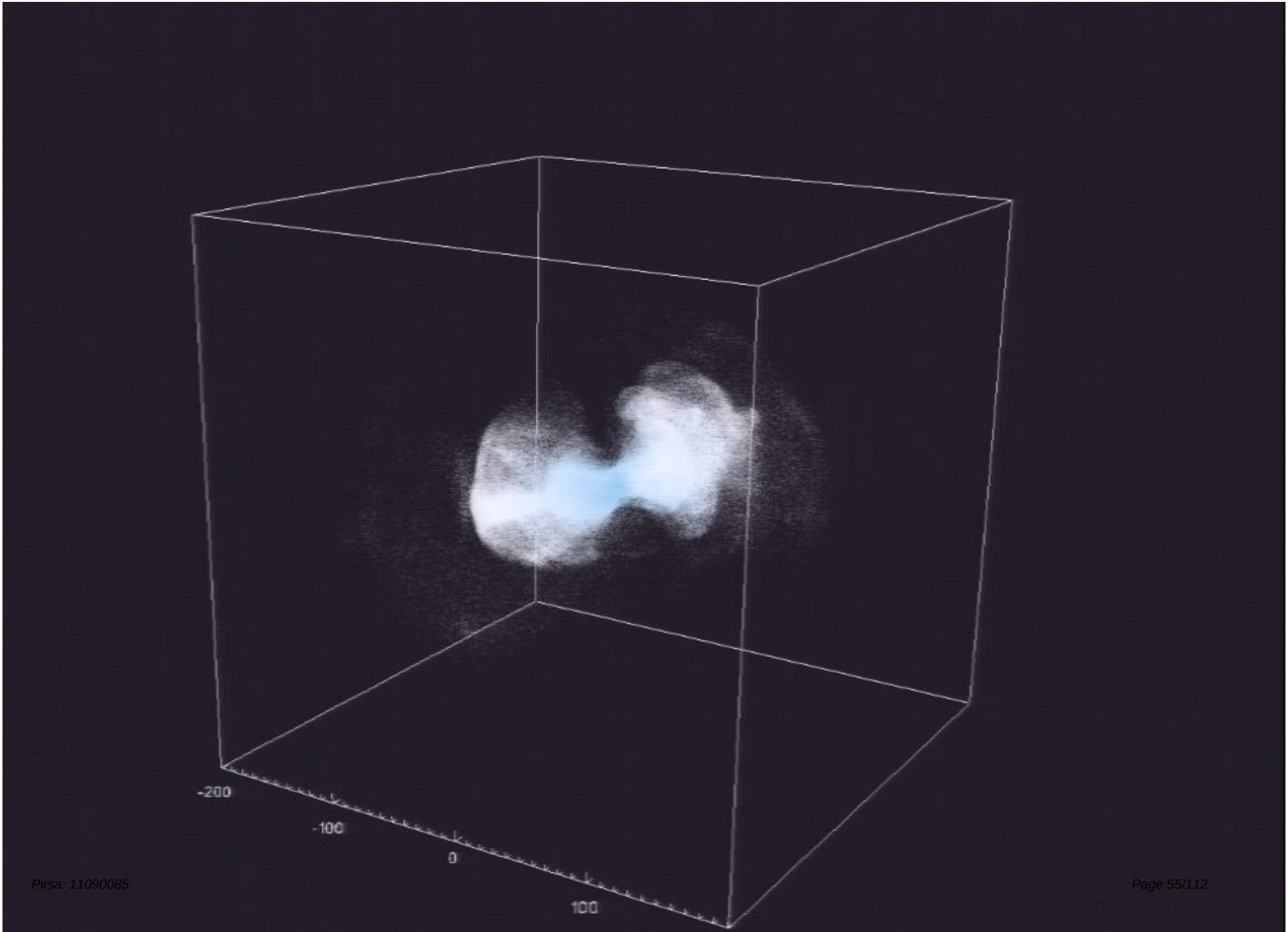
-200
-100
0
100

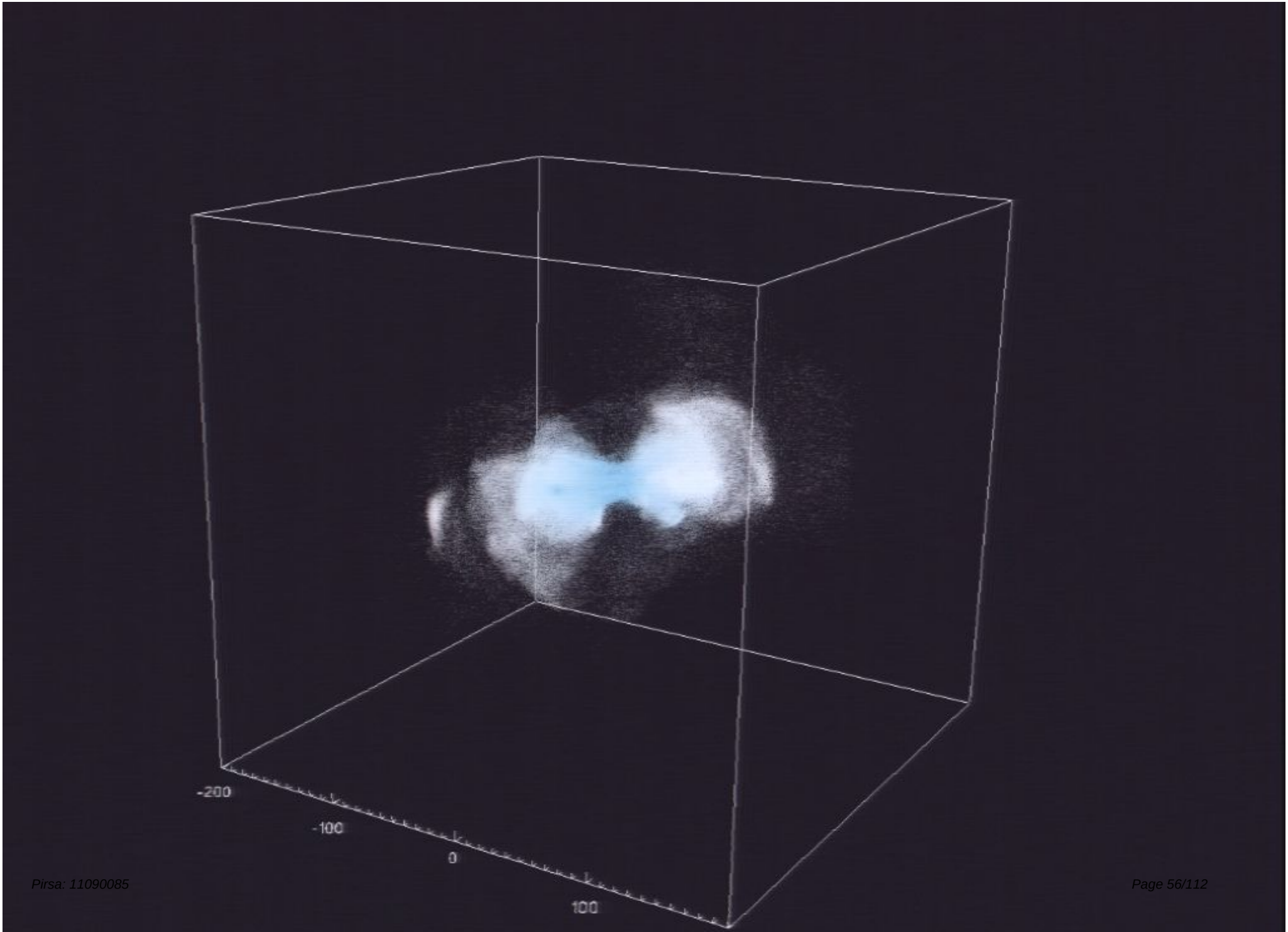
-200
-100
0
100

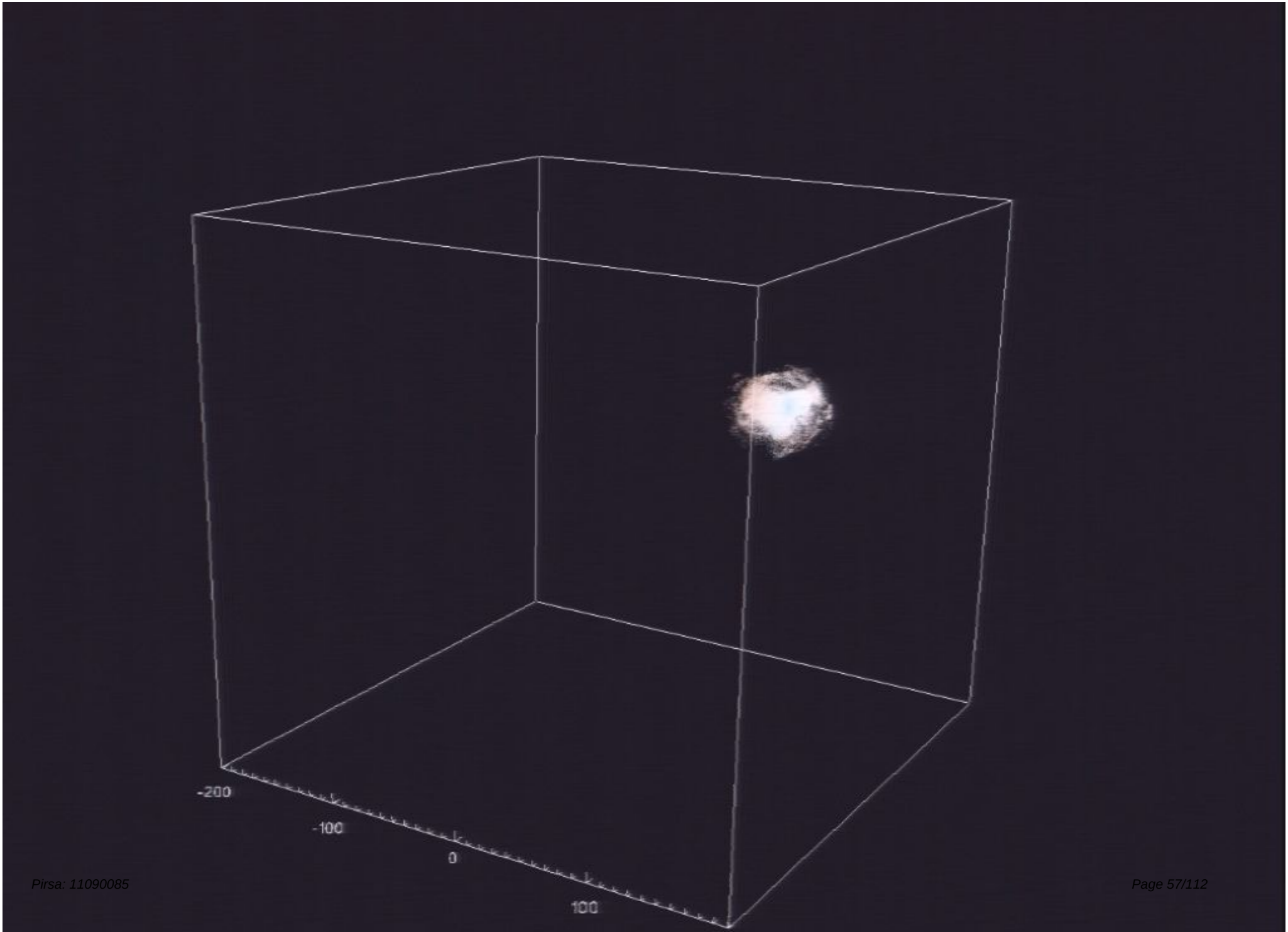
-200
-100
0
100

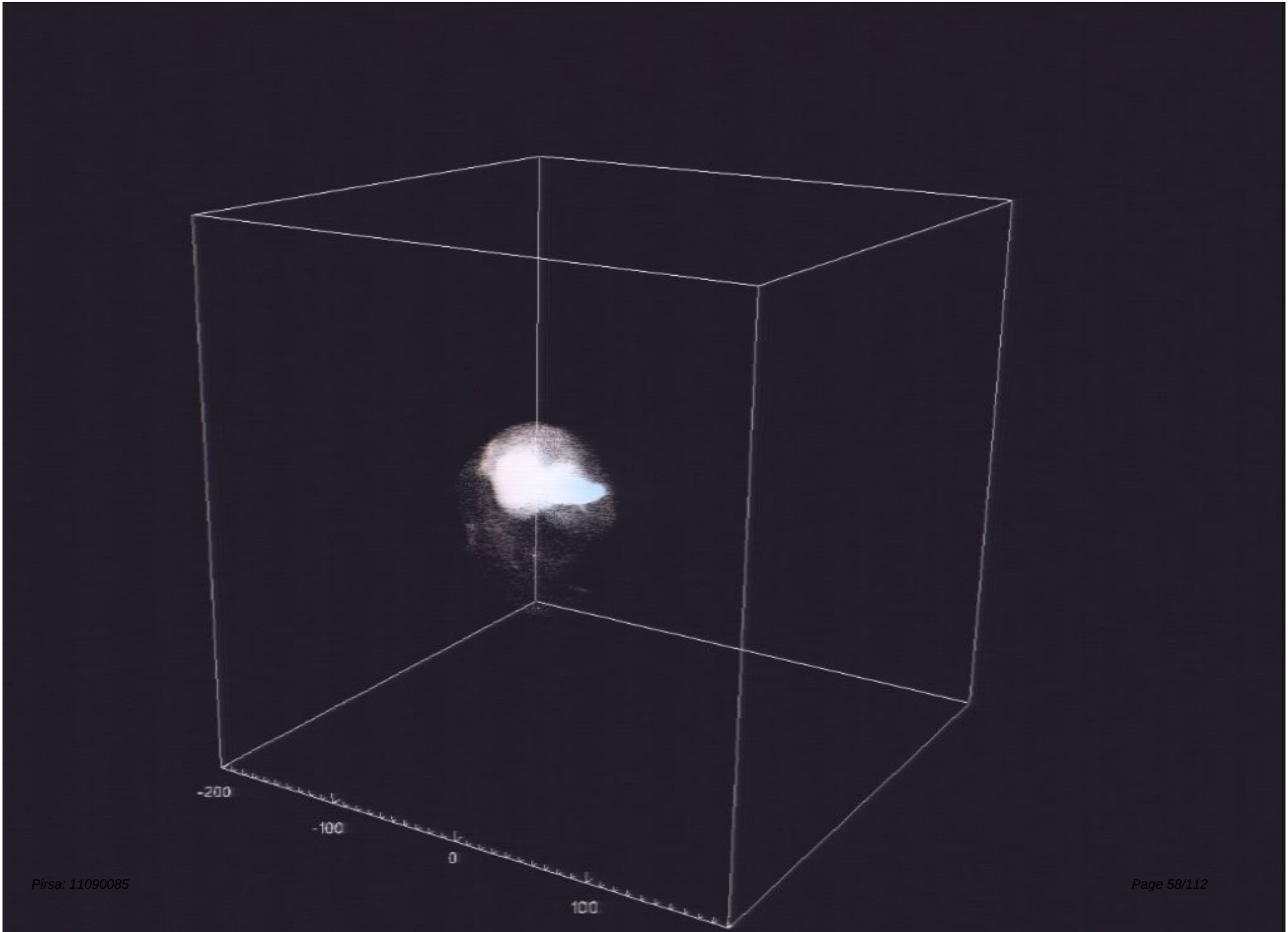
-200
-100
0
100

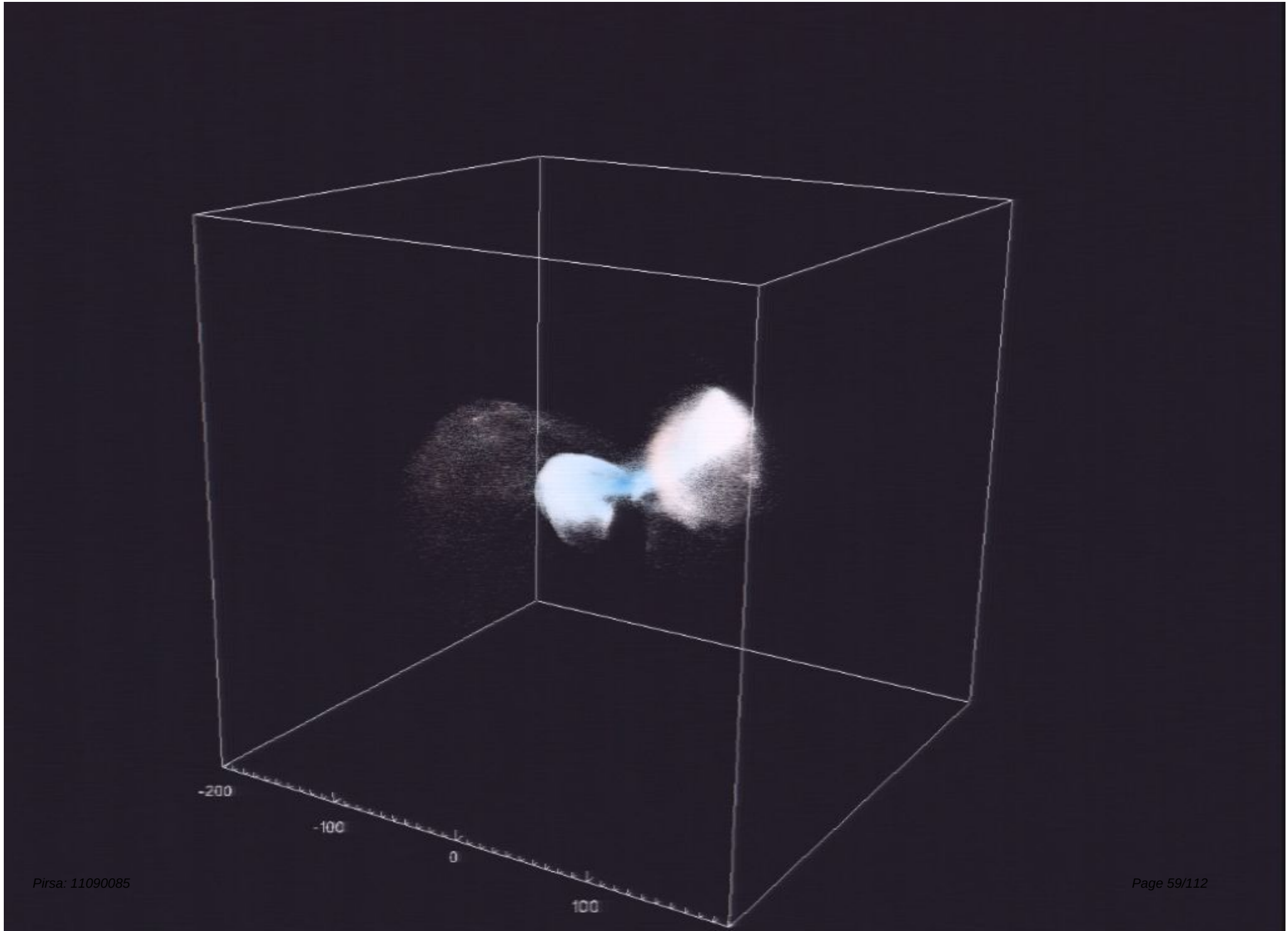
-200
-100
0
100

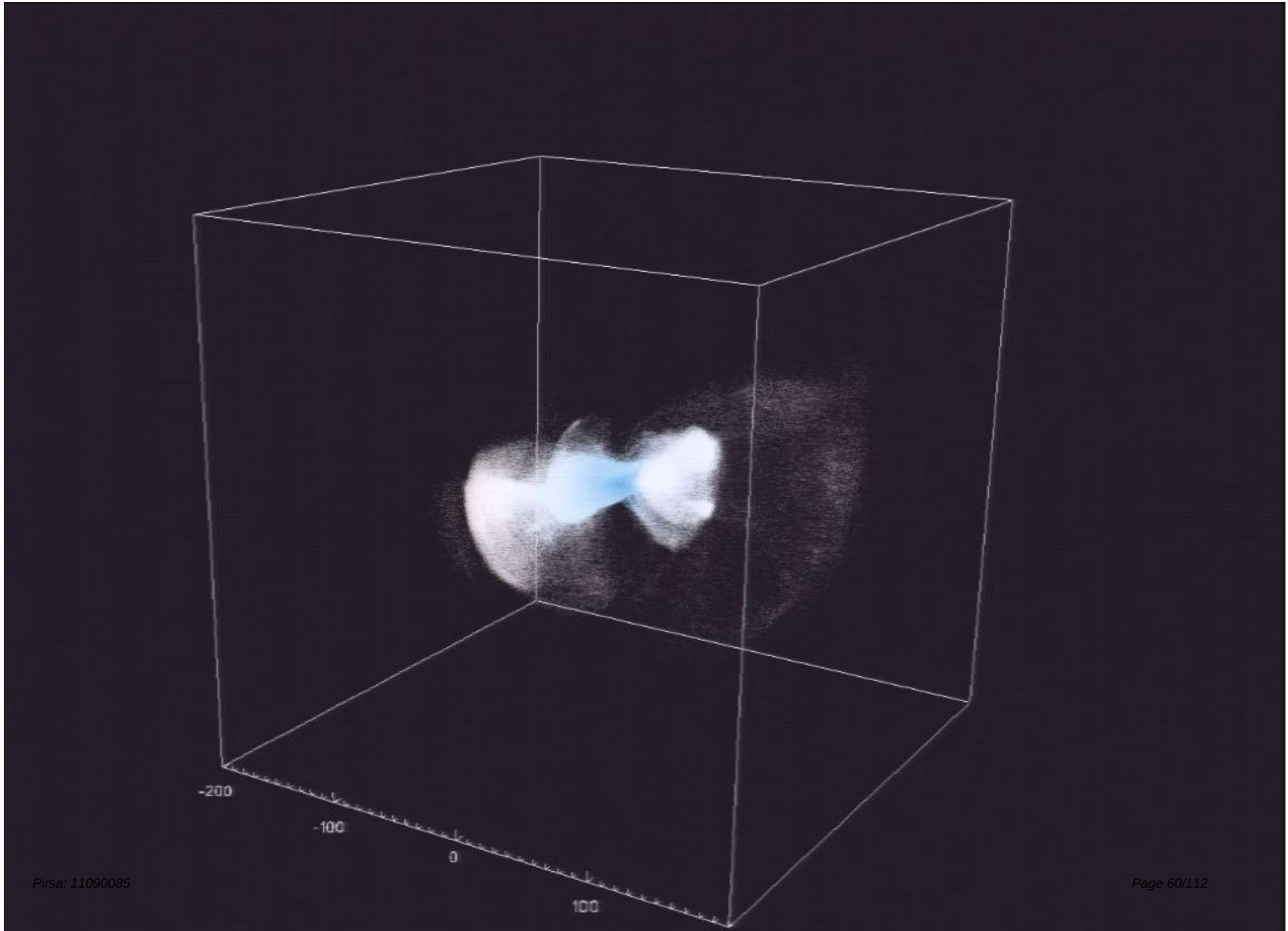
-200
-100
0
100

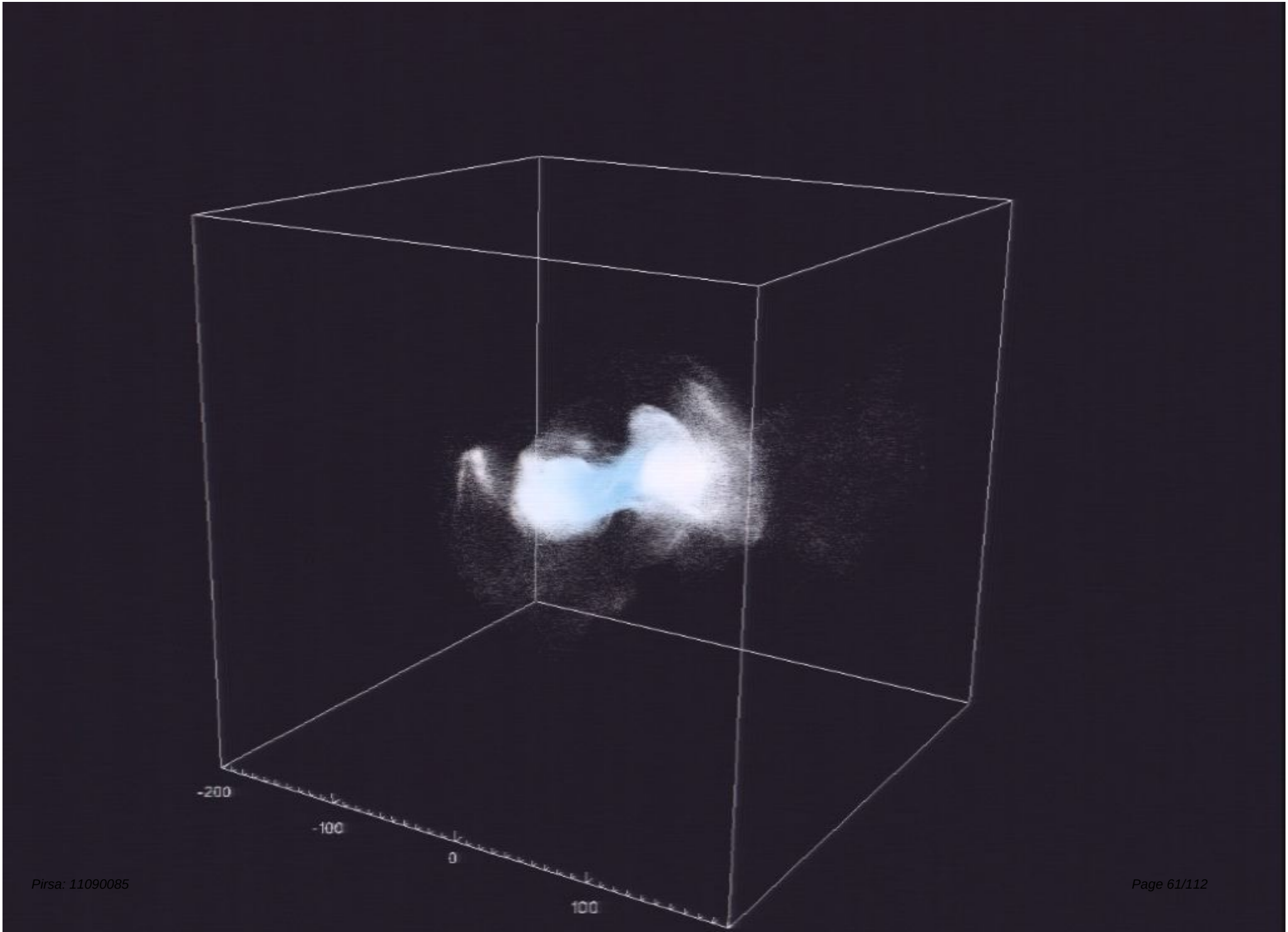
-200
-100
0
100

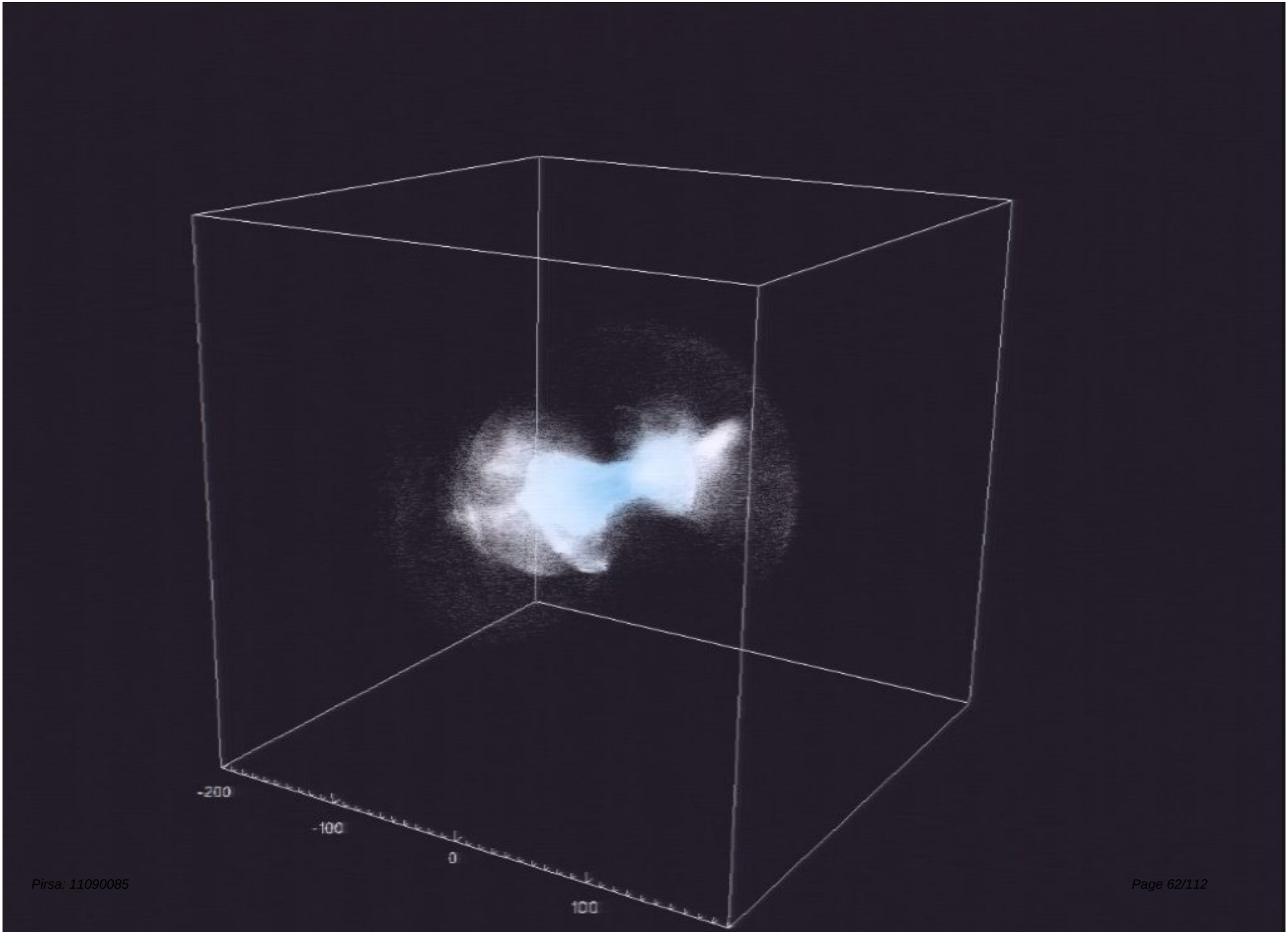
-200
-100
0
100

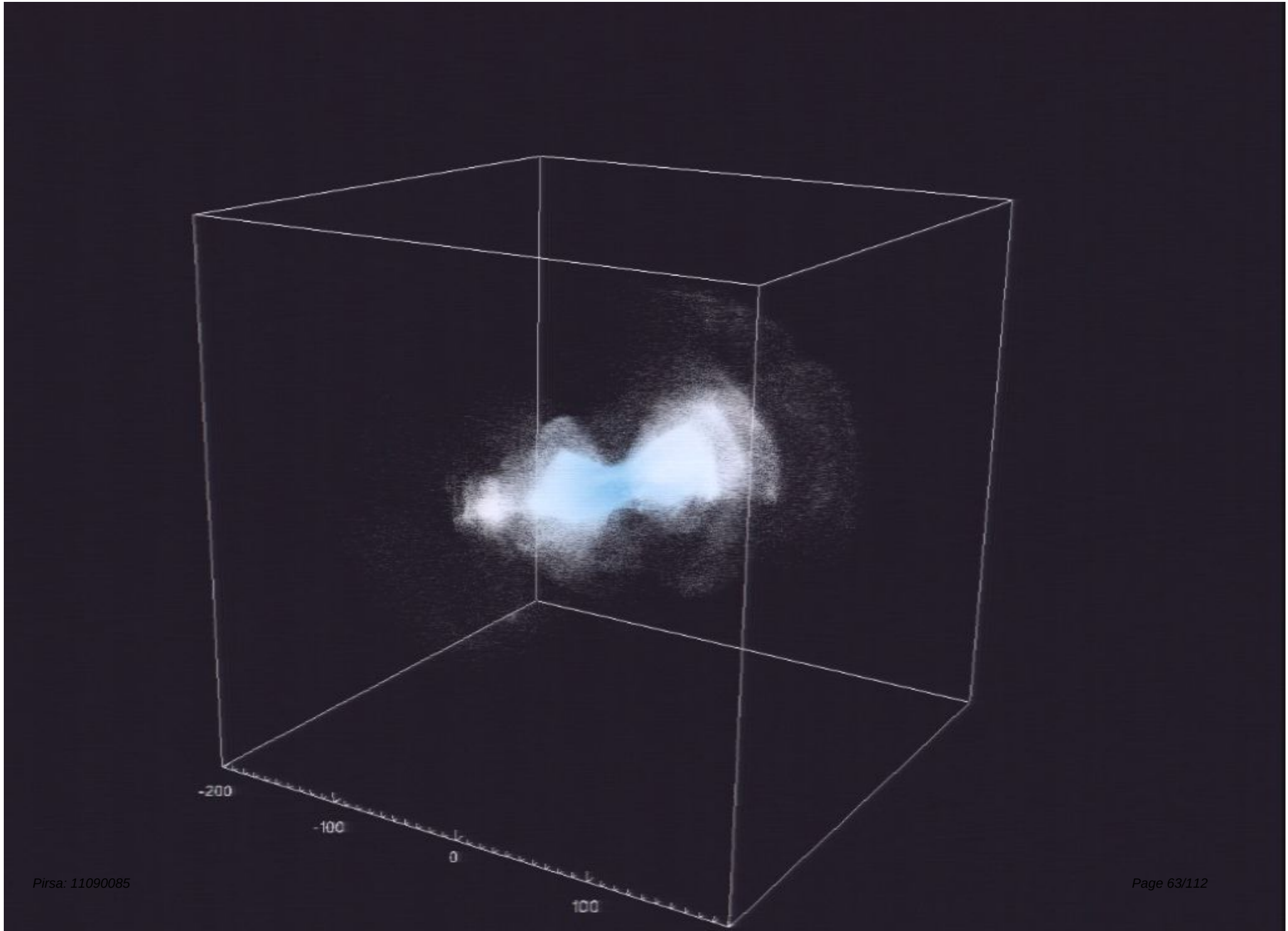
-200
-100
0
100

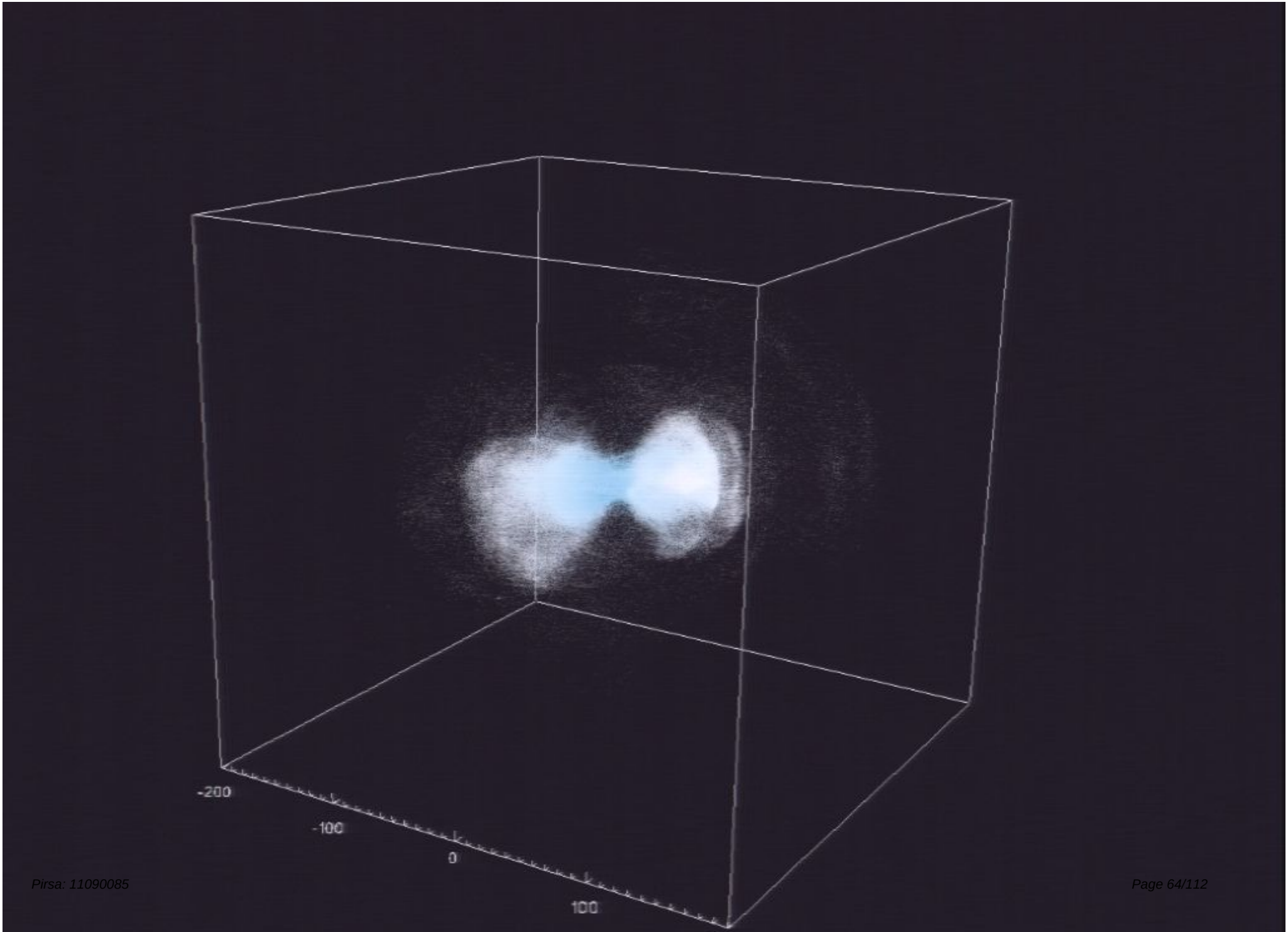
-200
-100
0
100

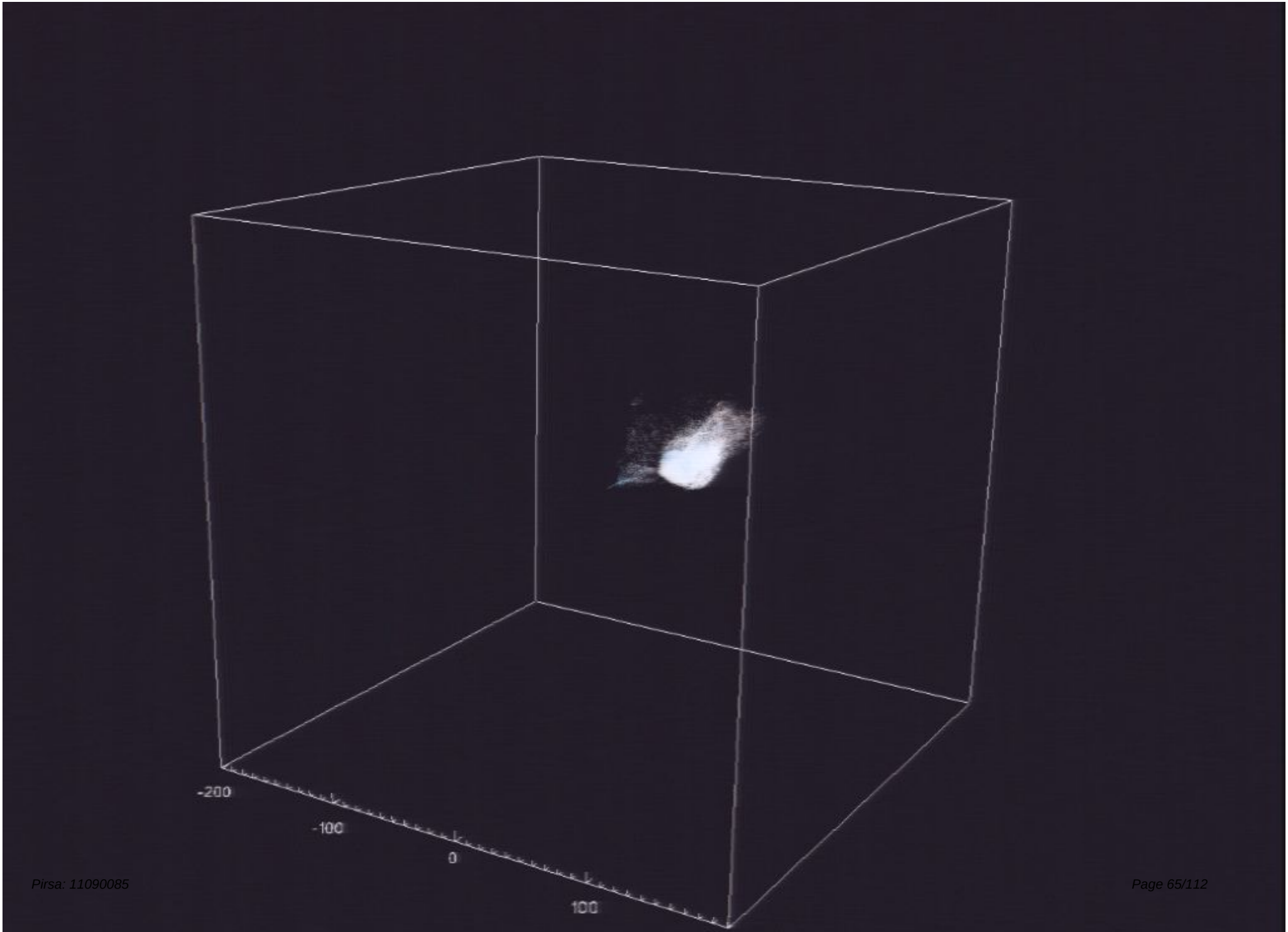
-200
-100
0
100

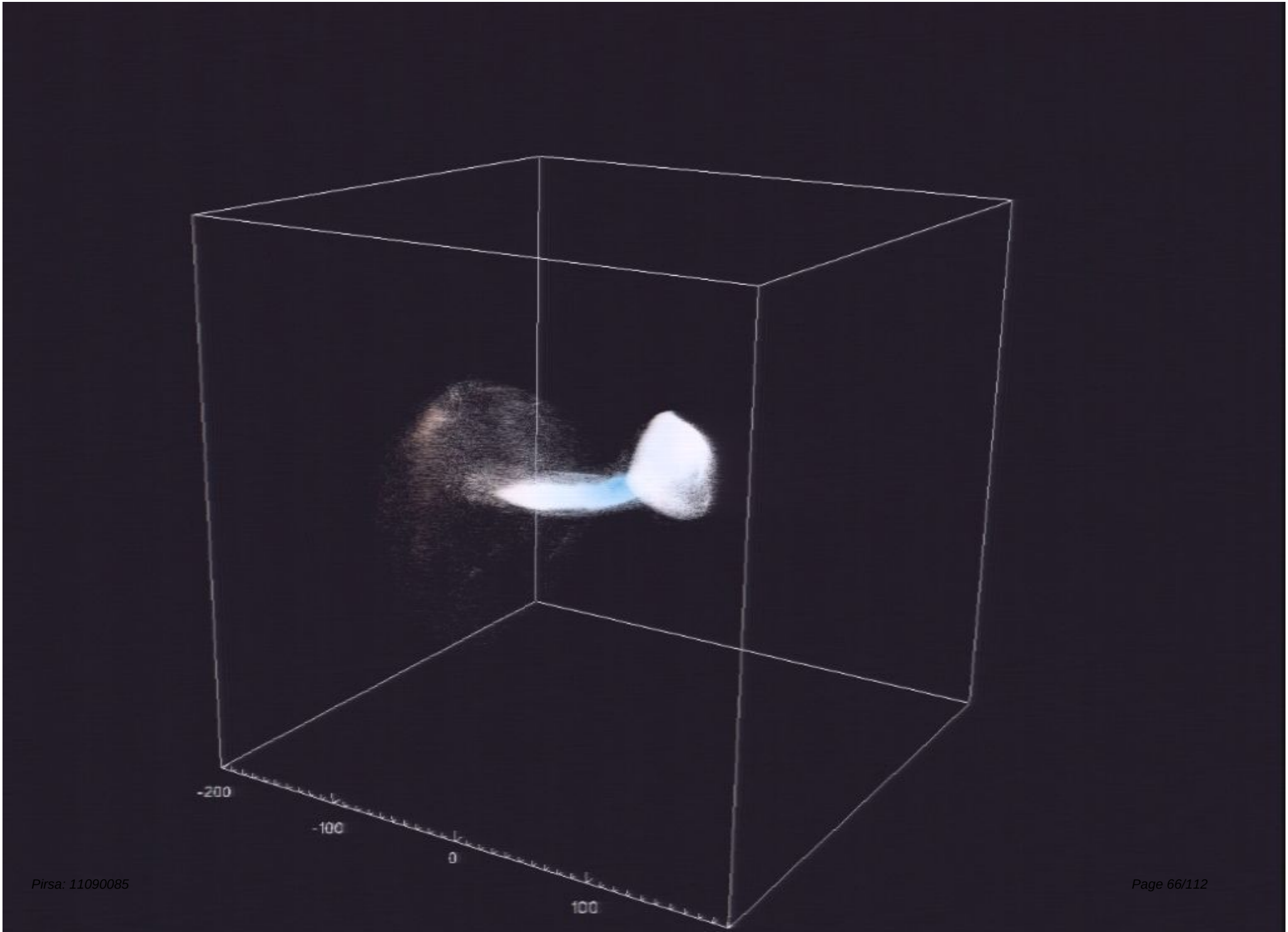
-200
-100
0
100

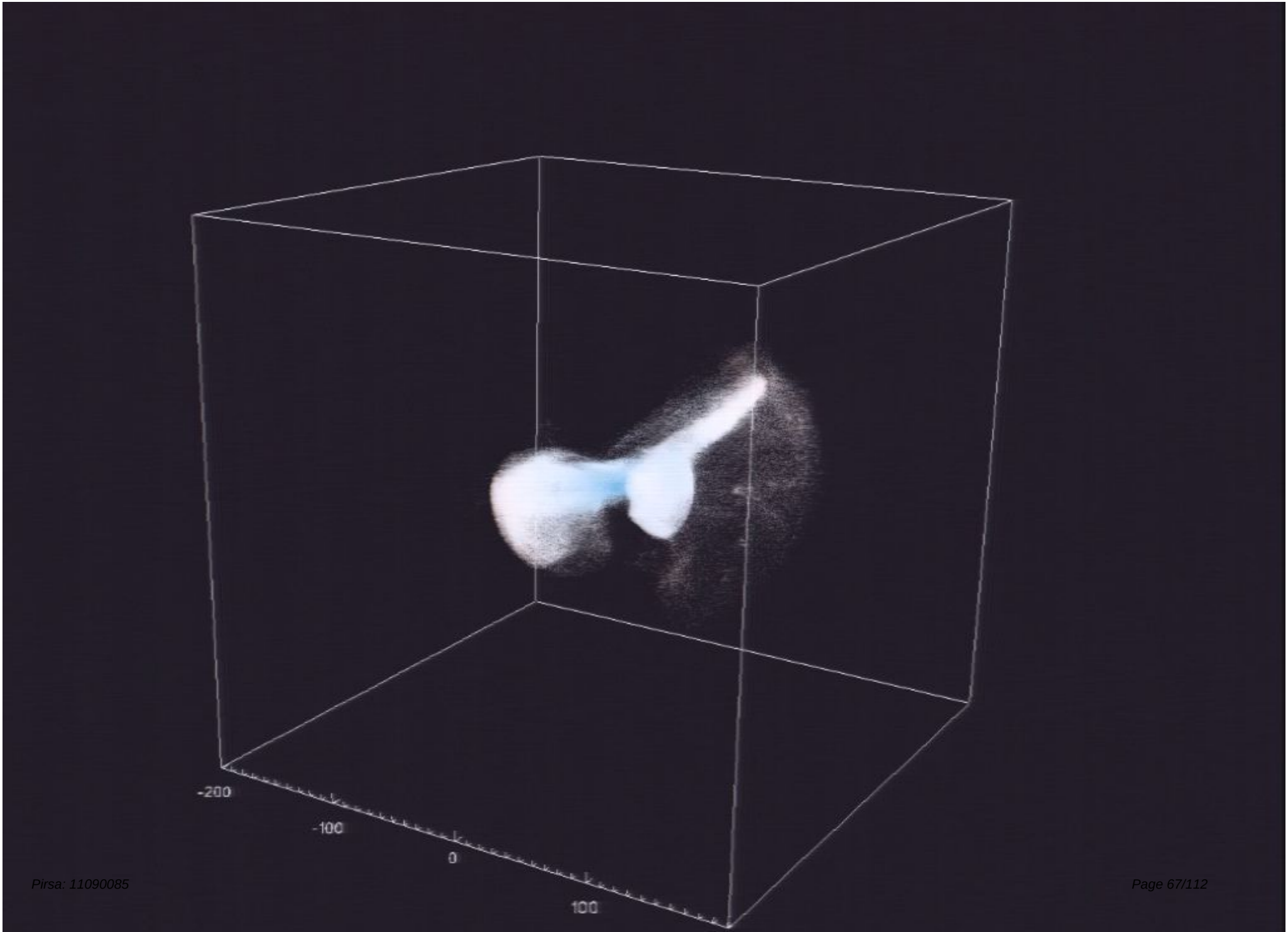
-200
-100
0
100

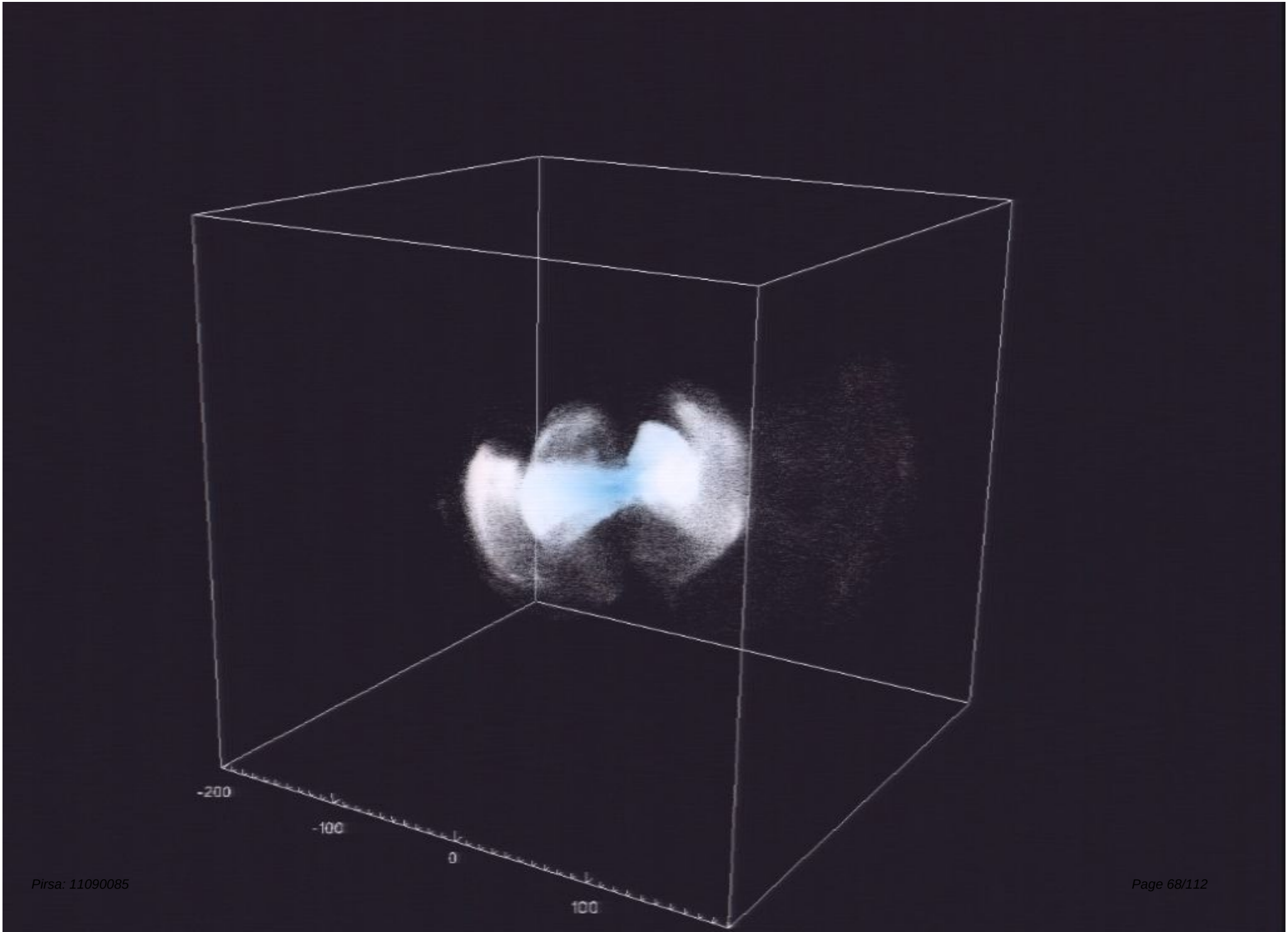
-200
-100
0
100

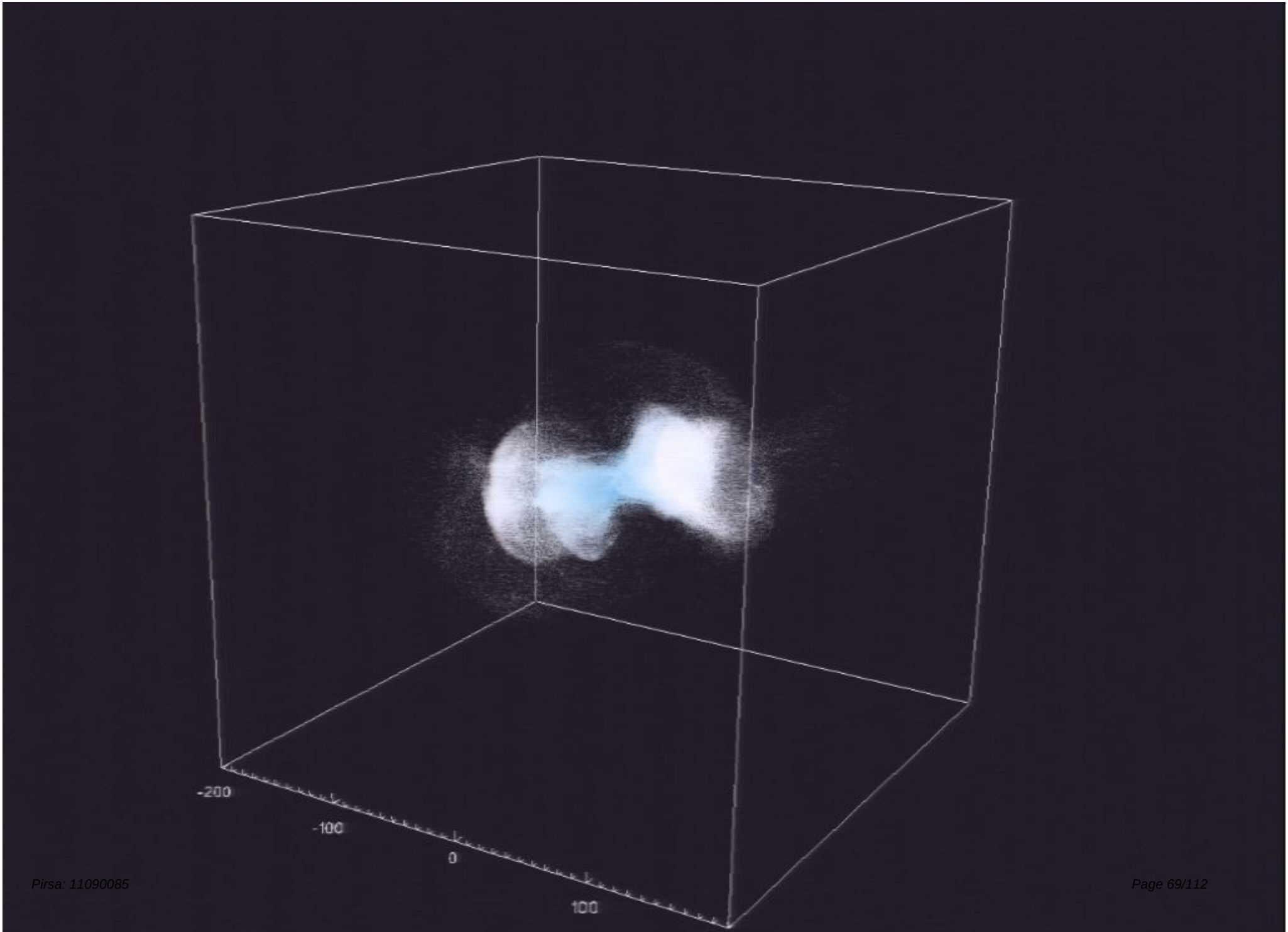
-200
-100
0
100

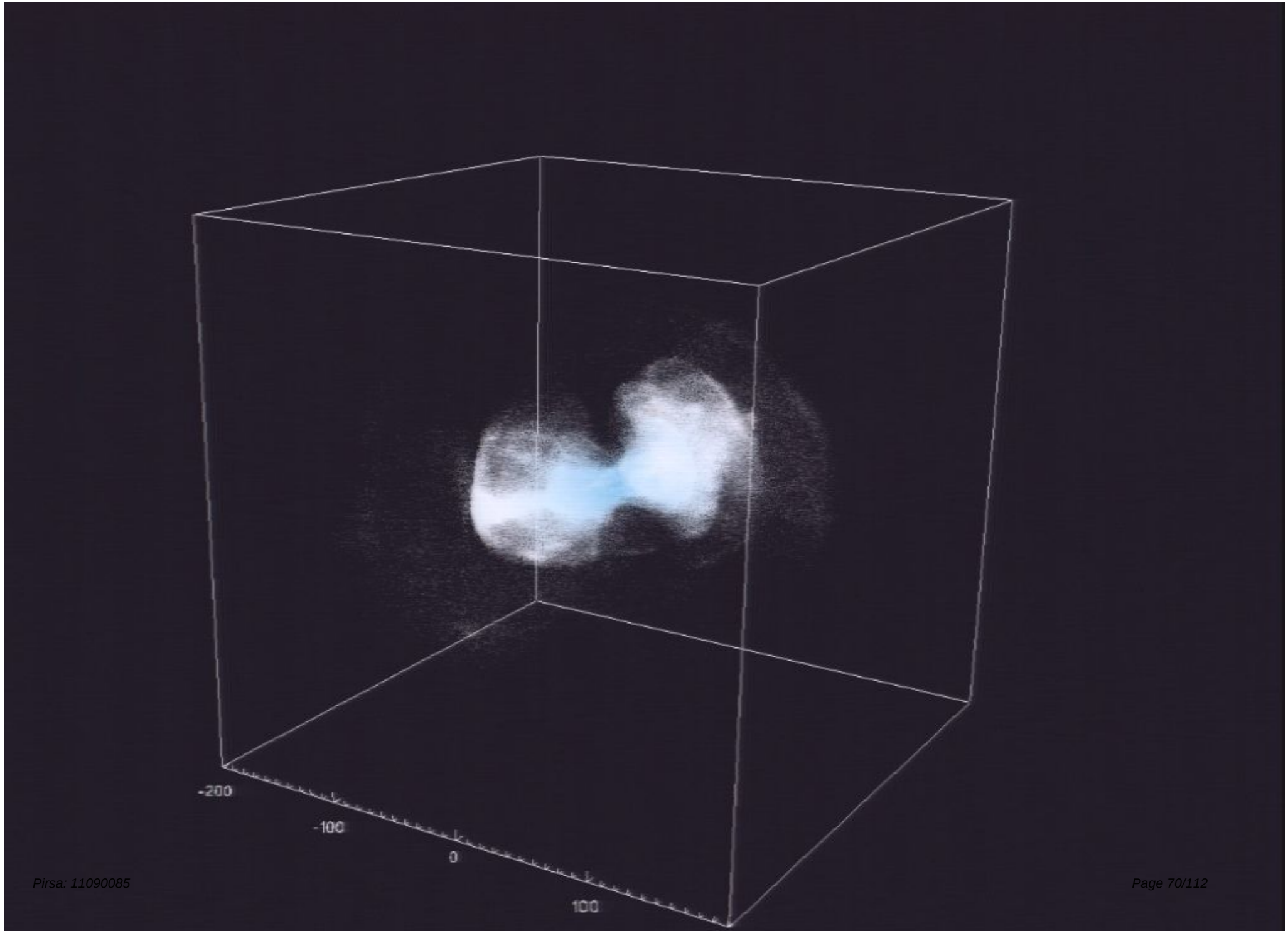
-200
-100
0
100

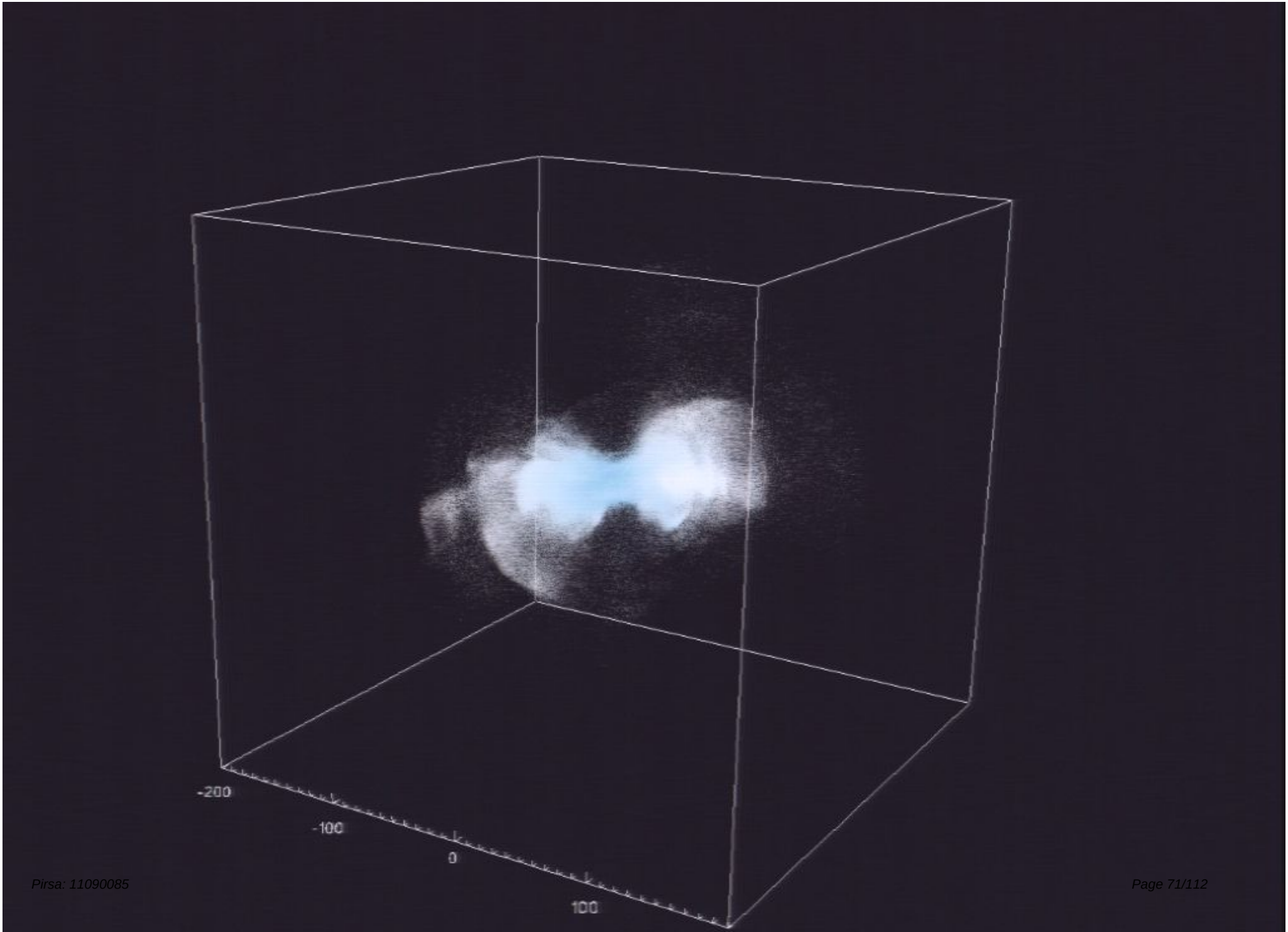
-200
-100
0
100

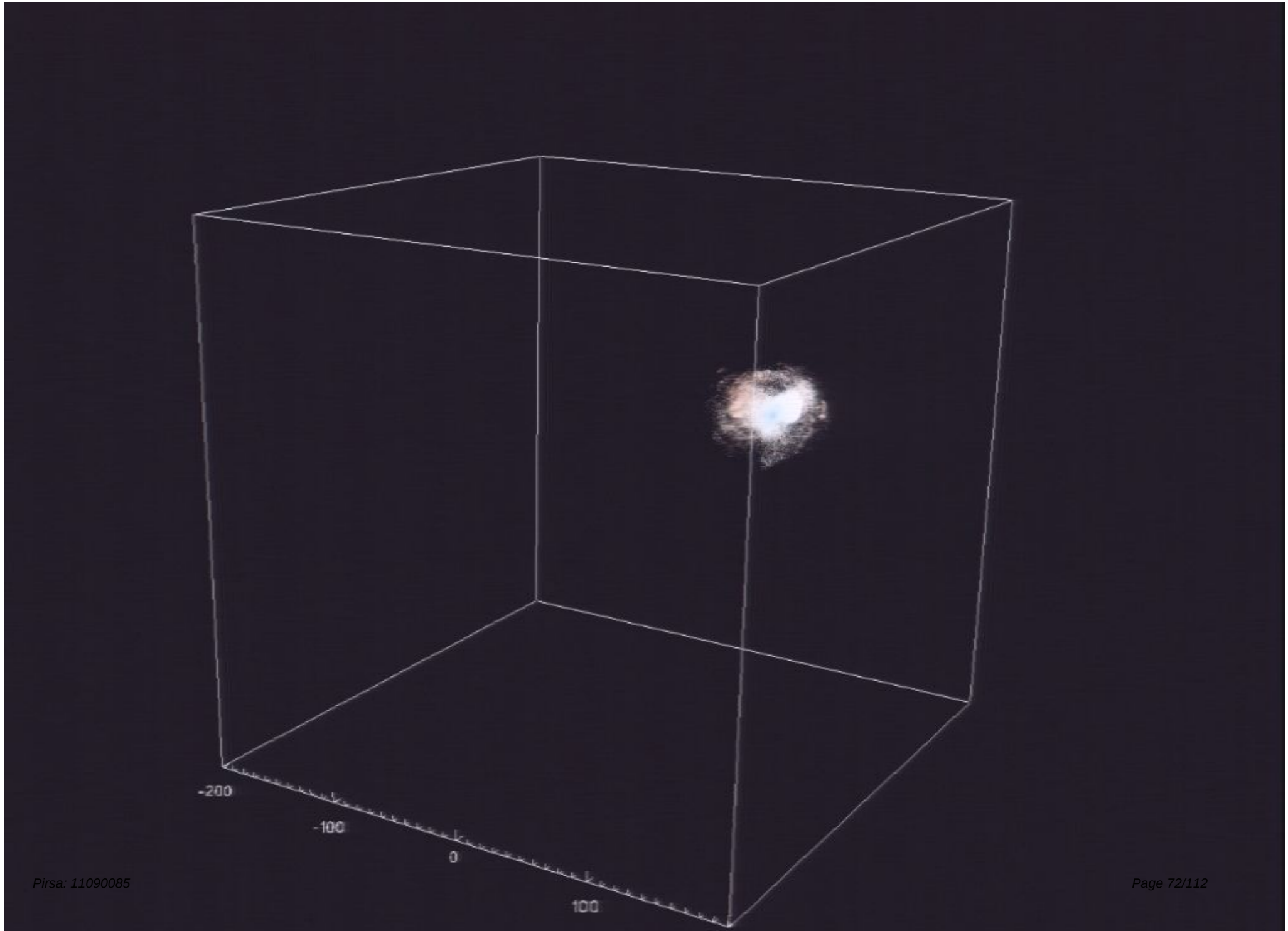
-200
-100
0
100

Velocity Space Substructure: Debris Flow

Recent work with M. Lisanti – **Work in Progress!**

Study of the origin of the velocity space structure by tracking (sub)halo particles though time in the simulation.

Debris ≡ particles that were at some earlier time bound to a subhalo but are unbound at z=0.

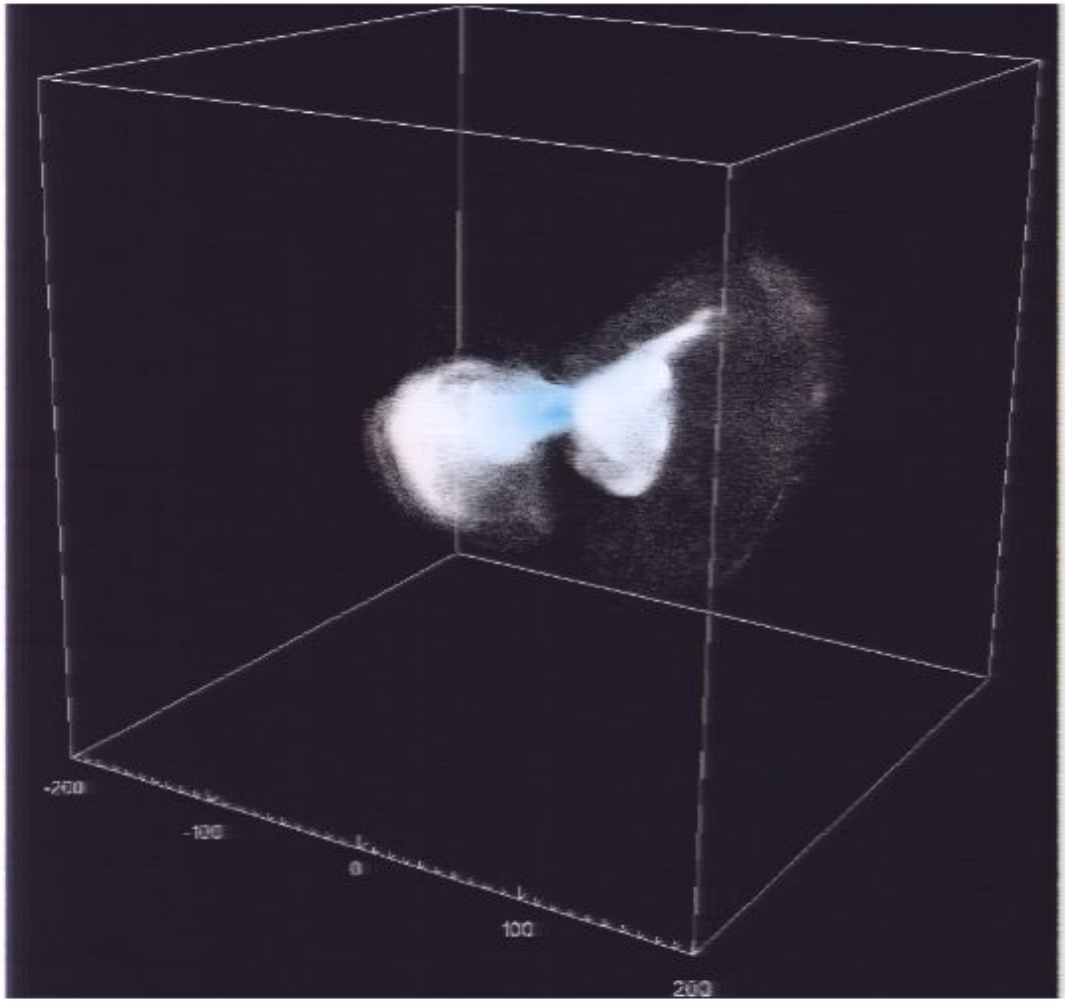

[First pointed out in Lisanti & Spergel 2011 (arXiv:1105.4166)]

Velocity Space Substructure: Debris Flow

Recent work with M. Lisanti – **Work in Progress!**

1) The fraction of debris particles is quite large at high velocities!

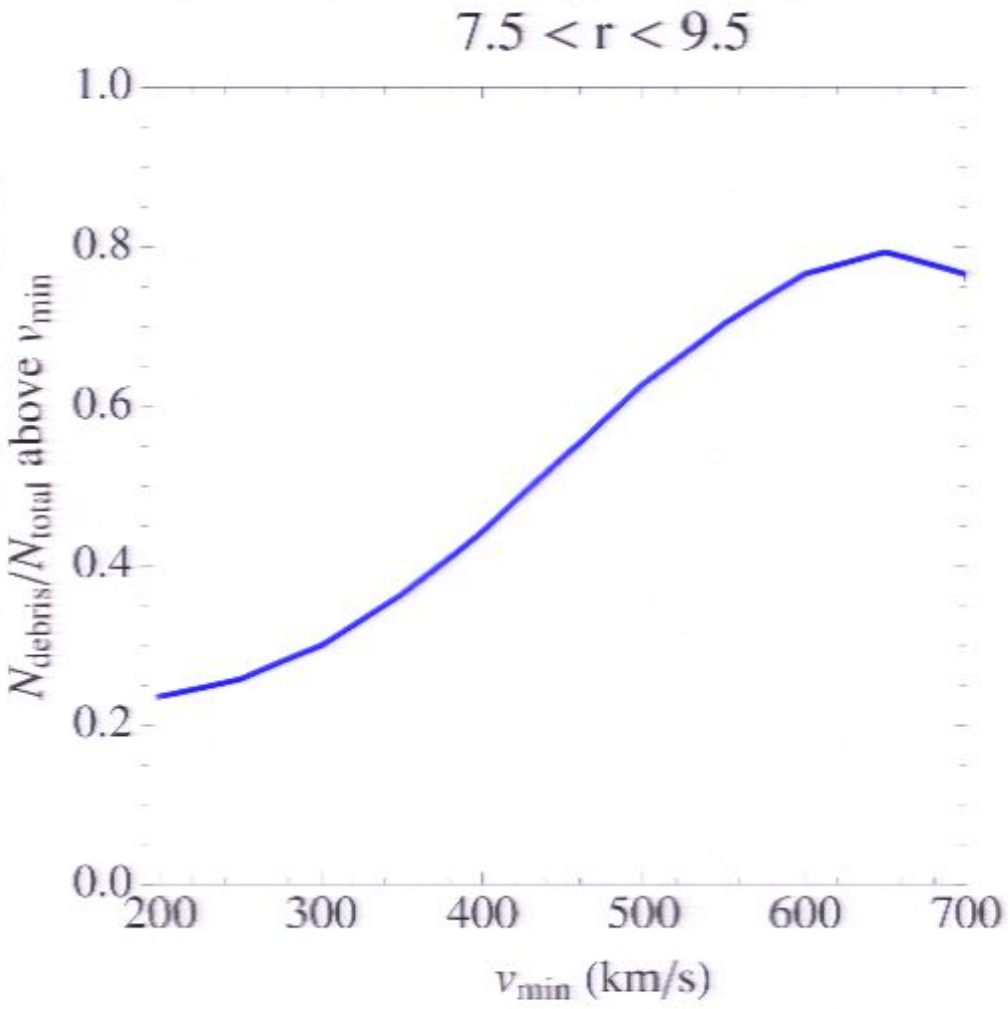

Velocity Space Substructure: Debris Flow

Recent work with M. Lisanti – **Work in Progress!**

1) The fraction of debris particles is quite large at high velocities!

2) **Majority of debris is accreted after z=3 (in last 10 Gyr).**

Redshift Origin of Debris

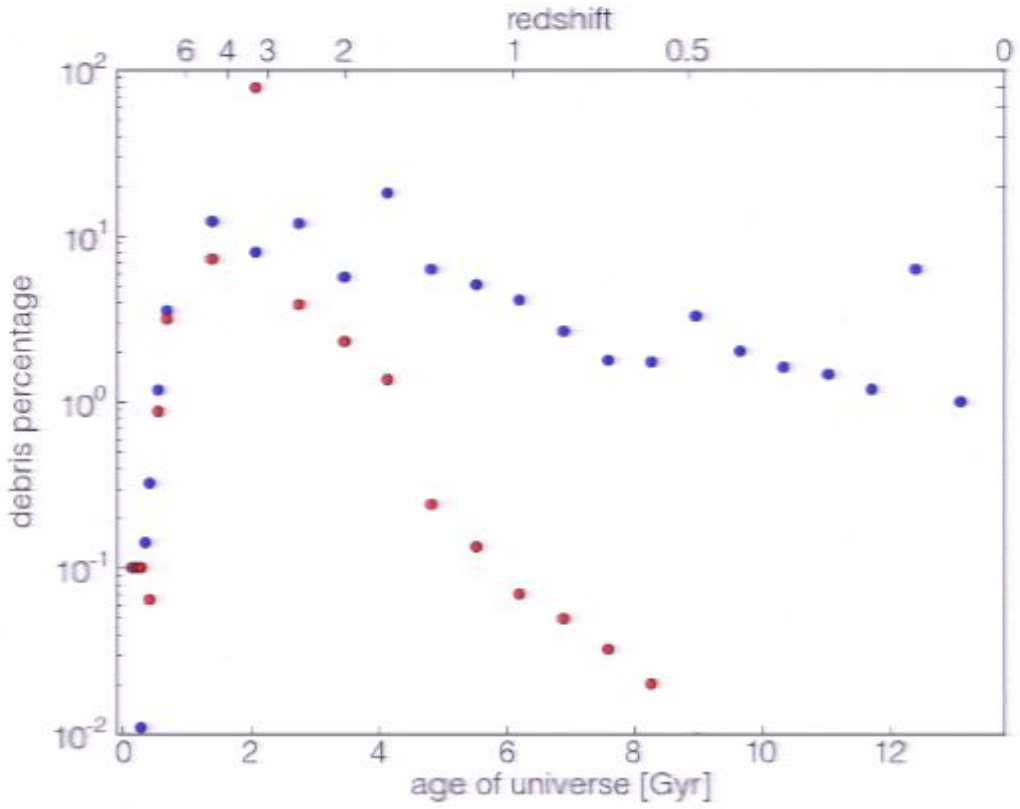

Velocity Space Substructure: Debris Flow

Recent work with M. Lisanti – **Work in Progress!**

1) The fraction of debris particles is quite large at high velocities!

2) Majority of debris is accreted after z=3 (in last 10 Gyr).

3) **Early accreted material is virialized. Later material shows large departures from Maxwellian.**

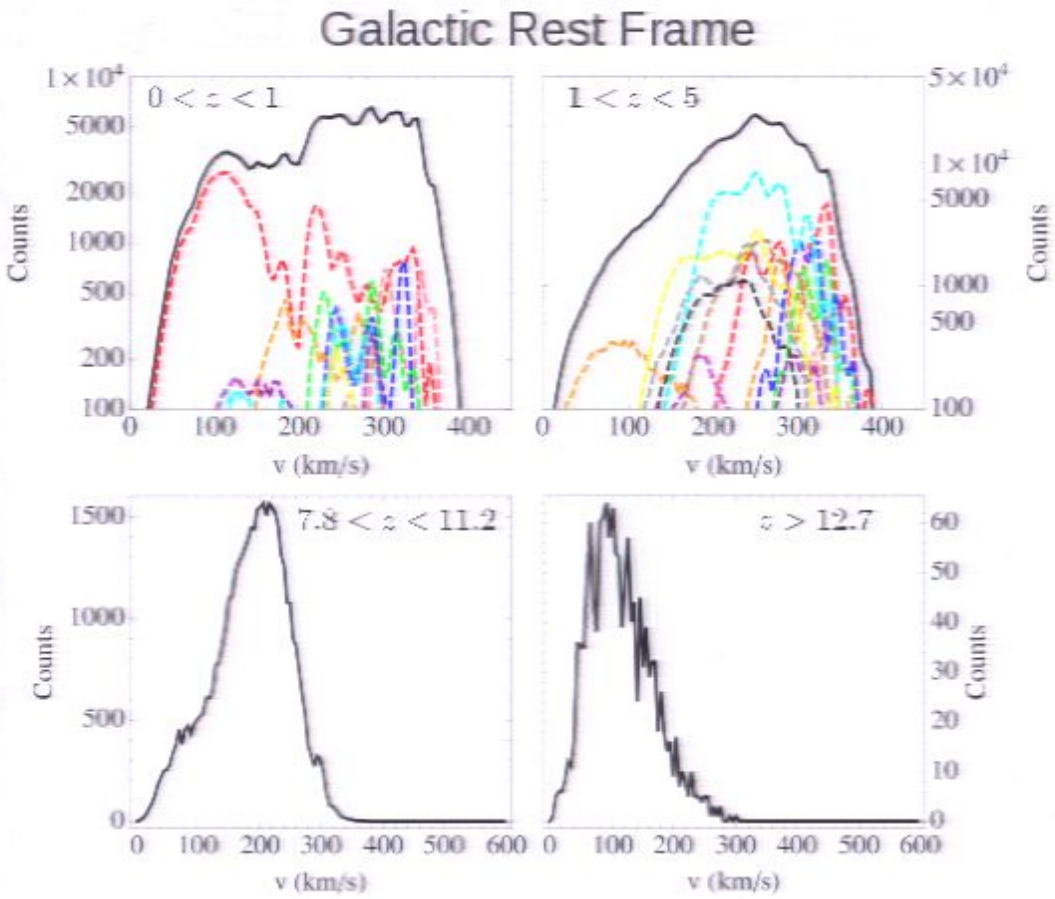

Velocity Space Substructure: Debris Flow

Recent work with M. Lisanti – **Work in Progress!**

1) The fraction of debris particles is quite large at high velocities!

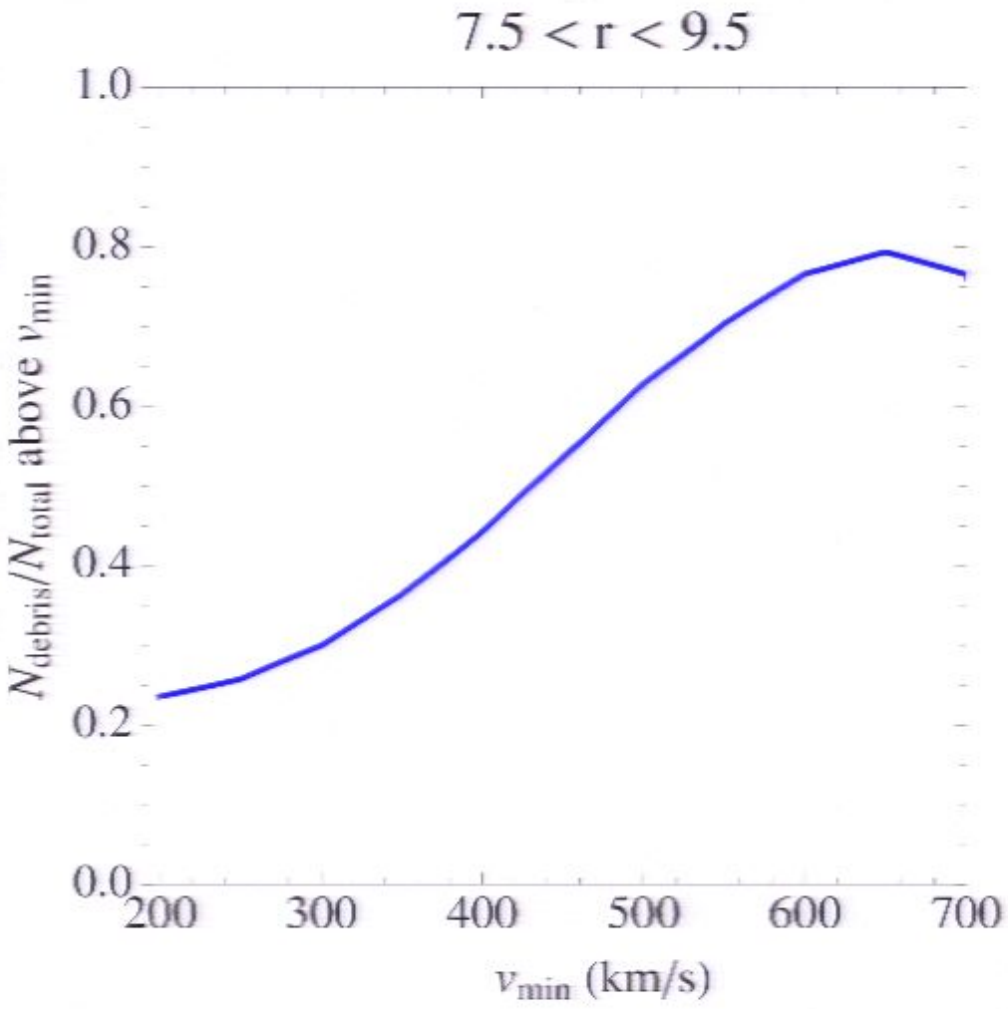

Velocity Space Substructure: Debris Flow

Recent work with M. Lisanti – **Work in Progress!**

1) The fraction of debris particles is quite large at high velocities!

2) Majority of debris is accreted after z=3 (in last 10 Gyr).

3) **Early accreted material is virialized. Later material shows large departures from Maxwellian.**

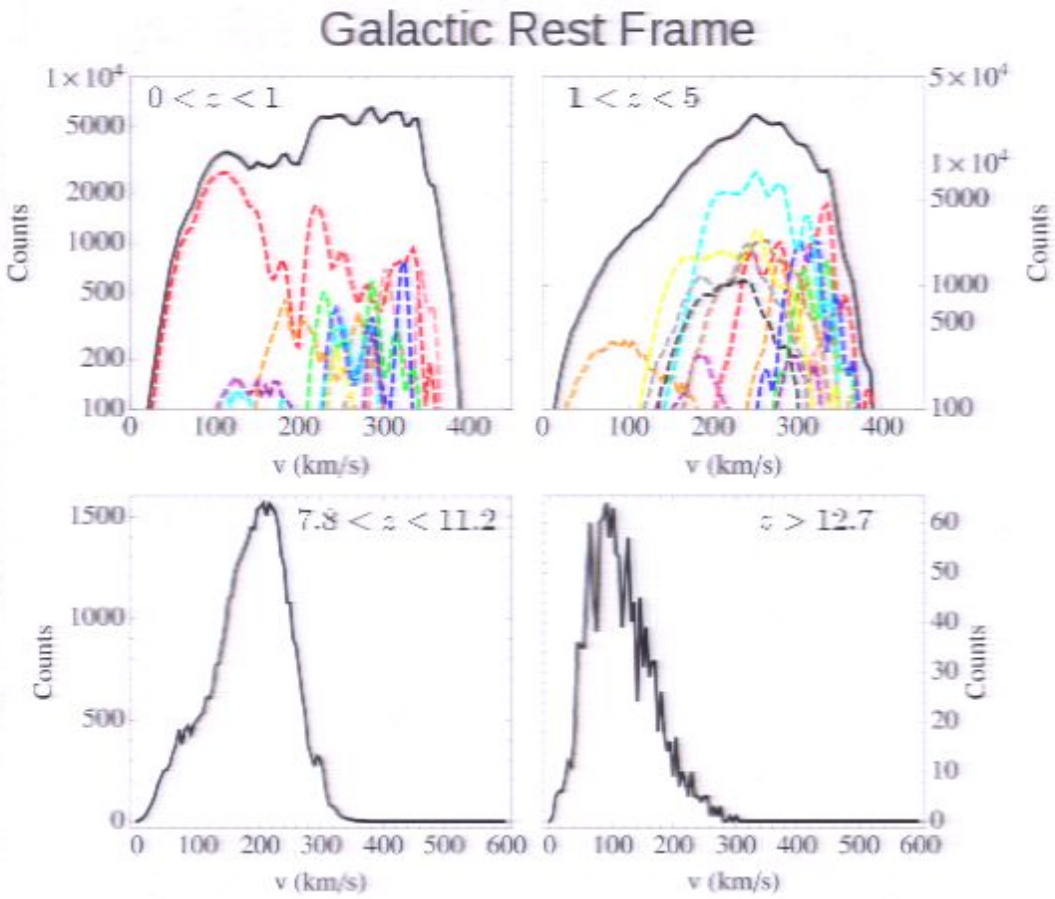

Velocity Space Substructure: Debris Flow

Recent work with M. Lisanti – **Work in Progress!**

1) The fraction of debris particles is quite large at high velocities!

2) **Majority of debris is accreted after z=3 (in last 10 Gyr).**

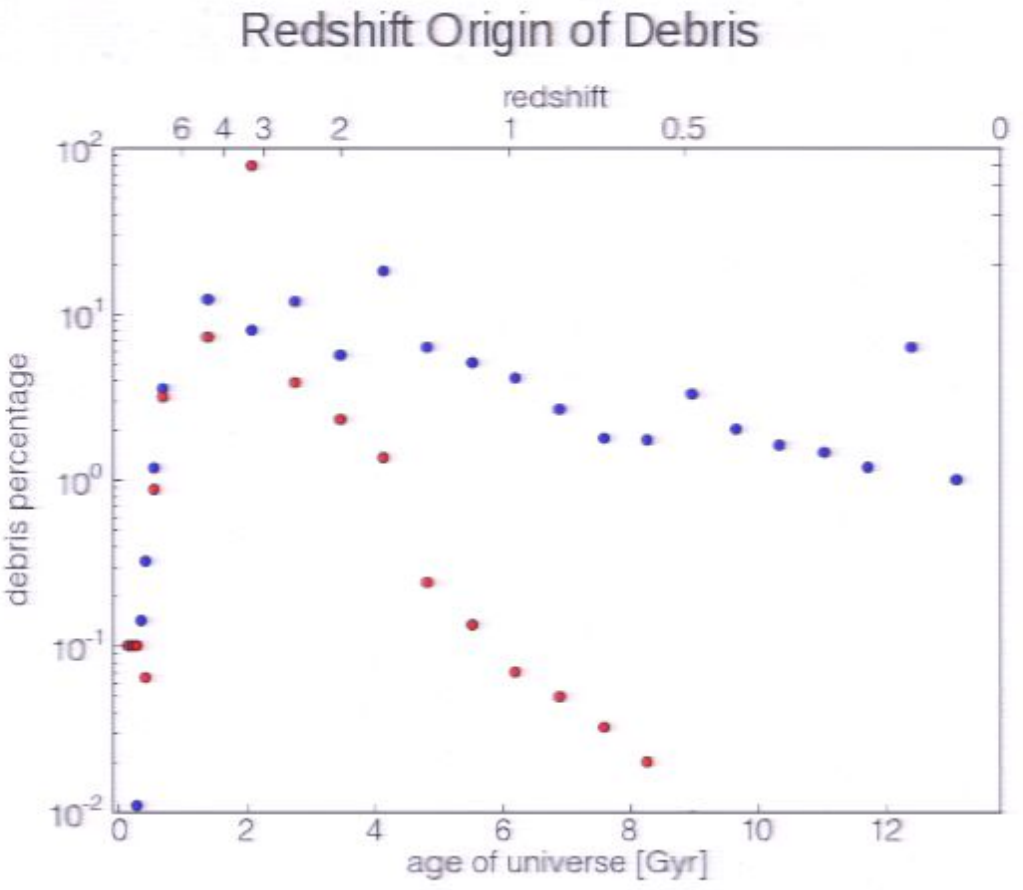

Velocity Space Substructure: Debris Flow

Recent work with M. Lisanti – **Work in Progress!**

1) The fraction of debris particles is quite large at high velocities!

2) Majority of debris is accreted after z=3 (in last 10 Gyr).

3) **Early accreted material is virialized. Later material shows large departures from Maxwellian.**

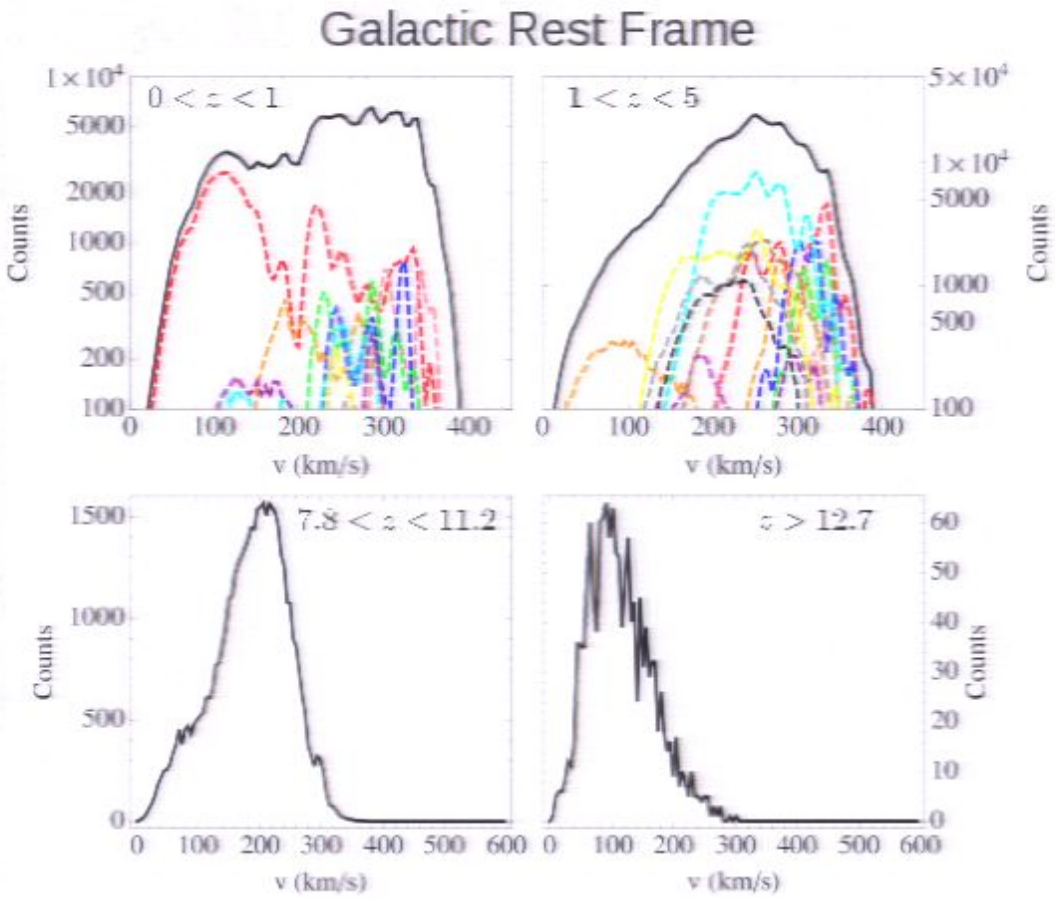

Velocity Space Substructure: Debris Flow

Recent work with M. Lisanti – **Work in Progress!**

1) The fraction of debris particles is quite large at high velocities!

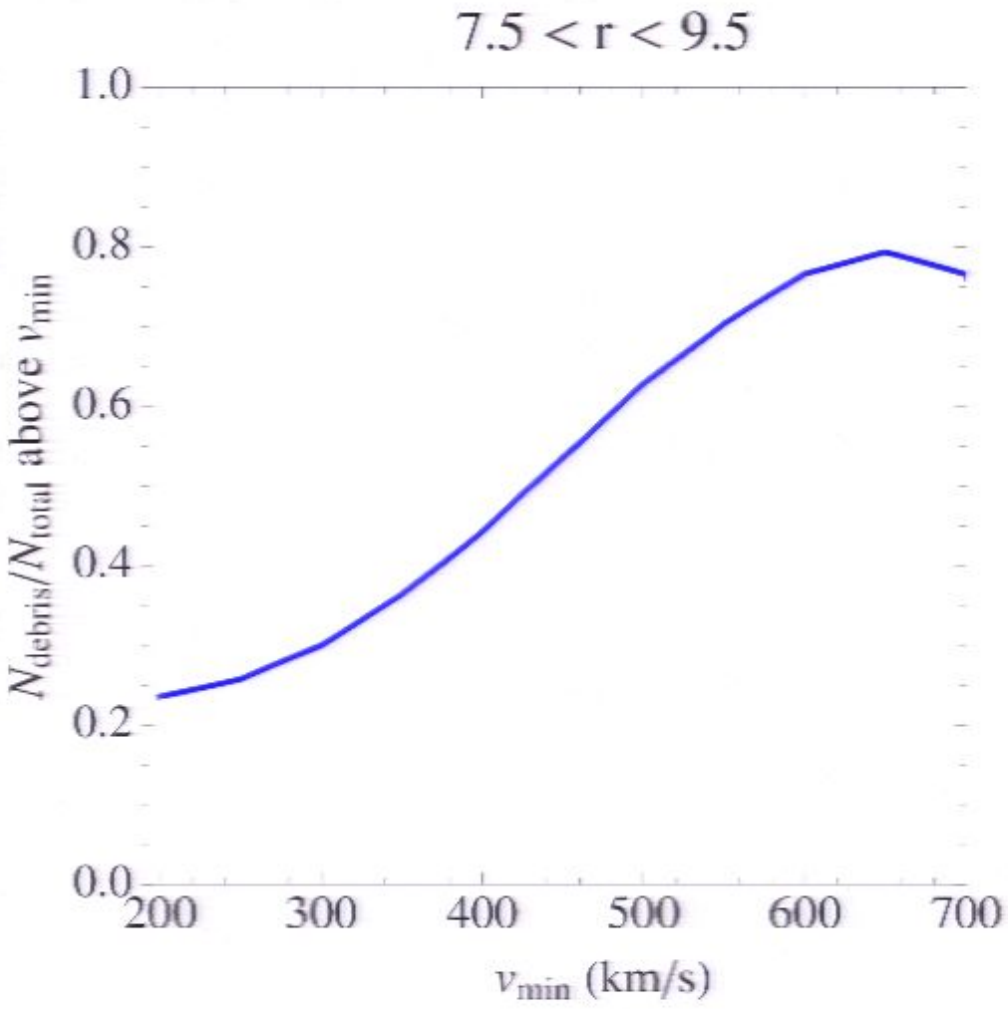

Velocity Space Substructure: Debris Flow

Recent work with M. Lisanti – **Work in Progress!**

1) The fraction of debris particles is quite large at high velocities!

2) Majority of debris is accreted after z=3 (in last 10 Gyr).

3) **Early accreted material is virialized. Later material shows large departures from Maxwellian.**

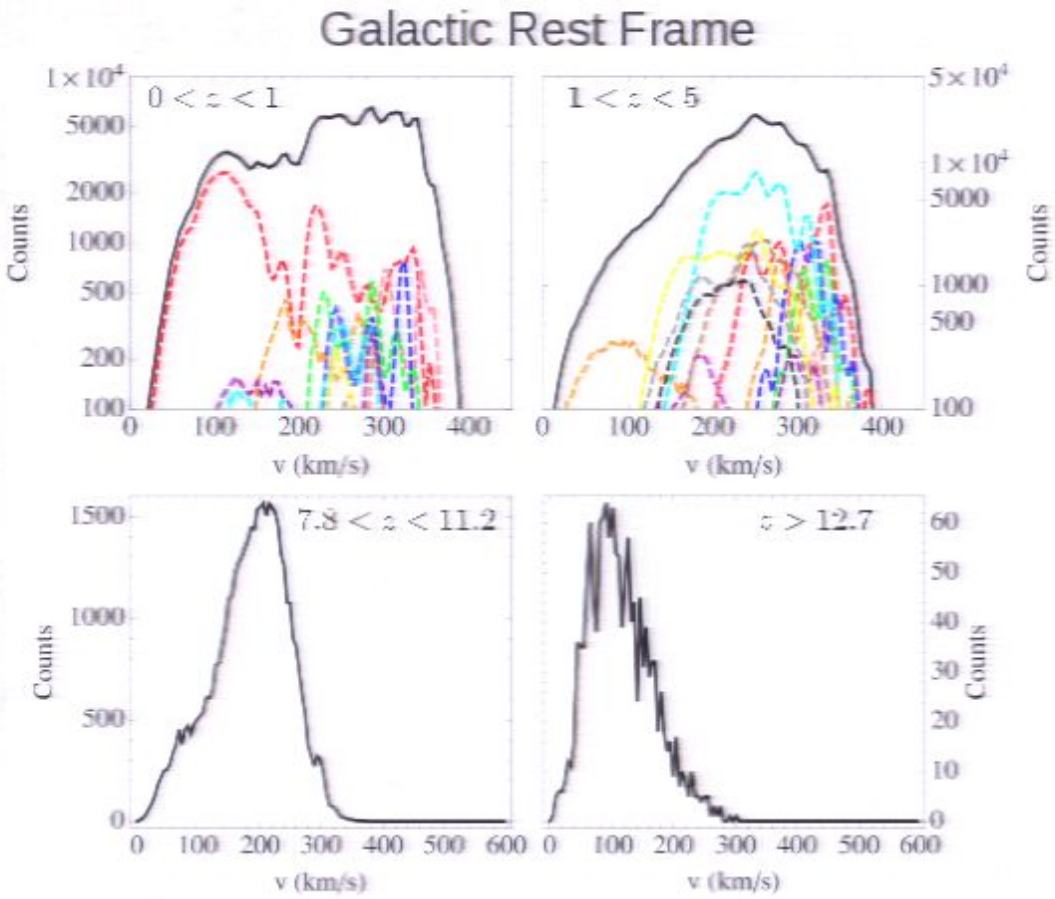

Velocity Space Substructure: Debris Flow

Recent work with M. Lisanti – **Work in Progress!**

1) The fraction of debris particles is quite large at high velocities!

2) Majority of debris is accreted after $z=3$ (in last 10 Gyr).

3) **Early accreted material is virialized. Later material shows large departures from Maxwellian.**

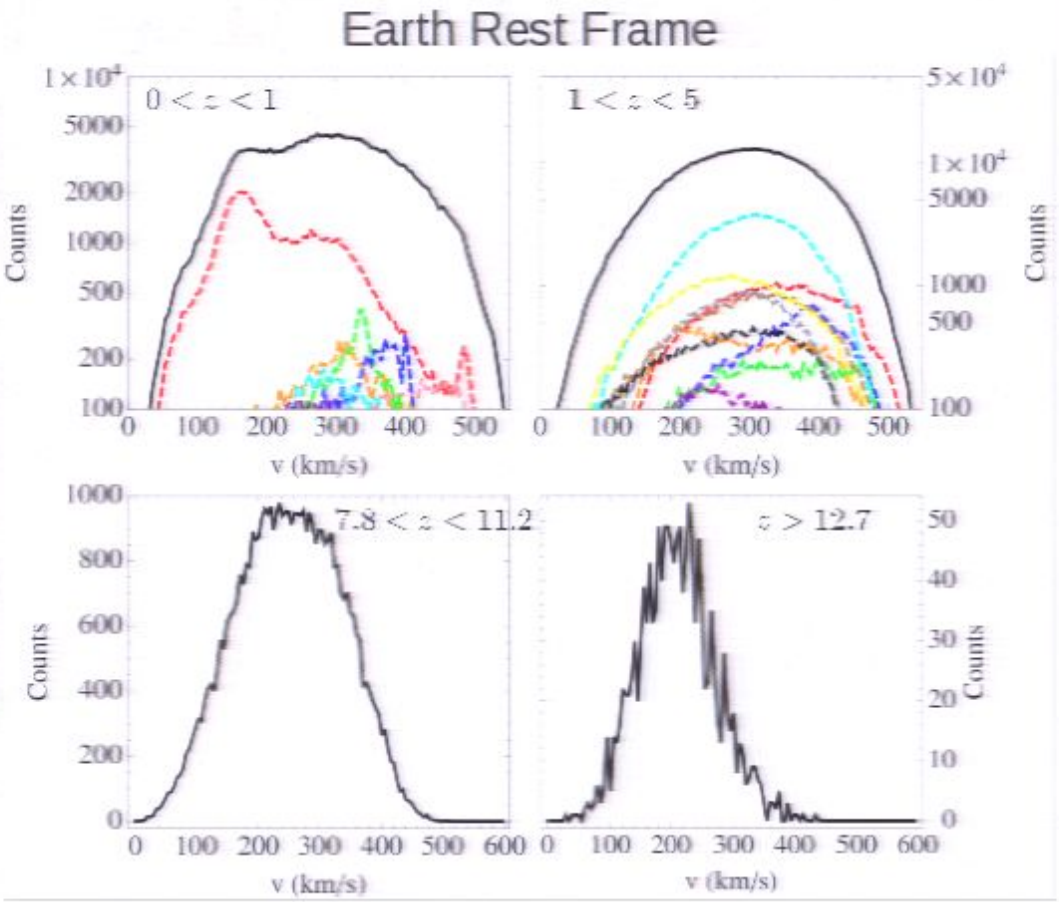

Velocity Space Substructure: Debris Flow

Some example halo orbits:

ID: 15782

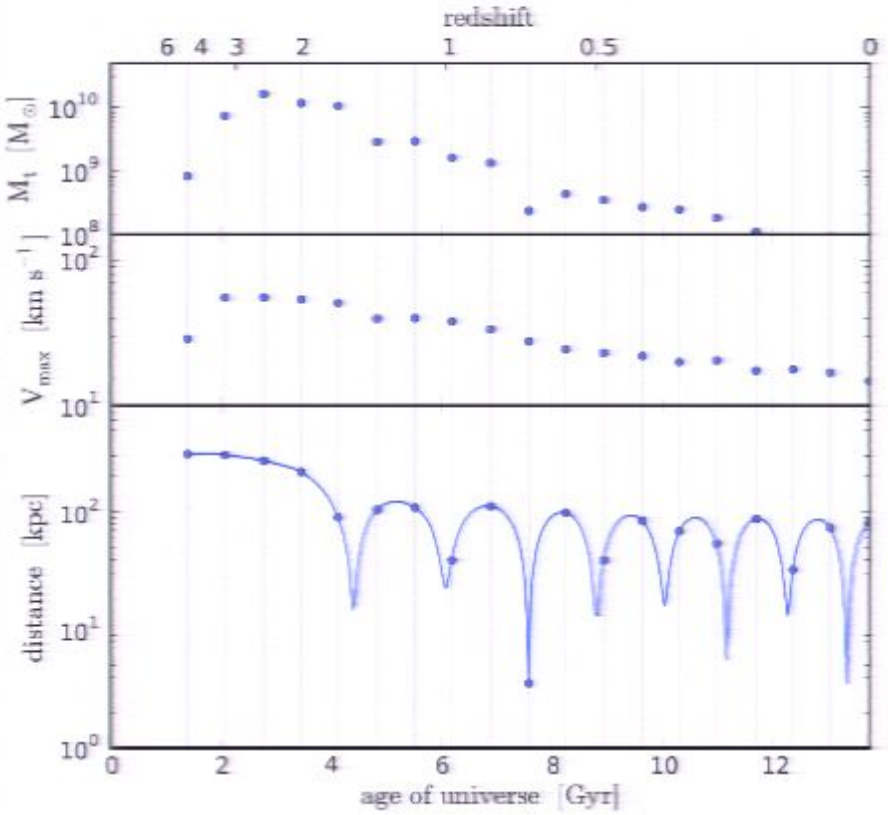

ID: 19624

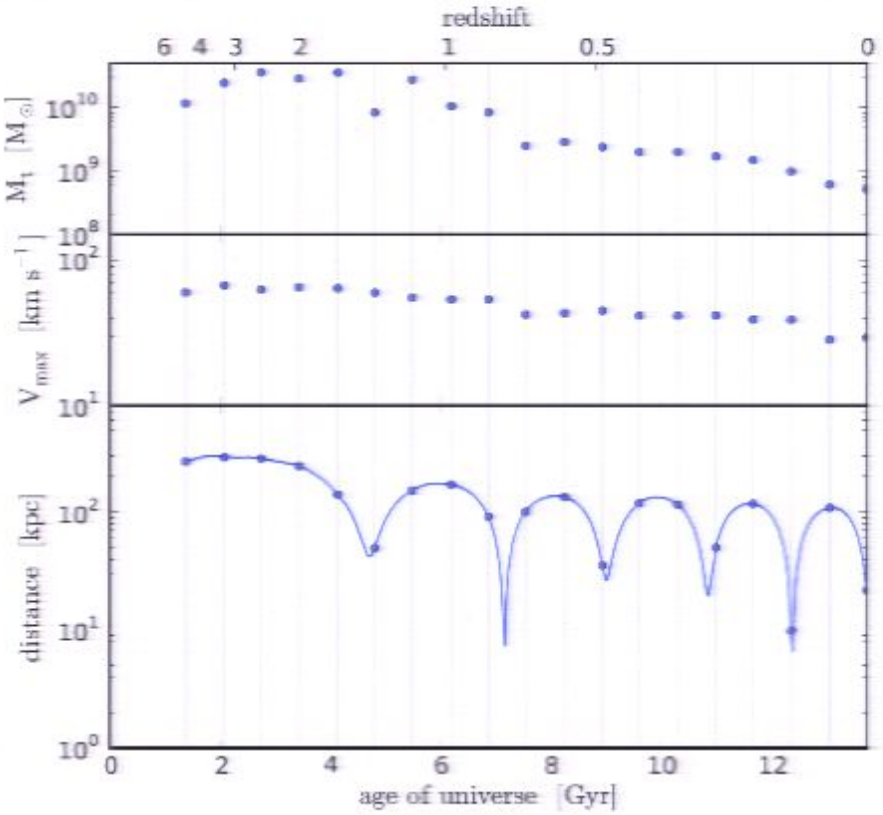

Recent work with M. Lisanti – **Work in Progress!**

Velocity Space Substructure: Debris Flow

Recent work with M. Lisanti – **Work in Progress!**

1) The fraction of debris particles is quite large at high velocities!

2) Majority of debris is accreted after z=3 (in last 10 Gyr).

3) **Early accreted material is virialized. Later material shows large departures from Maxwellian.**

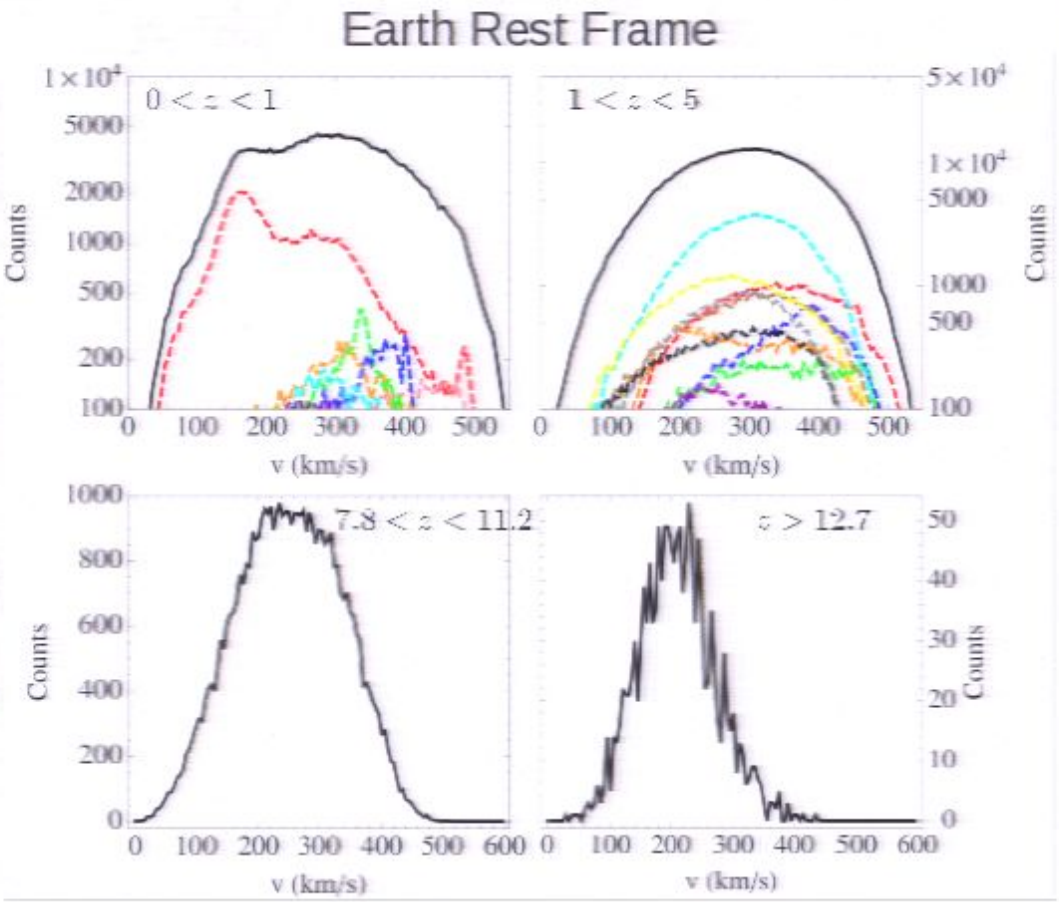

Velocity Space Substructure: Debris Flow

Some example halo orbits:

ID: 15782

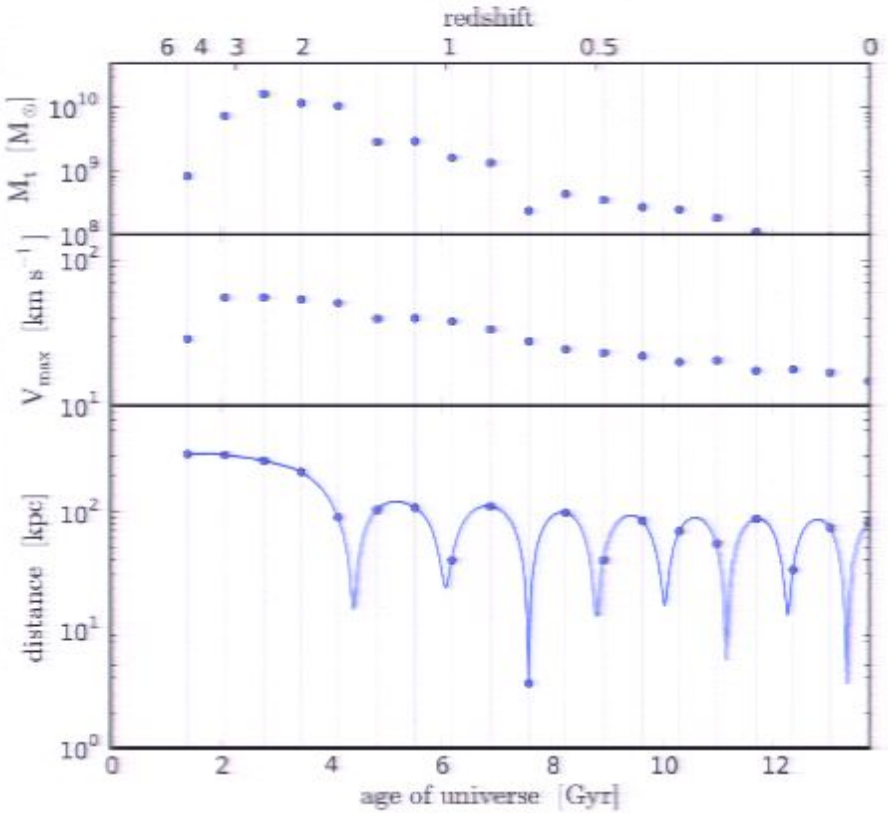

ID: 19624

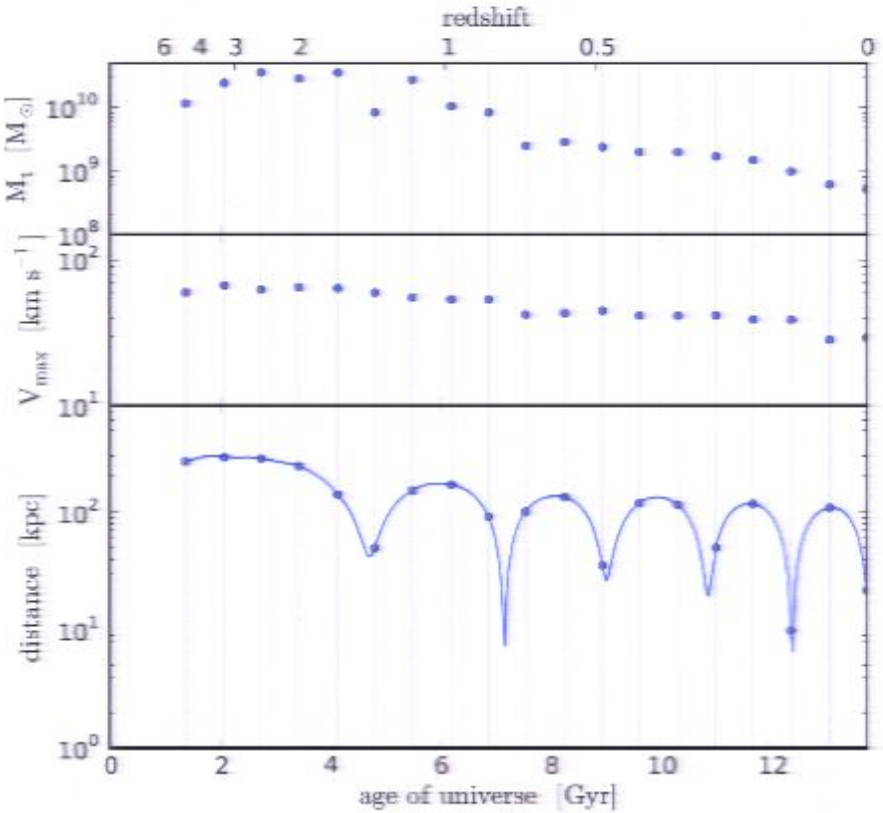

Recent work with M. Lisanti – **Work in Progress!**

Velocity Space Substructure: Debris Flow

Some example halo orbits:

ID: 19728

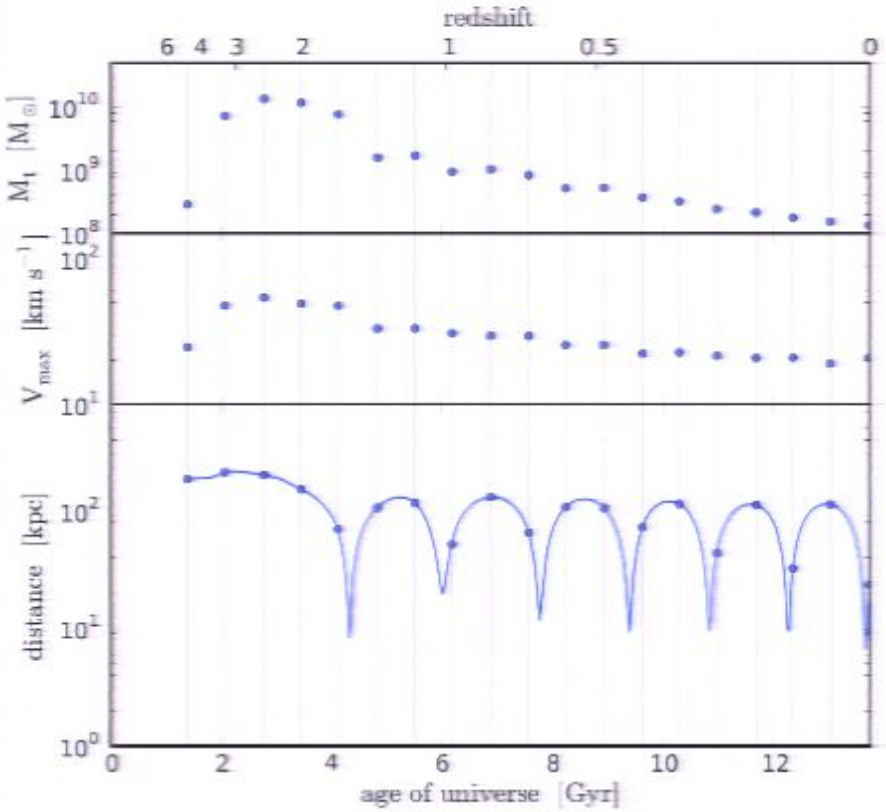

ID: 19765

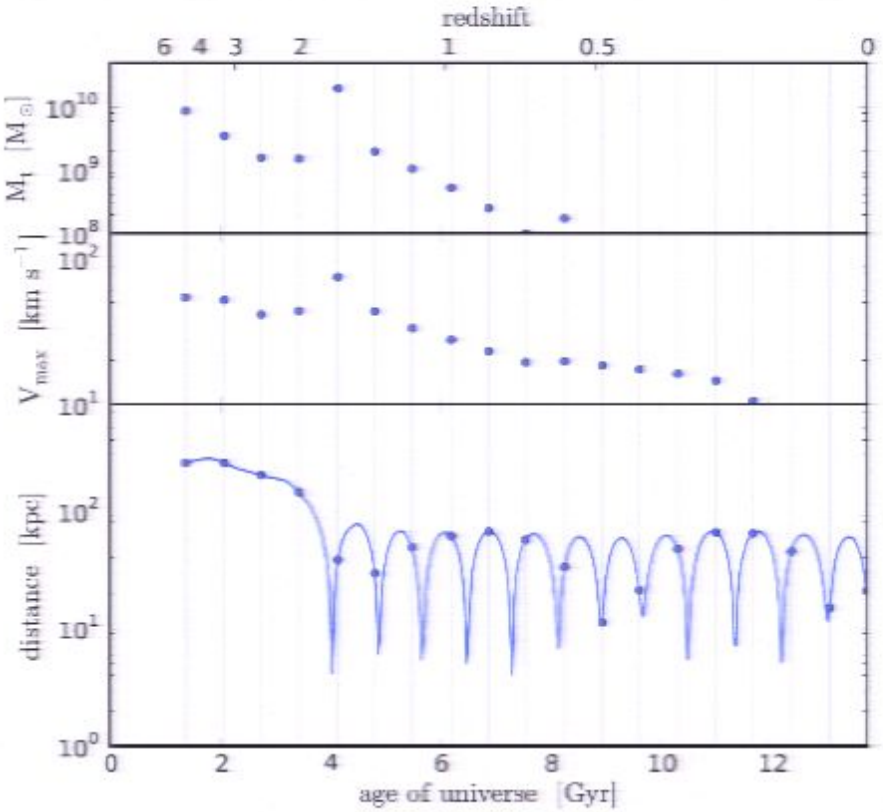

Recent work with M. Lisanti – **Work in Progress!**

Velocity Space Substructure: Debris Flow

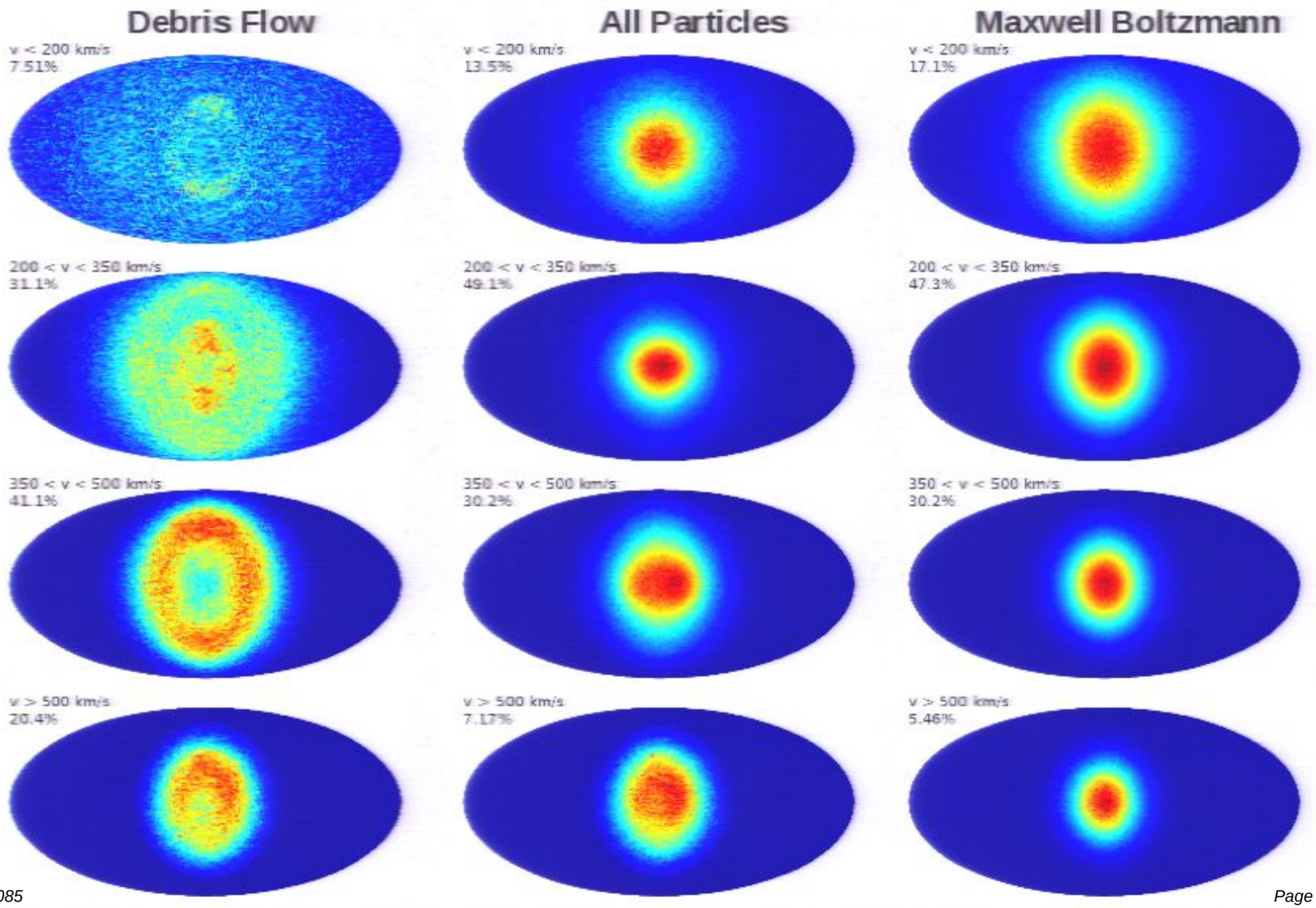

The Eris Simulation

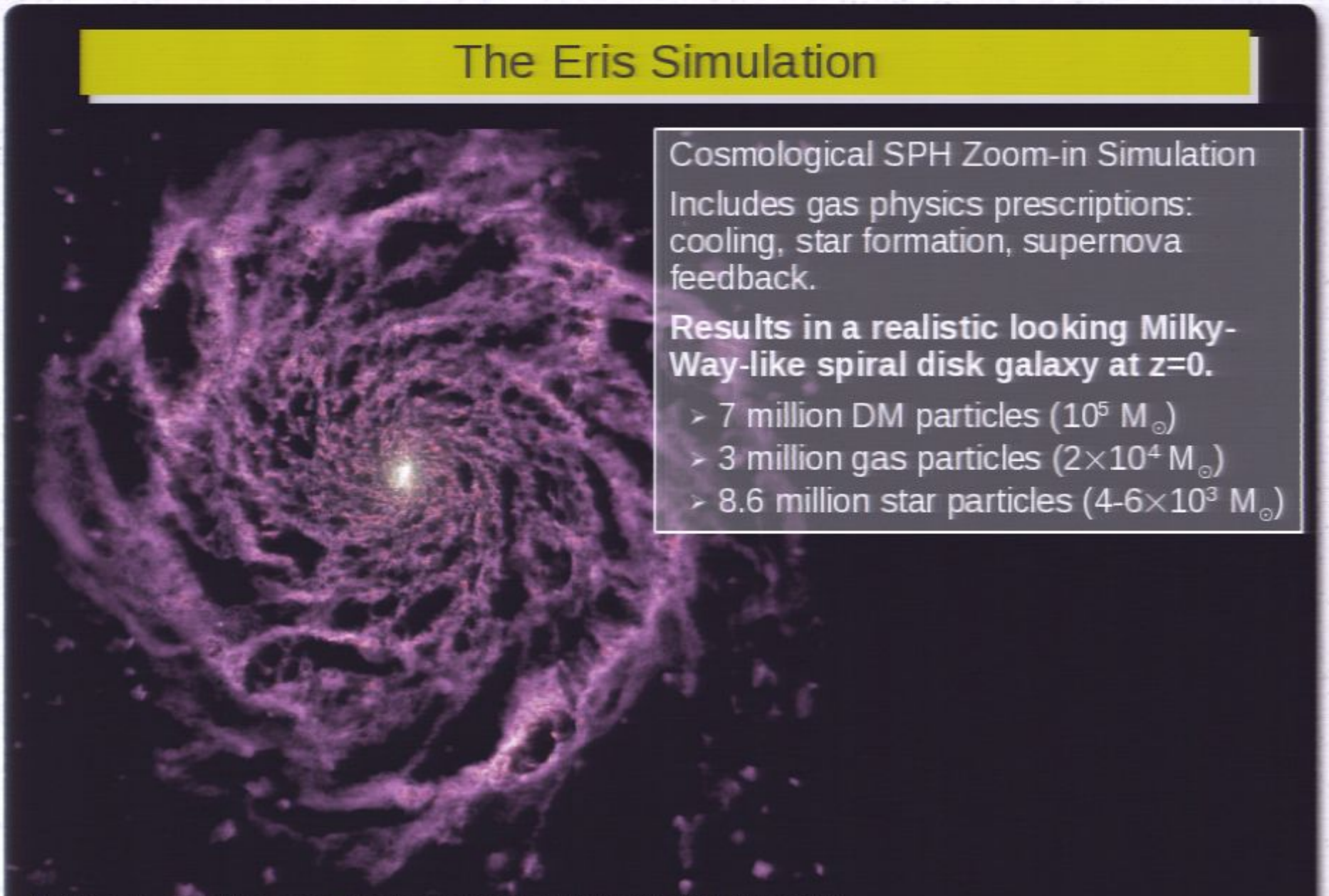

Cosmological SPH Zoom-in Simulation

Includes gas physics prescriptions: cooling, star formation, supernova feedback.

Results in a realistic looking Milky-Way-like spiral disk galaxy at z=0.

- 7 million DM particles (10^5 $M_\odot$)
- 3 million gas particles (2×10^4 $M_\odot$)
- 8.6 million star particles ($4\text{-}6\times10^3$ $M_\odot$)

For more details see Guedes et al. 2011 (arXiv/1103.6030)

The Eris Simulation

Cosmological SPH Zoom-in Simulation

Includes gas physics prescriptions: cooling, star formation, supernova feedback.

Results in a realistic looking Milky-Way-like spiral disk galaxy at z=0.

- 7 million DM particles (10^5 $M_\odot$)
- 3 million gas particles (2×10^4 $M_\odot$)
- 8.6 million star particles ($4\text{-}6\times10^3$ $M_\odot$)

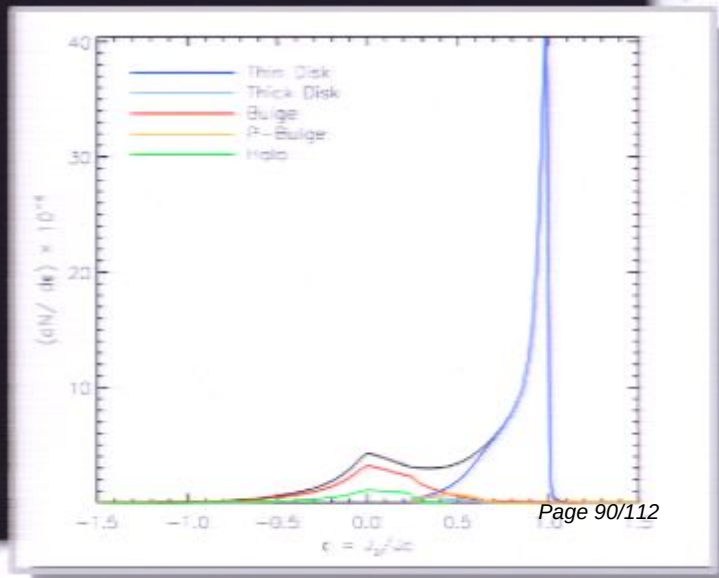

For more details see Guedes et al. 2011 (arXiv/1103.6030)

The Eris Simulation

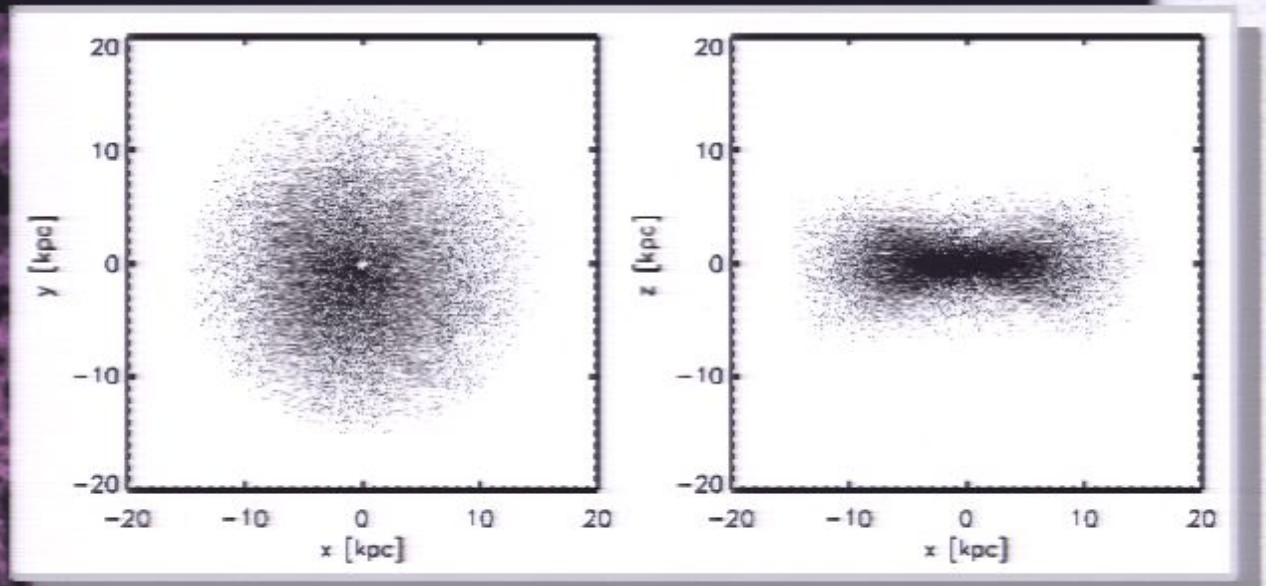

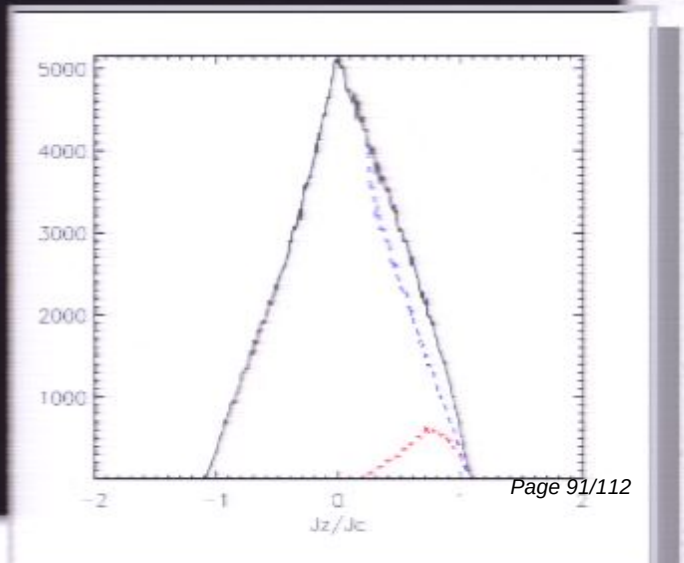

For more details see Guedes et al. 2011 (arXiv/1103.6030)

The Eris Simulation

Density profile in the disk (Δz<0.1kpc):

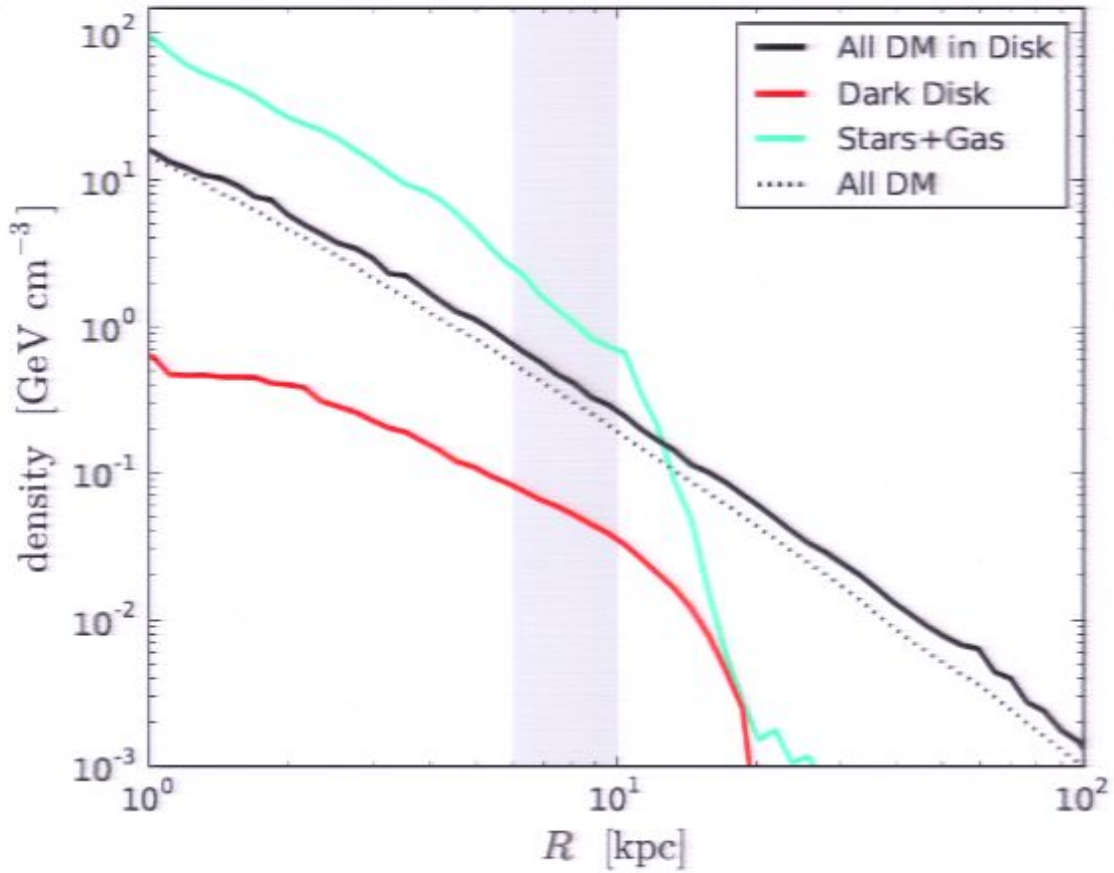

The dark disk contributes about 10% of the mass at R ~ 8 kpc.

In the plane the DM density is ~30% higher than the spherical average.

The density (and potential) in the disk is baryon dominated at R<10 kpc.

The Eris Simulation

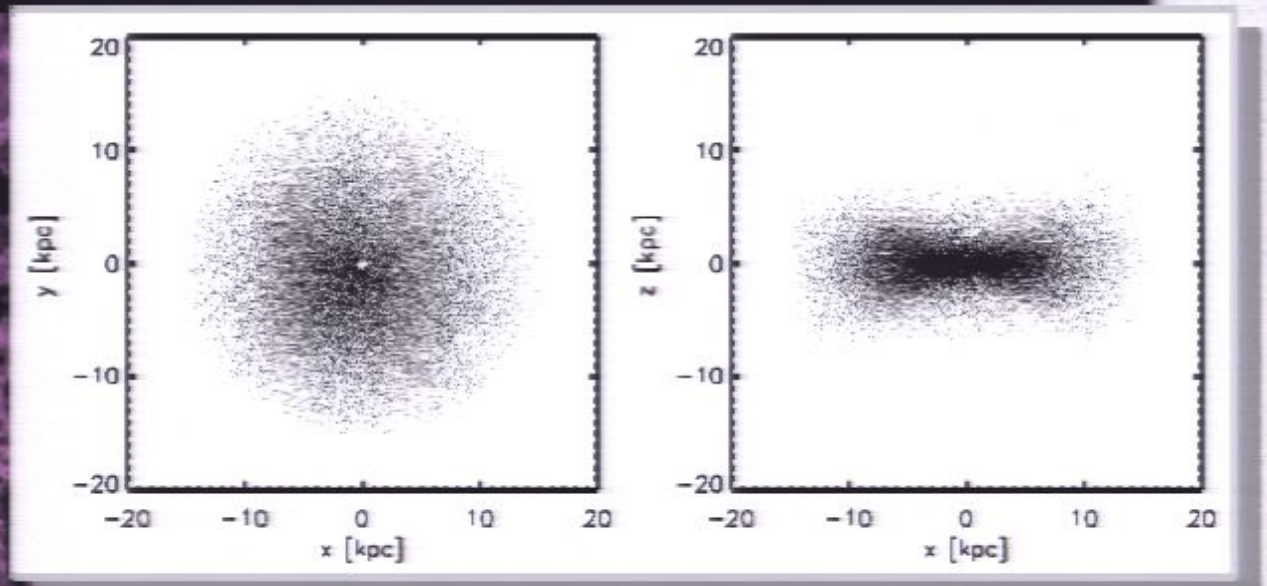

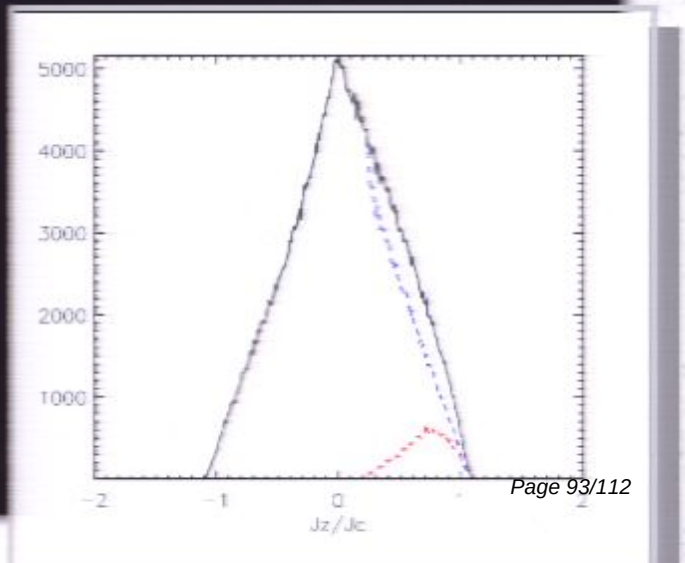

For more details see Guedes et al. 2011 (arXiv/1103.6030)

The Eris Simulation

Density profile in the disk (Δz<0.1kpc):

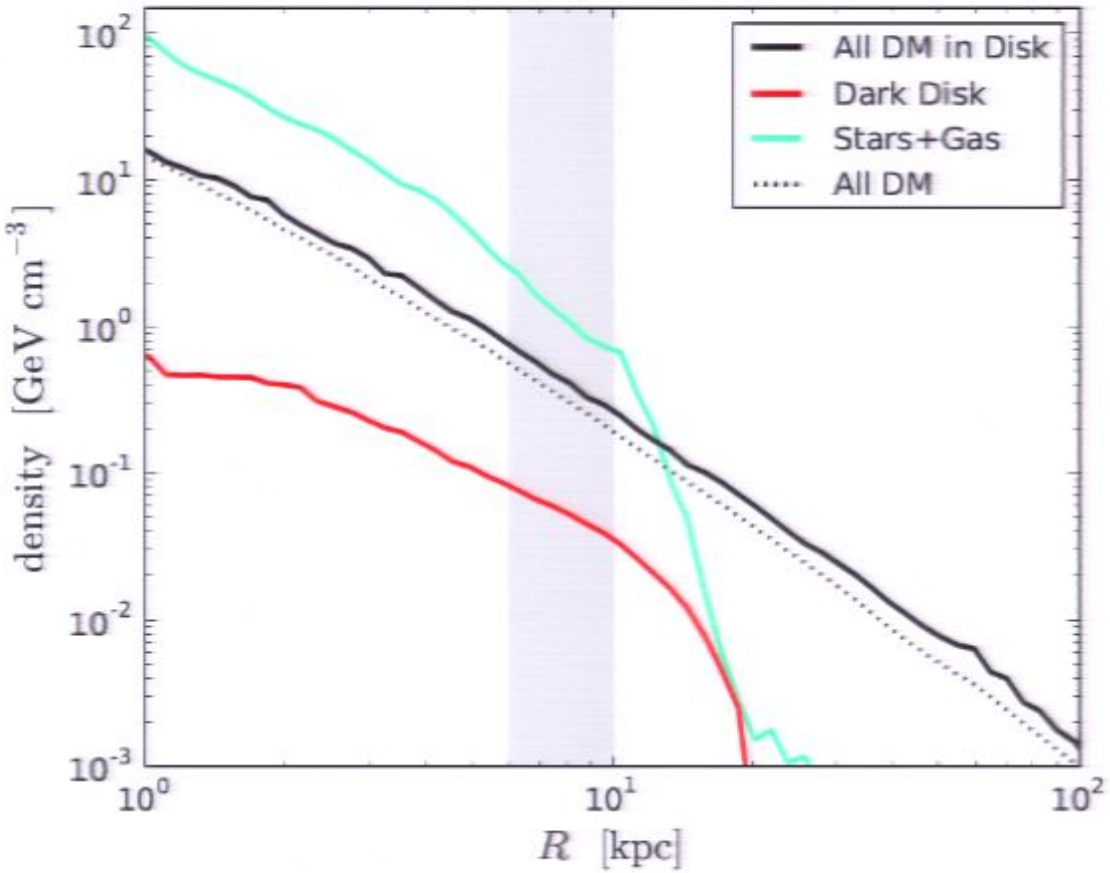

The dark disk contributes about 10% of the mass at R ~ 8 kpc.

In the plane the DM density is ~30% higher than the spherical average.

The density (and potential) in the disk is baryon dominated at R<10 kpc.

Halo Rest Frame Velocity Distributions

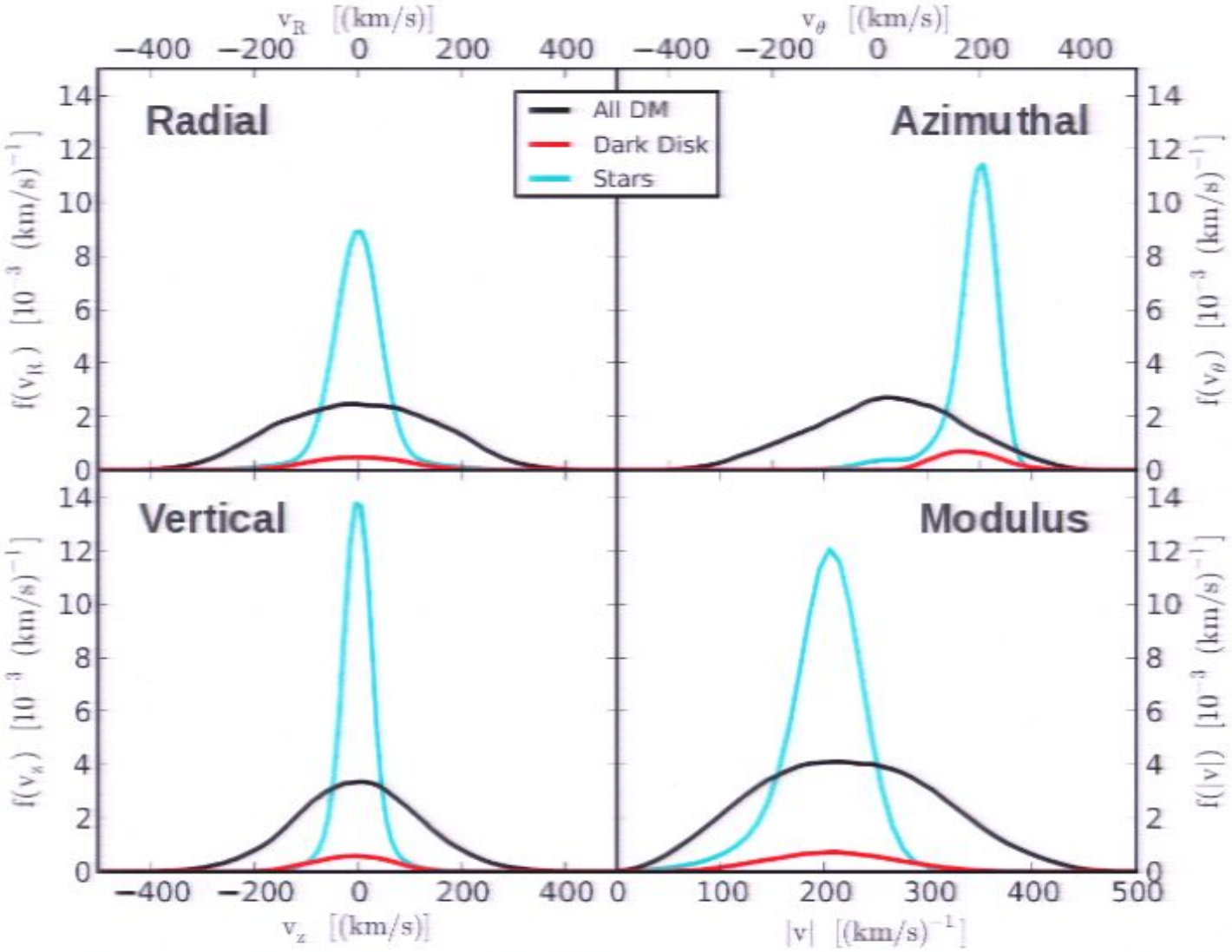

Halo Rest Frame Velocity Distributions

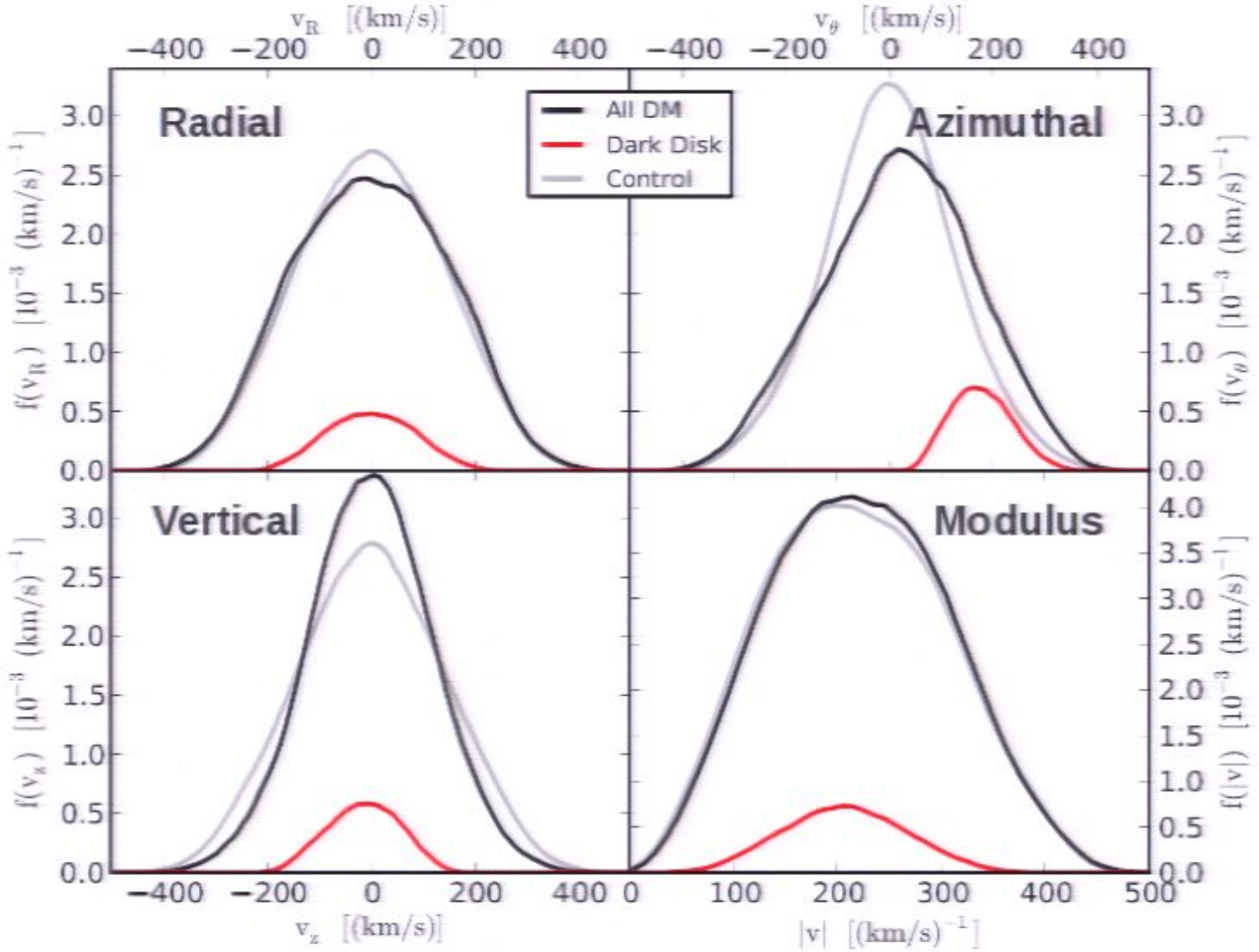

Earth Rest Frame (Summer) Velocity Distributions

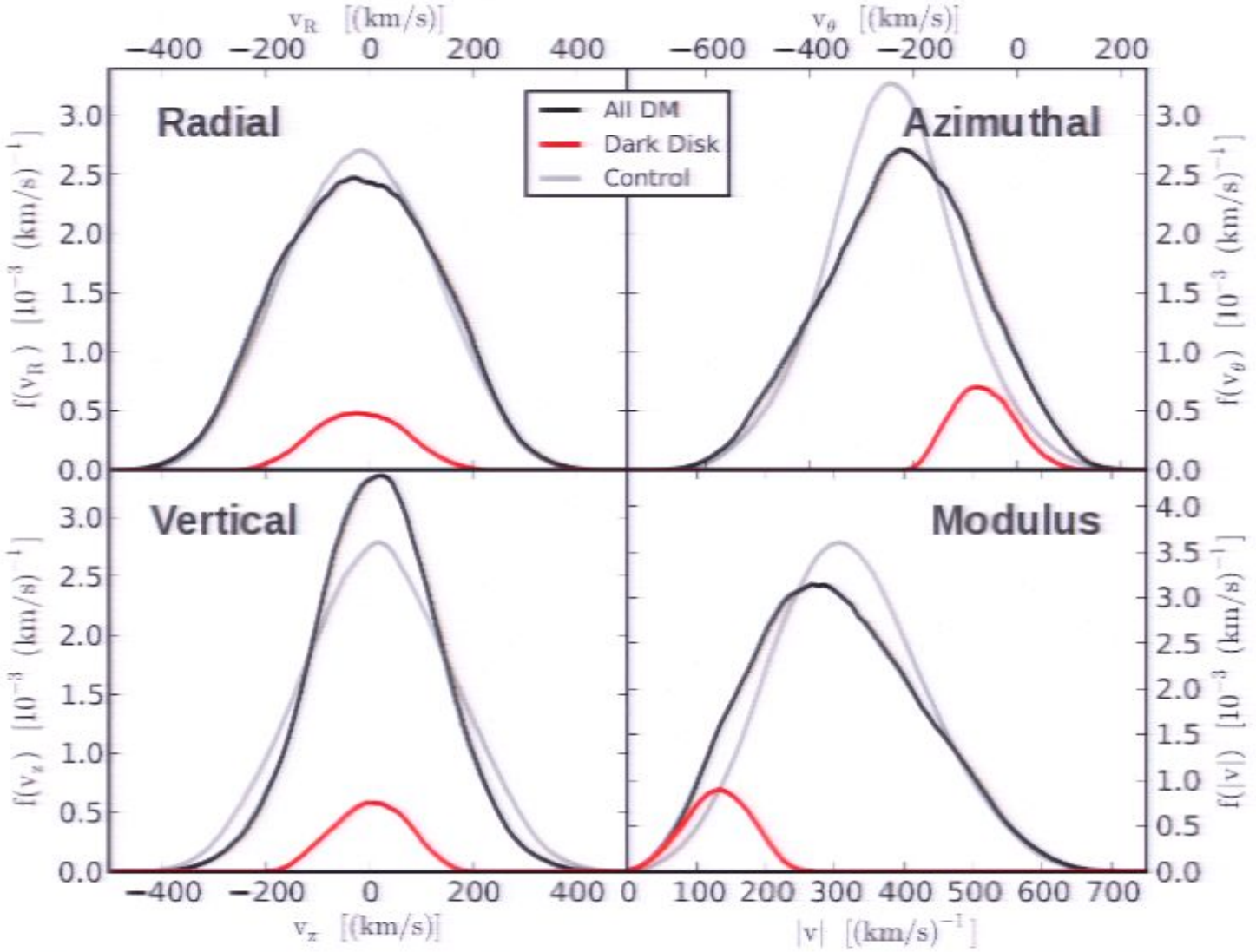

Time-averaged Signal

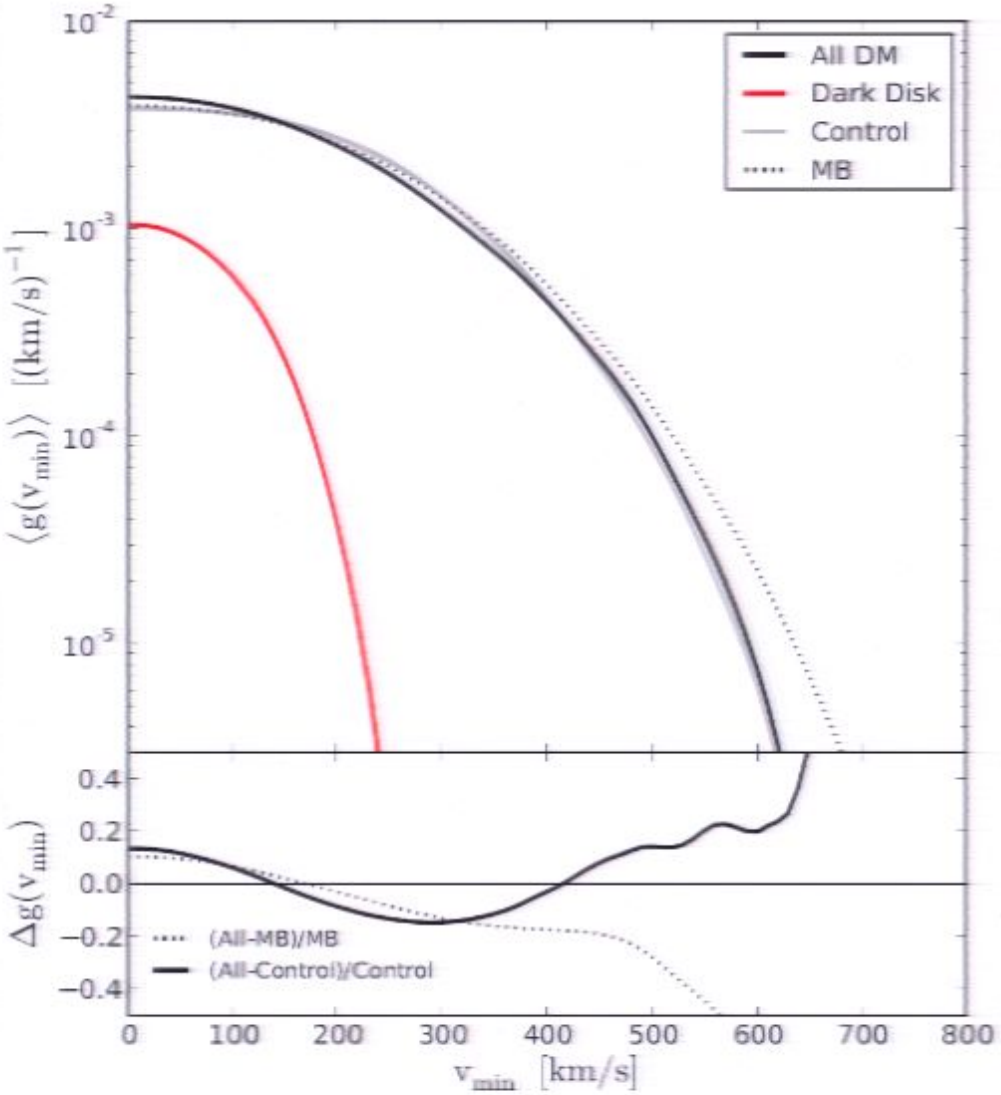

$$g(v_{\rm min}) \equiv \int_{v_{\rm min}}^{\infty} \frac{f(v)}{v}\, dv$$

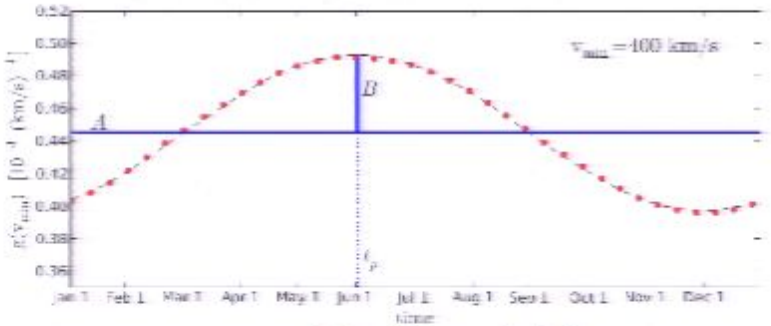

$$A + B \sin\left(\frac{2\pi(t - t_p)}{365\,\text{days}}\right)$$

- Deviations from control and MB sample around 10 – 20%, higher at v_{min} > 500 km/s.
- Compared to Control sample, the Dark Disk increases the signal at both low and high v_{min}, and suppresses it in between.

Experimental Benchmarks

Name	Experiment	Element	(Z, A)	m_χ [GeV]	E_{recoil} [keV_{nr}]	v_{min} [km s^{-1}]	Reference	Comments
CDMS_Ge_50GeV	CDMS-II	Ge	(32, 73)	50.0	[10.0, 100.0]	[193.1, 610.8]	0912.3592	
CDMS_Ge_100GeV	—	—	—	100.0	—	[135.8, 429.5]	—	
CDMS_Ge_500GeV	—	—	—	500.0	—	[89.98, 284.5]	—	
CDMS_Si_50GeV	CDMS-II	Si	(14, 28)	50.0	[10.0, 100.0]	[197.8, 625.4]	0912.3592	
CDMS_Si_100GeV	—	—	8—	100.0	—	[162.3, 513.1]	—	
CDMS_Si_500GeV	—	—	—	500.0	—	[133.9, 423.3]	—	
CDMS_Ge_lowE	CDMS-II	Ge	(32, 73)	7.0	[2.3, 11.6]	[430.3, 966.4]	1107.0717	matched to CoGeNT
CDMS_Si_lowE	—	Si	(14, 28)	7.0	[4.5, 22.8]	[425.2, 957.1]	—	matched to CoGeNT
Xenon_50GeV	Xenon100	Xe	(54, 131)	50.0	[8.4, 44.6]	[194.5, 448.1]	1005.0380	
Xenon_100GeV	—	—	—	100.0	—	[124.1, 285.9]	—	
Xenon_500GeV	—	—	—	500.0	—	[67.89, 156.2]	—	
Xenon_lowE	Xenon100	Xe	(54, 131)	7.0	[1.4, 7.0]	[431.3, 966.7]	1107.0717	matched to CoGeNT
DAMA_Na_10GeV	DAMA	Na	(11, 23)	10.0	[6.7, 20.0]	[377.8, 652.8]	1002.1028	Q(Na) = 0.3
DAMA_I_100GeV	—	I	(53, 127)	100.0	[25.0, 75.0]	[213.6, 370.1]	—	Q(I) = 0.08
DAMA_Na_lowE	DAMA	Na	(11, 23)	7.0	[5.0, 25.3]	[423.9, 954.1]	1107.0717	matched to CoGeNT
CoGeNT_7GeV	CoGeNT	Ge	(32, 73)	7.0	[2.3, 11.6]	[430.3, 966.4]	1106.0650	
CRESST_O_10GeV	CRESST	O	(8, 16)	10.0	[12.0, 40.0]	[477.7, 872.1]	1109.0702	
CRESST_Ca_15GeV	—	Ca	(20, 40)	15.0	—	[426.0, 777.8]	—	
CRESST_W_50GeV	—	W	(74, 184)	50.0	—	[253.5, 462.9]	—	
CRESST_O_lowE	CRESST	O	(8, 16)	7.0	[5.8, 29.8]	[419.7, 951.2]	1107.0717	matched to CoGeNT

Time-averaged Signal

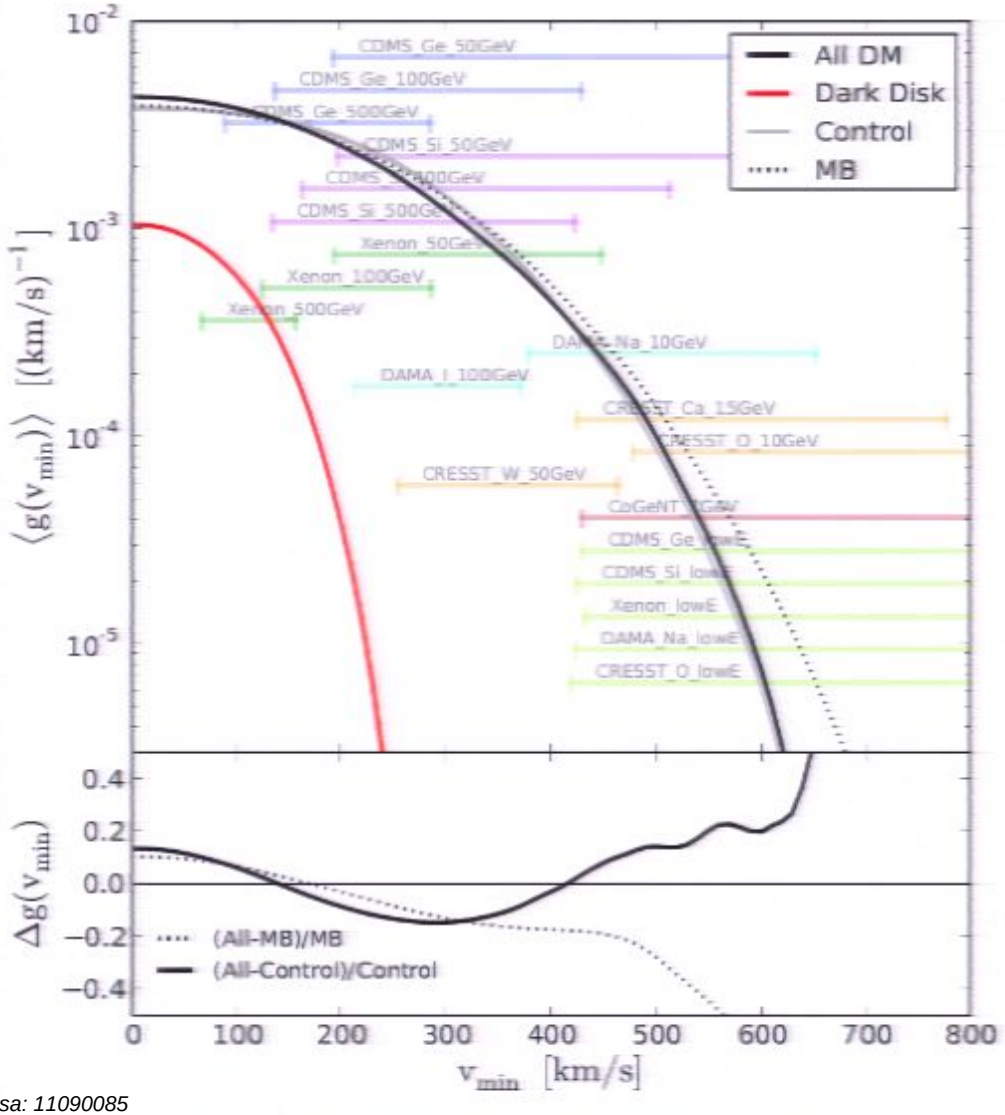

$$g(v_{\min}) \equiv \int_{v_{\min}}^{\infty} \frac{f(v)}{v}\, dv$$

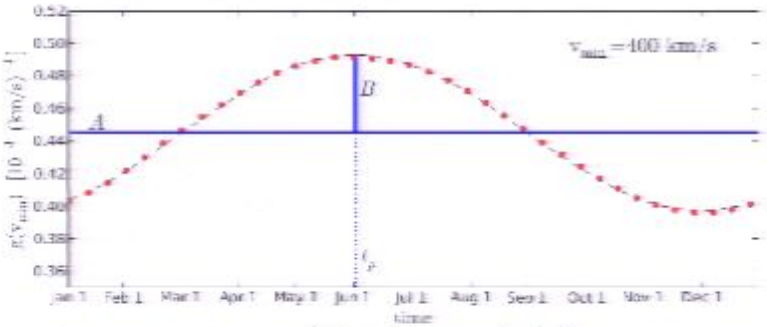

$$A + B \sin\left(\frac{2\pi(t - t_p)}{365\,\text{days}}\right)$$

- Deviations from control and MB sample around 10 – 20%, higher at v_{min} > 500 km/s.
- Compared to Control sample, the Dark Disk increases the signal at both low and high v_{min}, and suppresses it in between.

The Annual Modulation

$$A + B\sin\left(\frac{2\pi(t - t_p)}{365\,\text{days}}\right)$$

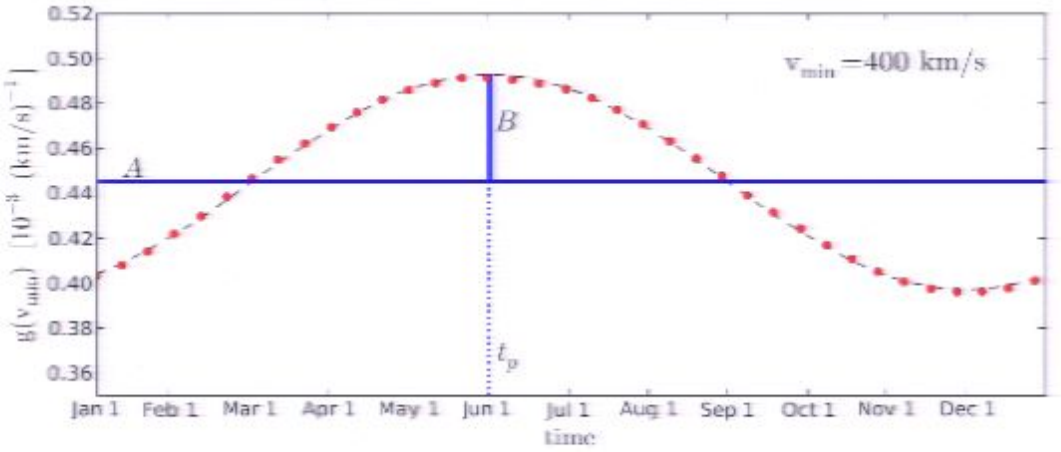

Modulation Amplitude (*B*)

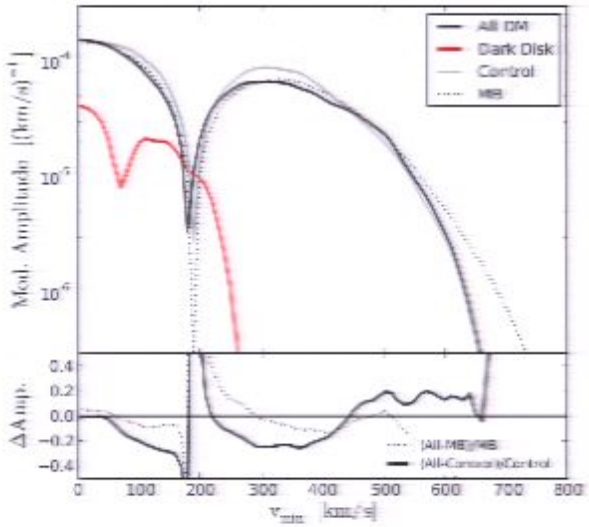

Modulation Fraction (*B*/*A*)

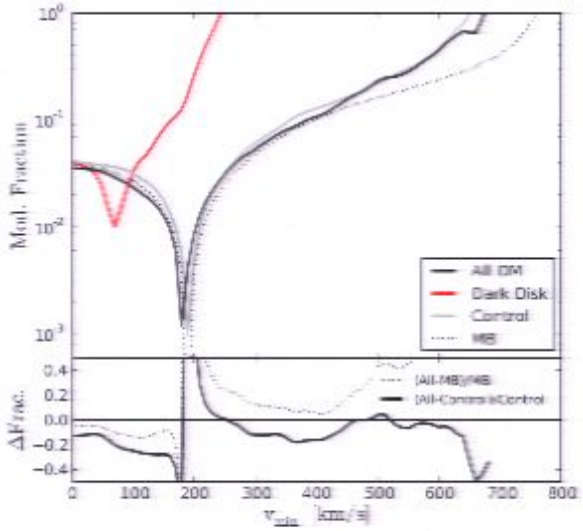

Modulation Peak Day (t_p)

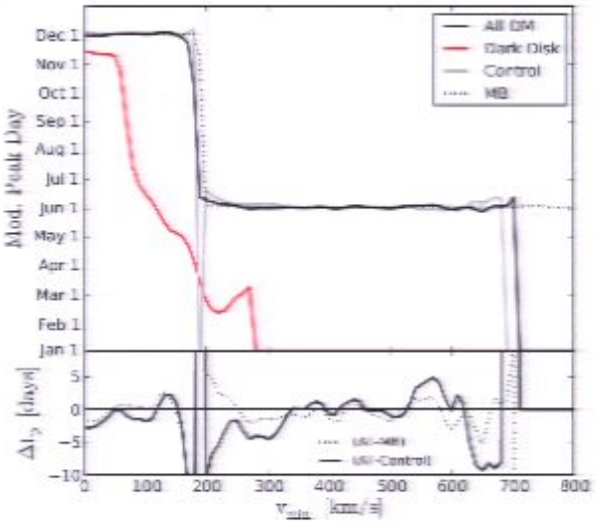

A Retrograde Disk?

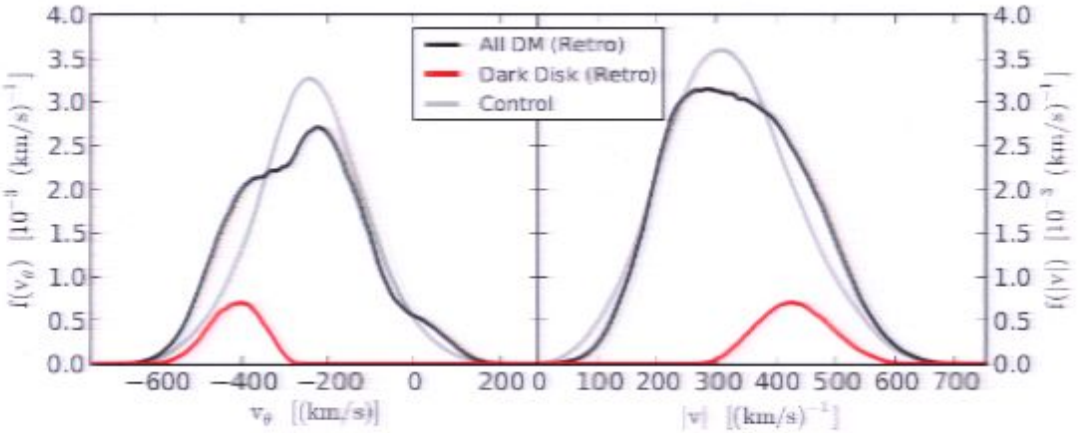

- Model a retrograde dark disk by simply flipping the sign of v_θ of all dark disk particles.
- Retro-DD particles add constructively to the Sun's orbital velocity.
- Effects shift to larger v_{min} and become more prominent: up to 40%.

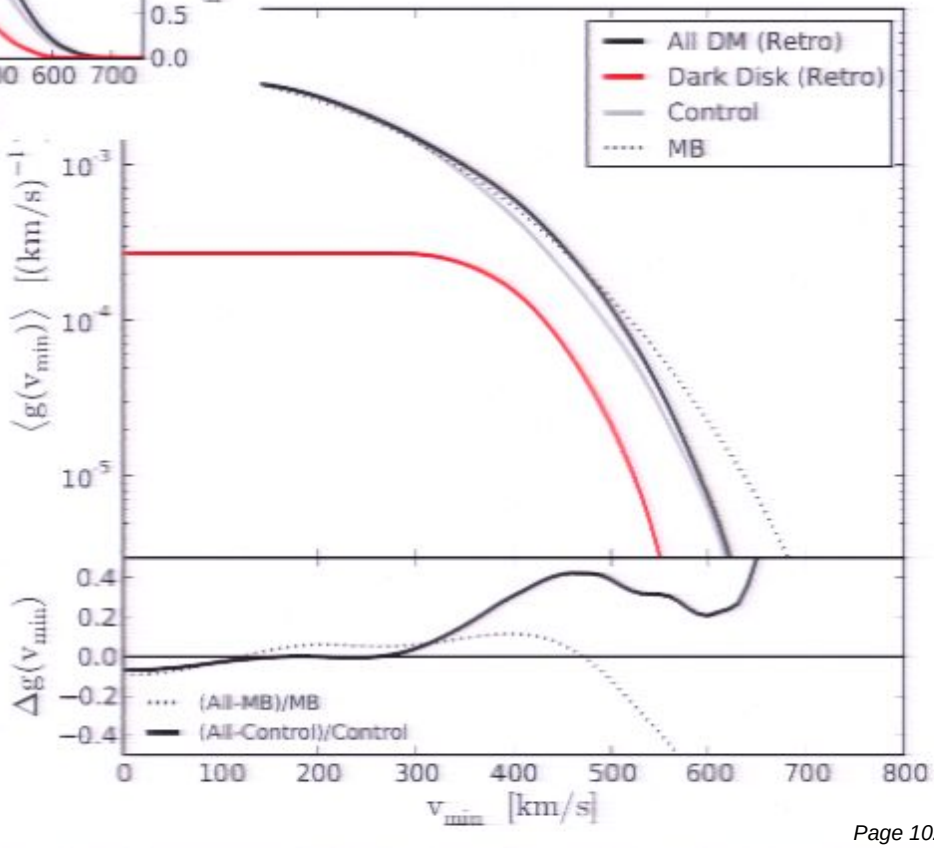

Conclusions

- According to ultrahigh resolution dark-matter only simulations **f(v) is not strictly Maxwellian**.

Conclusions

- According to ultrahigh resolution dark-matter only simulations **f(v) is not strictly Maxwellian**.
- Departures occur at all velocities, but **most notable at high velocities**. Relevant for light dark matter (and inelastic, and directionally sensitive experiments).

Conclusions

- According to ultrahigh resolution dark-matter only simulations **f(v) is not strictly Maxwellian**.
- Departures occur at all velocities, but **most notable at high velocities**. Relevant for light dark matter (and inelastic, and directionally sensitive experiments).
- Velocity substructure: both spatially localized (**subhalos and tidal streams**) and "global" (**debris flow**).

Conclusions

- According to ultrahigh resolution dark-matter only simulations **f(v) is not strictly Maxwellian**.
- Departures occur at all velocities, but **most notable at high velocities**. Relevant for light dark matter (and inelastic, and directionally sensitive experiments).
- Velocity substructure: both spatially localized (**subhalos and tidal streams**) and "global" (**debris flow**).
- **Debris flow is non-virialized bulk motion** of particles stripped from accreted subhalos that is incompletely phase-mixed. **It is dominant at high |v|**, and can interesting effects in the arrival direction of DM.

Conclusions

- According to ultrahigh resolution dark-matter only simulations **f(v) is not strictly Maxwellian**.
- Departures occur at all velocities, but **most notable at high velocities**. Relevant for light dark matter (and inelastic, and directionally sensitive experiments).
- Velocity substructure: both spatially localized (**subhalos and tidal streams**) and "global" (**debris flow**).
- **Debris flow is non-virialized bulk motion** of particles stripped from accreted subhalos that is incompletely phase-mixed. **It is dominant at high |v|**, and can interesting effects in the arrival direction of DM.
- It is becoming possible to **go beyond pure-DM simulations** of galaxy formation.

Caveats: much lower resolution, hidden dependence of implementation of baryonic physics (hydrodynamics, cooling, star formation, feedback, etc.).

Conclusions

- According to ultrahigh resolution dark-matter only simulations **f(v) is not strictly Maxwellian**.
- Departures occur at all velocities, but **most notable at high velocities**. Relevant for light dark matter (and inelastic, and directionally sensitive experiments).
- Velocity substructure: both spatially localized (**subhalos and tidal streams**) and "global" (**debris flow**).
- **Debris flow is non-virialized bulk motion** of particles stripped from accreted subhalos that is incompletely phase-mixed. **It is dominant at high |v|**, and can interesting effects in the arrival direction of DM.
- It is becoming possible to **go beyond pure-DM simulations** of galaxy formation.

  Caveats: much lower resolution, hidden dependence of implementation of baryonic physics (hydrodynamics, cooling, star formation, feedback, etc.).
- The **Eris simulation** is one such example: it exhibits a **kinematically distinct dark disk**, a component of the DM halo rotating in the Galactic disk plane (prograde).

Conclusions

- According to ultrahigh resolution dark-matter only simulations **f(v) is not strictly Maxwellian**.
- Departures occur at all velocities, but **most notable at high velocities**. Relevant for light dark matter (and inelastic, and directionally sensitive experiments).
- Velocity substructure: both spatially localized (**subhalos and tidal streams**) and "global" (**debris flow**).
- **Debris flow is non-virialized bulk motion** of particles stripped from accreted subhalos that is incompletely phase-mixed. **It is dominant at high |v|**, and can interesting effects in the arrival direction of DM.
- It is becoming possible to **go beyond pure-DM simulations** of galaxy formation.

  Caveats: much lower resolution, hidden dependence of implementation of baryonic physics (hydrodynamics, cooling, star formation, feedback, etc.).
- The **Eris simulation** is one such example: it exhibits a **kinematically distinct dark disk**, a component of the DM halo rotating in the Galactic disk plane (prograde).
- The dark disk makes up about **10% of the local density, and affects scattering rates and the annual modulation at the 10-20% level.**

The Annual Modulation

$$A + B\sin\left(\frac{2\pi(t - t_p)}{365\,\text{days}}\right)$$

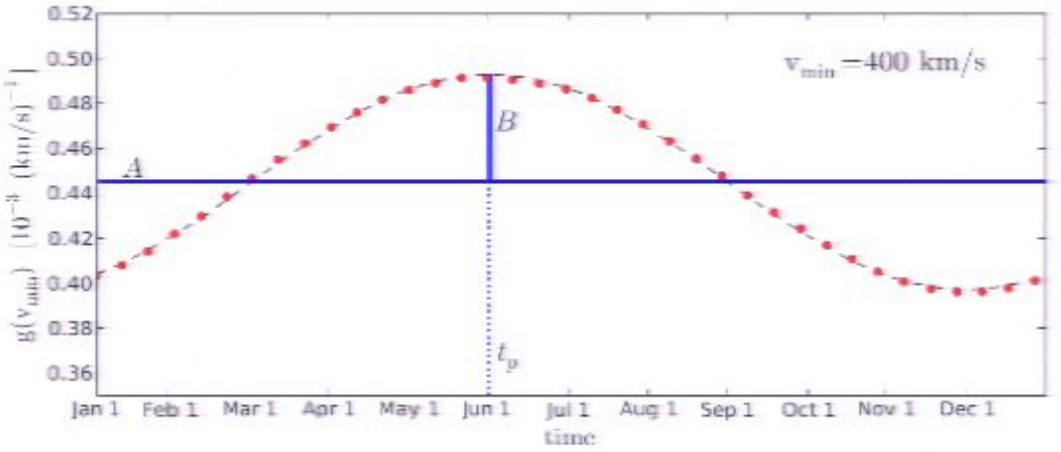

Modulation Amplitude (*B*)

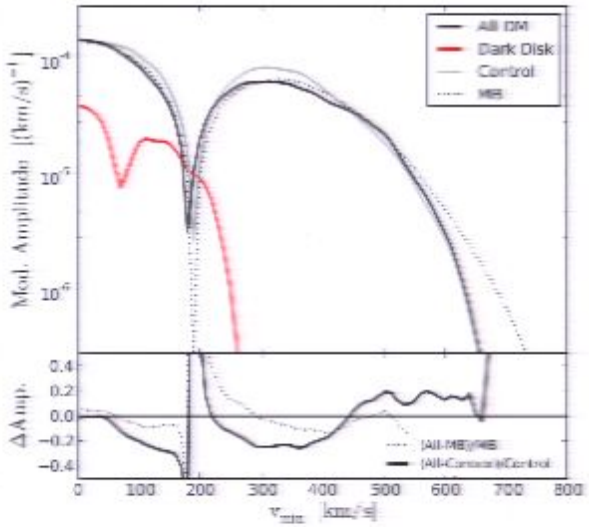

Modulation Fraction (*B*/*A*)

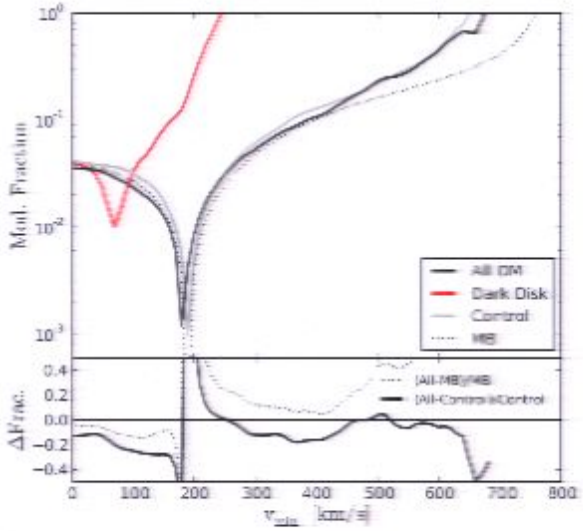

Modulation Peak Day (t_p)

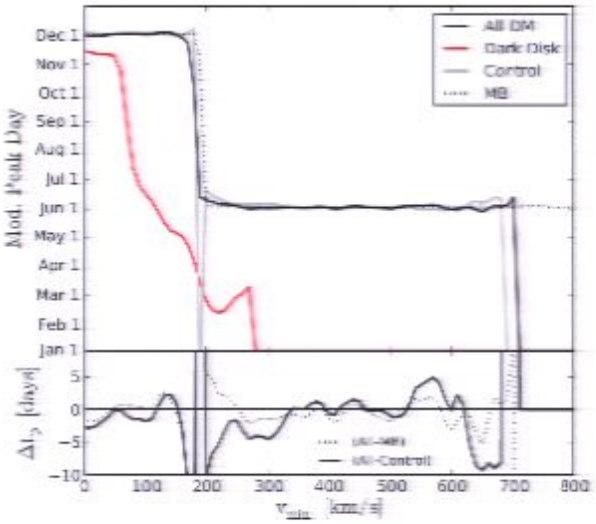

The Eris Simulation

Density profile in the disk (Δz<0.1kpc):

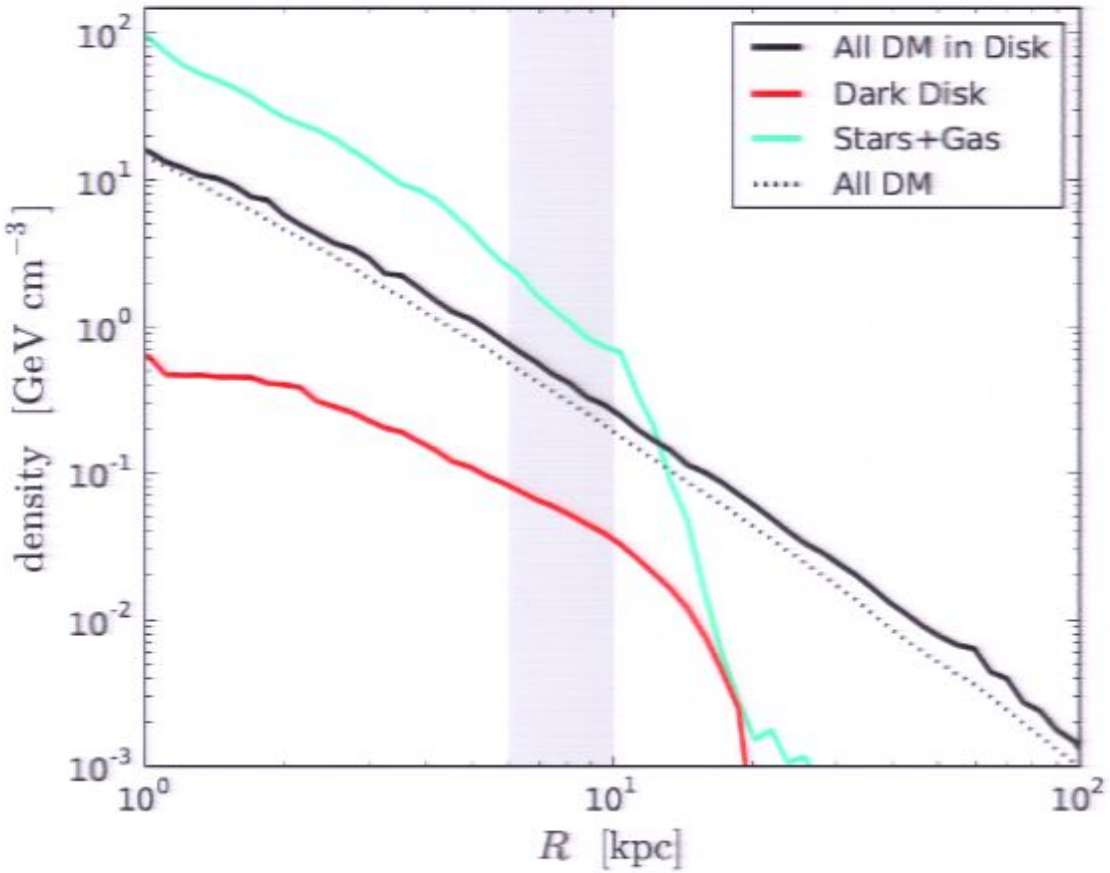

The dark disk contributes about 10% of the mass at R ~ 8 kpc.

In the plane the DM density is ~30% higher than the spherical average.

The density (and potential) in the disk is baryon dominated at R<10 kpc.

The Eris Simulation

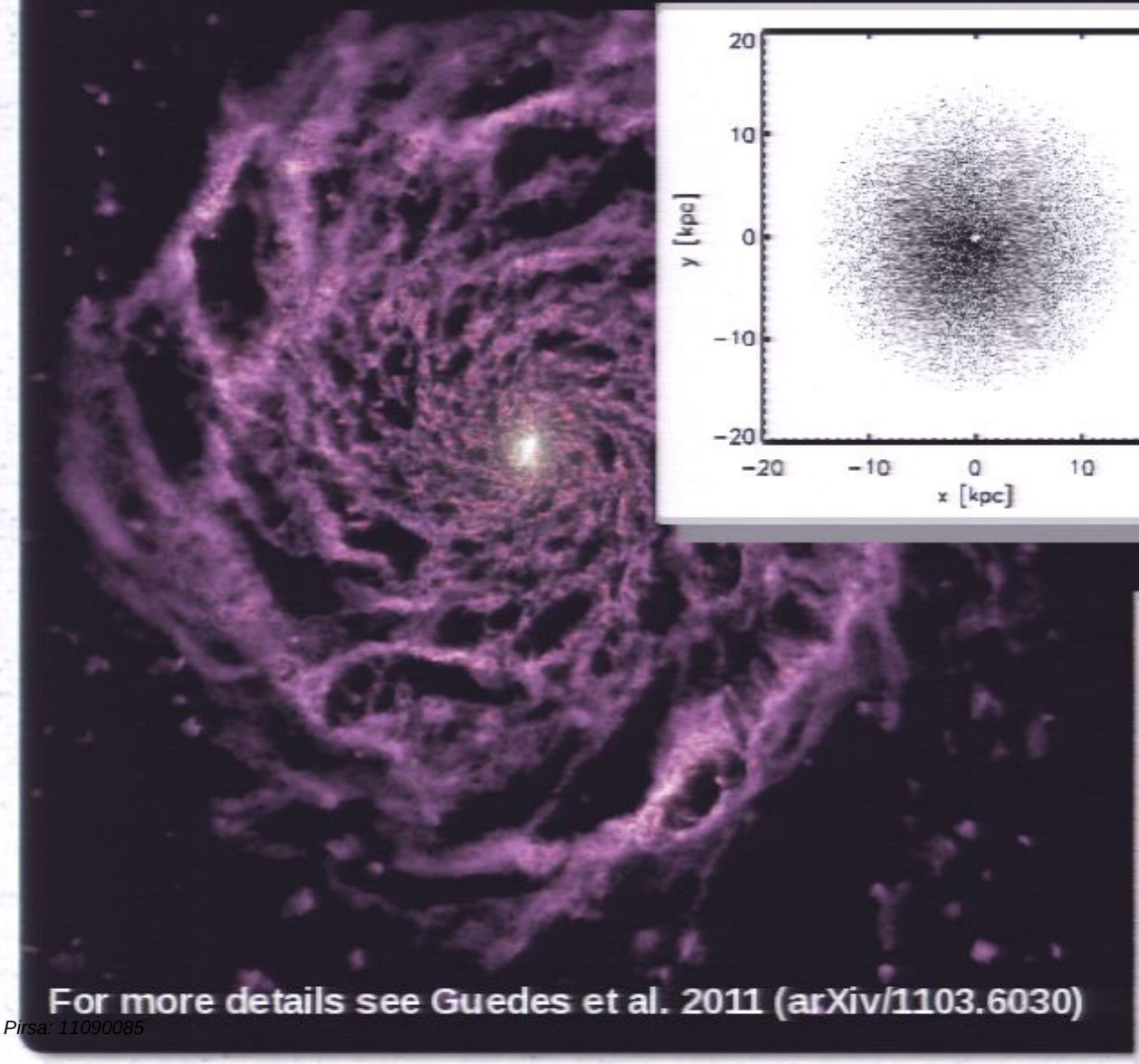

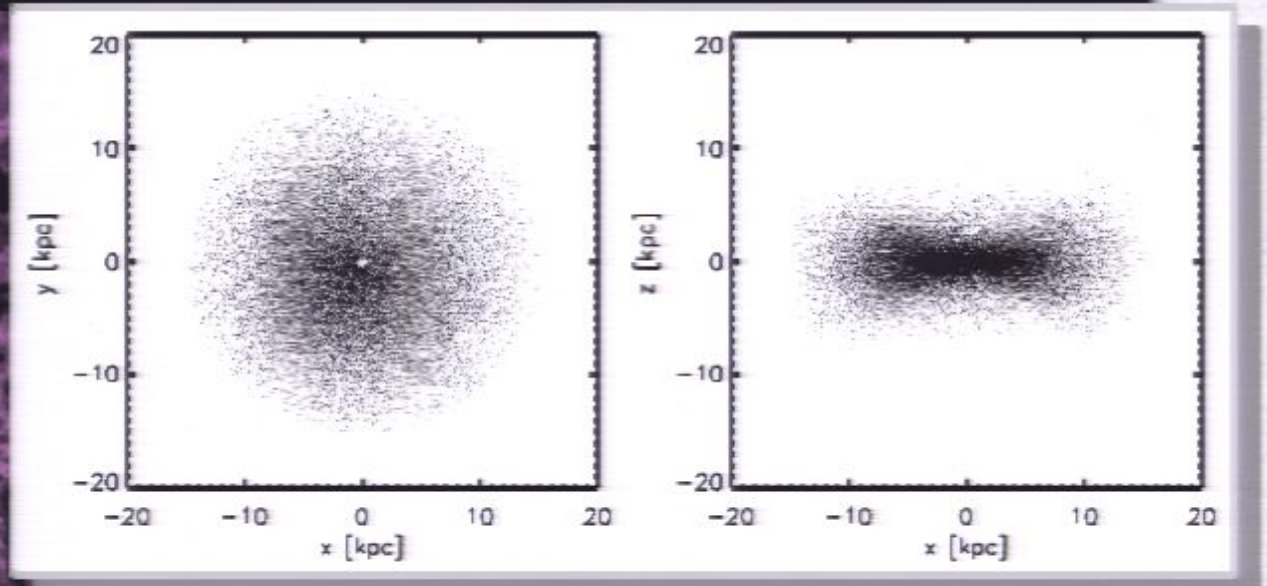

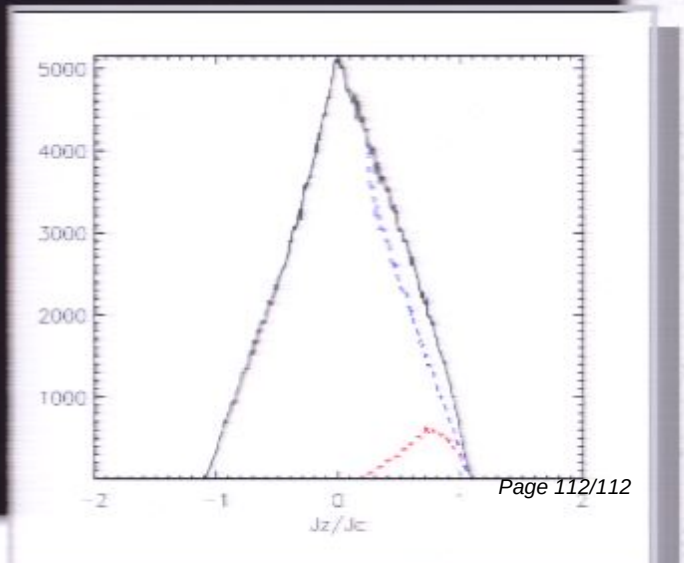

For more details see Guedes et al. 2011 (arXiv/1103.6030)